Univerzita Karlova

Přírodovědecká fakulta

Studijní program: Biologie

Studijní obor: Fyziologie živočichů

Bc. Tomáš Knotek

Vliv kanonické Wnt signální dráhy na diferenciaci polydendrocytů po ischemickém poranění nervové tkáně

The effect of the canonical Wnt signalling pathway on the differentiation of polydendrocytes after ischemic injury

Diplomová práce

Vedoucí diplomové práce: Ing. Miroslava Anděrová, CSc.

Praha, 2018

Prohlášení:

Prohlašuji, že jsem závěrečnou práci zpracoval samostatně a že jsem uvedl všechny použité informační zdroje a literaturu. Tato práce ani její podstatná část nebyla předložena k získání jiného nebo stejného akademického titulu.

V Praze 30. 4. 2018

Podpis:

Poděkování:

Rád bych na tomto místě poděkoval své školitelce Ing. Miroslavě Anděrové, CSc. za odborné vedení mé práce, trpělivost a cenné rady. Dále bych chtěl poděkovat Mgr. Jánu Kriškovi za pomoc při práci v laboratoři.

Abstract:

Polydendrocytes, or NG2 glia, are fourth type of glial cells in mammal central nervous system. In the adult brain, NG2 glia represent important cell type with respect to their role in gliogenesis and nervous tissue regeneration following injury. Ligands from the Wingless/Int (Wnt) family play key role in proliferation and differentiation of NG2 glia and they can also influence regeneration of nervous tissue after ischemia. The aim of this thesis was to elucidate the role of NG2 glia in neurogenesis and gliogenesis following ischemic brain injury and investigate the impact of Wnt signalling on the reaction of NG2 glia to this type of injury. To fulfil these aims, transgenic mouse strains with tamoxifen-inducible recombination, that enabled simultaneous expression of red fluorescent dye and either activation or inhibition of the Wnt signalling pathway in NG2 glia, were employed. To induce ischemic injury, middle cerebral artery occlusion model was used. Changes in differentiation and electrophysiological properties of NG2 glia were analysed using patch-clamp technique. Activation of the Wnt signalling pathway under physiological conditions and 7 days after ischemic injury led to increased differentiation of NG2 glia toward astrocytes, while 3 days after ischemic injury activation of this signalling pathway supported neurogenesis. Differentiation of NG2 glia was not affected by Wnt signalling inhibition.

Key words: Polydendrocytes; NG2 glia; CNS; Differentiation; Brain ischemia; Wnt signalling pathway

Abstrakt:

Polydendrocyty, také nazývané NG2 glie, jsou čtvrtým typem gliových buněk v savčím centrálním nervovém systému. V dospělém mozku představují NG2 glie důležitý buněčný typ vzhledem k jejich roli v gliogenezi a regeneraci nervové tkáně po poškození. Ligandy z rodiny Wnt mohou hrát klíčovou roli v proliferaci a diferenciaci NG2 glií a mají také vliv na průběh regenerace nervové tkáně po ischemii. Cílem této práce bylo objasnit roli NG2 glií v neurogenezi a gliogenezi po ischemickém poškození mozku a prozkoumat, jaký vliv měla v reakci NG2 glií na tento typ poškození Wnt signální dráha. K dosažení cílů byly použity transgenní myší kmeny s tamoxifenem indukovanou rekombinací, která umožňuje expresi červeného fluorescenčního proteinu tdTomato v NG2 gliích a současnou aktivaci či inhibici Wnt signální dráhy. K navození ischemického poškození byl použit model okluze střední mozkové arterie. Změny v diferenciaci a elektrofyziologických vlastnostech NG2 glií byly analyzovány metodou terčíkového zámku. Aktivace Wnt signální dráhy vedla za fyziologických podmínek a 7 dní po ischemickém poškození ke zvýšené diferenciaci NG2 glií v astrocyty, zatímco 3 dny po ischemickém poškození podporovala neurogenezi. Diferenciace NG2 glií nebyla ovlivněna při inhibici Wnt signalizace.

Klíčová slova: Polydendrocyty; NG2 glie; CNS; Diferenciace; Mozková ischemie; Wnt signální dráha

Table of contents

Abbreviations

aCSF – Artificial cerebrospinal fluid

AEP – Anterior entopeduncular area

Aldh1L1 – Aldehyde dehydrogenase 1 family, member L1

AMPA – α-amino-3-hydroxy-5-methyl-4-isoxazolepropionic acid

AP – Action potential

APC - Adenomatous polyposis coli

ATP – Adenosine triphosphate

ATPase – ATP hydrolase

BDNF – Brain-derived neurotrophic factor

BrdU – Bromodeoxyuridine

CamKII – Ca^{2+}/calmodulin-dependent protein kinase II

CGE – Caudal ganglionic eminence

Ci – Cubitus interruptus

CK1α – Casein kinase 1α

CM – Membrane capacitance

C-Myc - Myelocytomatosis cellular oncogene

CNP – 2',3'-cyclic-nucleotide 3'-phosphodiesterase

CNS – Central nervous systém

CSPG4 – Chondroitin sulphate proteoglycan 4

Daam1 – Dishevelled associated activator of morphogenesis 1

DAPI – 4′,6-diamidino-2-phenylindole

DCX – Doublecortin

Dkk1 – Dickkopf 1; also CSPG4-CreERT2/Rosa26-tdTomato-Dkk1 mouse strain

DMEM/F12 – Dulbecco's Modified Eagle Medium/Nutrient Mixture F-12

DNA - Deoxyribonucleic acid

Dsh – Dishevelled

E12.5 – 12.5 days of embryonic age

EAAT – Excitatory amino acid transporter

EGFP – Enhanced green fluorescent protein

EGTA – 5 Ethylene glycol-bis(2-aminoethylether)-N,N,N′,N′-tetraacetic acid

Ex3 – CSPG4-CreERT2/Rosa26-tdTomato/$Catnb^{lox(ex3)}$ mouse strain

FCI – Focal cerebral ischemia

FCS – Foetal calf serum

fEPSP – Field excitatory postsynaptic potential

Frz – Frizzled

GABA – γ-aminobutyric acid

GFAP – Glial fibrillary acidic protein

GLAST – Glutamate aspartate transporter

Gli - Glioblastoma proteins

Gln - Glutamine

GLT1 – Glutamate transporter 1

Glu - Glutamate

GSK3 – Glutamine synthase kinase 3

GTP – Guanosine triphosphate

GTPase – GTP hydrolases

HEPES – 2-[4-(2-hydroxyethyl)piperazin-1-yl]ethanesulfonic acid

HIF1 – Hypoxia-inducible factor 1

IL-1β – Interleukin 1β

IL-6 – Interleukin 6

IR – Input resistance

JNK – c-Jun N-terminal kinase

K2P – Two-pore domain K^+ channel

K_A – A-type K^+ channel

K_{Ca} – Calcium-activated K^+ channel

K_{DR} – Delayed outwardly rectifying K^+ channel

K_{IR} – Inwardly rectifying K^+ channel

LGE – Lateral ganglionic eminence

LRP5/6 – Low density lipoprotein related protein 5 and 6

LTP – Long term potentiation

MAP2 – Microtubule-associated protein 2

MBP – Myelin basic protein

MCAO – Middle cerebral artery occlusion

MCT1 – Monocarboxylate transporter 1

MGE – Medial ganglionic eminence

NeuN – Neuronal specific nuclear protein

NFAT – Nuclear factor of activated T-cells

NFκB – Nuclear factor-κB

NG2 – Nerve/glial antigen 2

Nkx – NK2 homeobox

NLK – Nemo-like kinase

NMDA – *N*-methyl-D-aspartate

nNOS – Neuronal nitric oxide synthase

NO – Nitric oxide

NS/PCs – Neural stem/progenitor cells

O-2A – Oligodendrocyte and type 2 astrocyte progenitors

OPC – Oligodendrocyte precursor cell

P6 – 6 days of postnatal age

PB – Phosphate buffer

PBS – Phosphate-buffered saline

PDGFαR – Platelet-derived grow factor receptor α

PDGFβR – Platelet-derived grow factor receptor β

PKA – Protein kinase A

PKC – Protein kinase C

PLC – Phospholipase C

PLL – Poly-L-lysine

PLP – Proteolipid protein

preOL – Immature oligodendrocyte

PNS - Peripheral nervous system

PPAR – Peroxisome proliferator-activated receptor;

PSA – Penicillin-Streptomycin-Amphotericin B solution

PTB – Pentobarbital

Ptch – Patched receptor

RNA – Ribonucleic acid

ROCK – Rho associated kinase

ROR2 – Receptor tyrosine kinase-like orphan receptor 2

ROS – Reactive oxygen species

Ryk – Receptor-like tyrosine kinase

S.E.M. – Standard error of the mean

Sfrp – Secreted frizzled-related protein

SGZ – Subgranular zone

Shh – Sonic hedgehog

Smo – Smoothened receptor

Sox10 – Sex region Y related high mobility group box 10

SVZ – Subventricular zone

TCA – Tricarboxylic acid

TCF/LEF – Transcription factors T-cell factor/lymphoid enhancer factor

TF – Transcription factor

TNFα – Tumor necrosis factor α

TTC – 2,3,5-Triphenyltetrazolium chloride

V_M – Resting membrane potential

WIF – Wnt inhibitory factors

Wnt – Wingless/Int

YFP – Yellow fluorescent protein

1 Introduction

Cerebral ischemia is the third most common cause of death in developed countries. It can be either caused by cardiac arrest or by occlusion of one of the major brain arteries, resulting in reduced blood flow through the brain or certain brain regions. Reduced blood supply results in numerous pathophysiological changes including neuronal death and loss of some of the brain functions. So far, the only effective approach to cerebral ischemia is restoration of blood flow; however, many studies focus on cellular mechanisms occurring in the ischemic brain.

Insufficient blood supply leads to neuronal apoptosis and necrosis; therefore, various studies concerning neuroprotection were conducted. However, glial cells are not a less interesting target for studies on ischemia since they play a major role in physiological and pathophysiological states of the brain and take on important events during ischemia. Glial cells are responsible for K^+ buffering, neurotransmitter uptake, metabolic support of neurons, regulation of blood flow, brain immunity and phagocytosis, and axonal myelination.

Nerve/glial antigen 2 (NG2) glia represent a newly discovered type of macroglia, which was found both in the grey and white matter. From the time of their discovery, they are characterized by their differentiation potential, which can be influenced by various brain injuries and pathologies.

The Wingless/Int (Wnt) signalling pathway is a major pathway in organism development, but it also influences various processes in the adult brain, including stem cell proliferation and differentiation. NG2 glia are affected by Wnt signalling as well, but the role of this signalling pathway in NG2 glia following ischemic stroke is not well understood. This thesis aims to shed light on the role of Wnt signalling in NG2 glia both under physiological and ischemic conditions.

2 Glial cells

In general, glial cells represent non-excitable cells of the nervous system. For a long time, they were viewed as a mere glue in the brain; however, with continuing research, various roles of these cells emerged. They play an important role in supporting neurons and maintaining stable environment of the neural system. Different types of homeostasis are upheld by glial cells, including stable ion concentrations, uptake of neurotransmitters or regulation of microcirculation. Glia also provide neurons with metabolites, help in formation

of blood-brain barrier, and are responsible for immune response in the nervous system (reviewed in Magaki *et al.*, 2017).

Glial cells can be divided into peripheral nervous system (PNS) glia and central nervous system (CNS) glia. In the CNS, glia are further divided into microglia, which are glia of the mesodermal origin with an immune function, and macroglia, a group of glial cells of the ectodermal origin, comprising oligodendrocytes, astrocytes, and NG2 glia. In the PNS, Schwann cells are the main class of glia.

2.1 Astrocytes

Astrocytes belong to group of macroglia in the CNS. This abundant and heterogeneous cell population is responsible mainly for brain homeostasis. Two distinct groups of astrocytes, grey matter protoplasmic astrocytes with fewer glial filaments and white matter fibrous astrocytes with numerous glial filaments, are recognized. However, astrocytes are more heterogeneous and more subtypes can be identified, based on their morphology, staining or location (Emsley and Macklis, 2006).

Widely used astrocytic marker is glial fibrillary acidic protein (GFAP); however, GFAP protein is predominantly present in white matter astrocytes and some astrocytes are not detectable with antibodies for this protein. To identify majority of astrocytes in the CNS, protein encoded by aldehyde dehydrogenase 1 family, member L1 (Aldh1L1) gene can be used, since it is expressed in all astrocytes and labels astrocytes specifically (Cahoy *et al.*, 2008).

Main function of astrocytes is to maintain homeostasis in the CNS. One of the key roles of astrocytes is uptake of glutamate from the proximity of neuronal synapses. Main transporters responsible for glutamate uptake in brain are excitatory amino acid transporters (EAAT) 1 and 2 (in human, in rodents called glutamate aspartate transporter, GLAST, and glutamate transporter 1, GLT1). These proteins are expressed both in astrocytes and neurons, but the expression in astrocytes is higher (Regan *et al.*, 2007; de Vivo *et al.*, 2010). After glutamate release, EAATs transport glutamate molecules to the cytosol to keep its extracellular concentration low. Glutamate is then converted to glutamine in astrocytes and released from the cells (**Figure 1**). In neurons, glutamine can be converted not only back to glutamate, but also to γ-aminobutyric acid (GABA) (Shen, 2013; Petr *et al.*, 2015). Moreover, glutamate in astrocytes can be degraded in the tricarboxylic acid (TCA) cycle (Yu *et al.*, 1982).

Glutamate also plays a role in communication between astrocytes and neurons. Both neurons and astrocytes can release glutamate and stimulate the other cell type (Parpura *et al.*, 1994; Porter and McCarthy, 1996).

Another crucial role of astrocytes is maintenance of K^+ homeostasis. Neuronal activity results in increased extracellular concentrations of K^+. Since higher concentrations of extracellular K^+ can alter numerous cell properties, such as maintenance of membrane potential or function of voltage gated channels, there is a need for K^+ buffering. There are two mechanisms for K^+ buffering: K^+ uptake and K^+ spatial buffering. K^+ buffering can be described as a process in which ions are transferred from regions of elevated extracellular concentrations to regions of lower extracellular concentrations. Entry of K^+ ions causes depolarization that spreads electrically through the network of astrocytes. Transport of K^+ ions within astrocytic network (syncytium) is maintained by inwardly rectifying K^+ (K_{IR}) channels 4.1. Potassium uptake is a process in which influx of K^+ is balanced with influx of anions or efflux of cations to keep the electrical neutrality and eventually, K^+ ions are released back to extracellular space. Uptake of K^+ is maintained predominantly by Na^+/K^+ – adenosine triphosphate (ATP) hydrolase (ATPase) and $Na^+/K^+/2Cl^-$ cotransporters (reviewed in Kofuji & Newman 2004).

Astrocytes also play a role in neuronal metabolism. They cooperate with neurons in a process known as astrocyte-neuron lactate shuttle, in which astrocytes metabolise glucose from blood in anaerobic glycolysis to pyruvate and then to lactate. Lactate is released from the cell to be taken by neurons and degraded in oxidative metabolism (**Figure 1**). It seems that astrocyte-neuron lactate shuttle plays a sustaining role after early oxidative metabolism of neuron (Kasischke *et al.*, 2004).

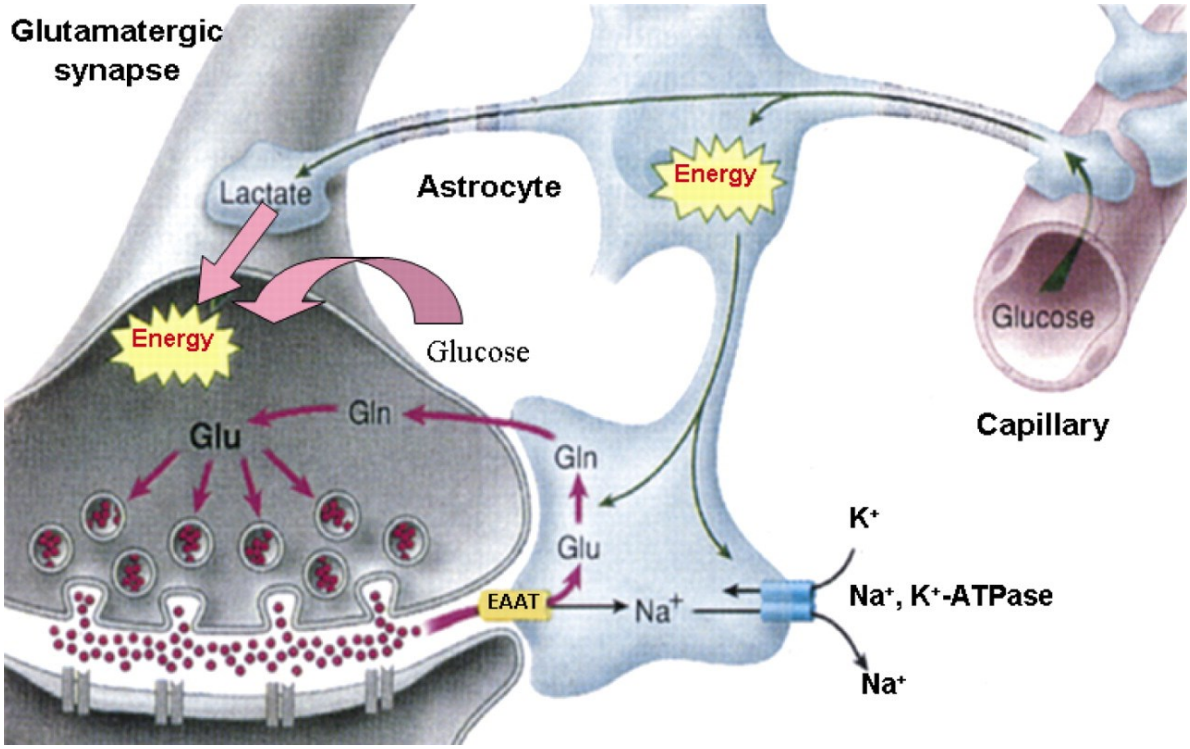

Figure 1: Glutamate uptake by astrocytes. Glutamate released at the synapse by neurons is transported by EAAT to astrocytes, where it is converted to glutamine. Substrates for energetic metabolism are taken by astrocytes from the capillaries not only for their own needs but also to support neuronal energetic metabolism with lactate. Neurons can also uptake glucose for energetic metabolism. Taken from Magistretti, 2011. **Abbreviations**: ATPase – Adenosine triphosphate hydrolase; EAAT – Excitatory amino acid transporter; Gln – Glutamine; Glu – Glutamate.

2.2 Oligodendrocytes

Oligodendrocytes are myelinating cells of the CNS, ensheathing multiple axons in multiple layers, and generating myelin. Myelination plays a crucial role in accelerating nerve conduction by restricting action potentials (APs) to unmyelinated segments called nodes of Ranvier. It increases conductivity of action potentials and decreases energetic demands of signal conduction (Wang *et al.*, 2008). Moreover, oligodendrocytes can metabolically support neurons with lactate released by monocarboxylate transporter 1 (MCT1) and dysfunction of this transporter can have a role in neurodegeneration (Lee *et al.*, 2012). The distribution of myelin along the axons is not uniform, and it seems that this distribution is a feature of neuronal identity (Tomassy *et al.*, 2014). Oligodendrocytes have been recently found to play a role in motor skill learning, because new oligodendrocytes and myelin are needed in this process (McKenzie *et al.*, 2014).

2.3 Microglia

Microglial cells are known mainly for their immunological function in the injured brain, but they also play an important role in the healthy brain. There are two major types of microglia in the brain: amoeboid and ramified. Amoeboid microglia are an active state of microglia, capable of proliferation, migration, and phagocytosis, while ramified microglia are a quiescent state (Parakalan *et al.*, 2012). In the healthy brain, microglia exhibit a morphology characterised by a small rod-shaped cell soma and numerous symmetrically extended thin ramified processes. Their distribution in the brain is homogeneous. While the microglial cells themselves remain static, their processes are highly motile, control the adjacent environment, and have a repellent effect on the processes of neighbouring microglia (Nimmerjahn *et al.*, 2005).

Microglia also play a role in the postnatal axonal development. Amoeboid microglia or microglia with thick processes accumulate along axonal tracts and exhibit a trophic effect on the neurons of layer V during early postnatal development (Ueno *et al.*, 2013). Both activated and non-activated microglial cells are able to produce various neurotrophic factors (Nakajima *et al.*, 2001). These cells can, however, stimulate not only neuronal survival, but also induce developmental neuronal death (Wakselman *et al.*, 2008). Moreover, microglia are in contact with synapses and play a role in synaptic pruning (Paolicelli *et al.*, 2011) and promote synapse formation in learning through brain-derived neurotrophic factor (BDNF) signalling (Parkhurst *et al.*, 2014).

2.4 NG2 glia

NG2 glia are fourth, newly discovered type of CNS glial cells, present in both grey and white matter. They differ in function, morphology and antigens from other glial cell types and their morphology is different in white and grey matter (Nishiyama *et al.*, 1996).

Glial cells staining with NG2 antibody, that were distinct from astrocytes and oligodendrocytes, were observed in the early 1980s (Stallcup, 1981) and a little later, progenitor cells responsive to A2B5 antigen, which gave rise to oligodendrocytes and type 2 astrocytes (O-2A), were observed (Raff *et al.*, 1983). These two publications describe the same glial type since 95 % of A2B5 positive cells are also positive for NG2 (Stallcup and Beasley, 1987).

NG2 glia are called by several names, based on their properties: NG2 glia based on their typical marker (chondroitin sulphate proteoglycan 4, CSPG4), synantocytes based on

their ability to make synapses with neurons, oligodendrocyte precursor cells (OPC) and O-2A cells based on their differentiation potential and polydendrocytes based on their morphology. These cells make 8-9 % of all white matter cells and 2-3 % of grey matter cells (Dawson *et al.*, 2003).

2.4.1 Morphology of NG2 glia

There are morphological differences between white matter and grey matter NG2 glia. Grey matter NG2 glia resemble astrocytes by their multiple processes extending to all directions, while white matter NG2 glia have elongated somas and processes parallel to the axons (Nishiyama *et al.*, 1996). Distinct morphology of NG2 glia is maintained during cell division, when they divide without retracting their processes, and the division is symmetric (Ge *et al.*, 2009). Typical morphology of these cells is changed after brain injury when processes of NG2 glia become thicker and shorter (Nishiyama *et al.*, 1997). When observed with electron microscope, NG2-labelled cells have pale nuclei with irregular outlines and pale cytoplasm, which distinguishes them from oligodendrocytes and microglia, and can resemble protoplasmic astrocytes. The cell bodies of NG2-labelled cells are irregular, but not as irregular as cell bodies of protoplasmic astrocytes. Chromatin of these cells is dispersed but a thin layer of heterochromatin can be observed beneath the nuclear envelope and this layer is more distinct than that observed in protoplasmic astrocytes. The cytoplasm of NG2-labelled cells contains few cisternae of endoplasmic reticulum that are highly covered by ribosomes, more than those of protoplasmic astrocytes. Another difference from protoplasmic astrocytes is that NG2-labelled cells lack intermediate filaments (Peters, 2004).

2.4.2 Identification of NG2 glia

NG2 glia possess several specific markers that can be used for their identification. One of these markers is CSPG4, also known as NG2 proteoglycan (**Figure 2**), however, this marker is not expressed exclusively by NG2 glia, but also by pericytes in the CNS and cardiomyocytes in smooth muscles of vessels (Ozerdem *et al.*, 2001) and can by transiently expressed by activated macrophages or microglia after induced injury (Bu *et al.*, 2001).

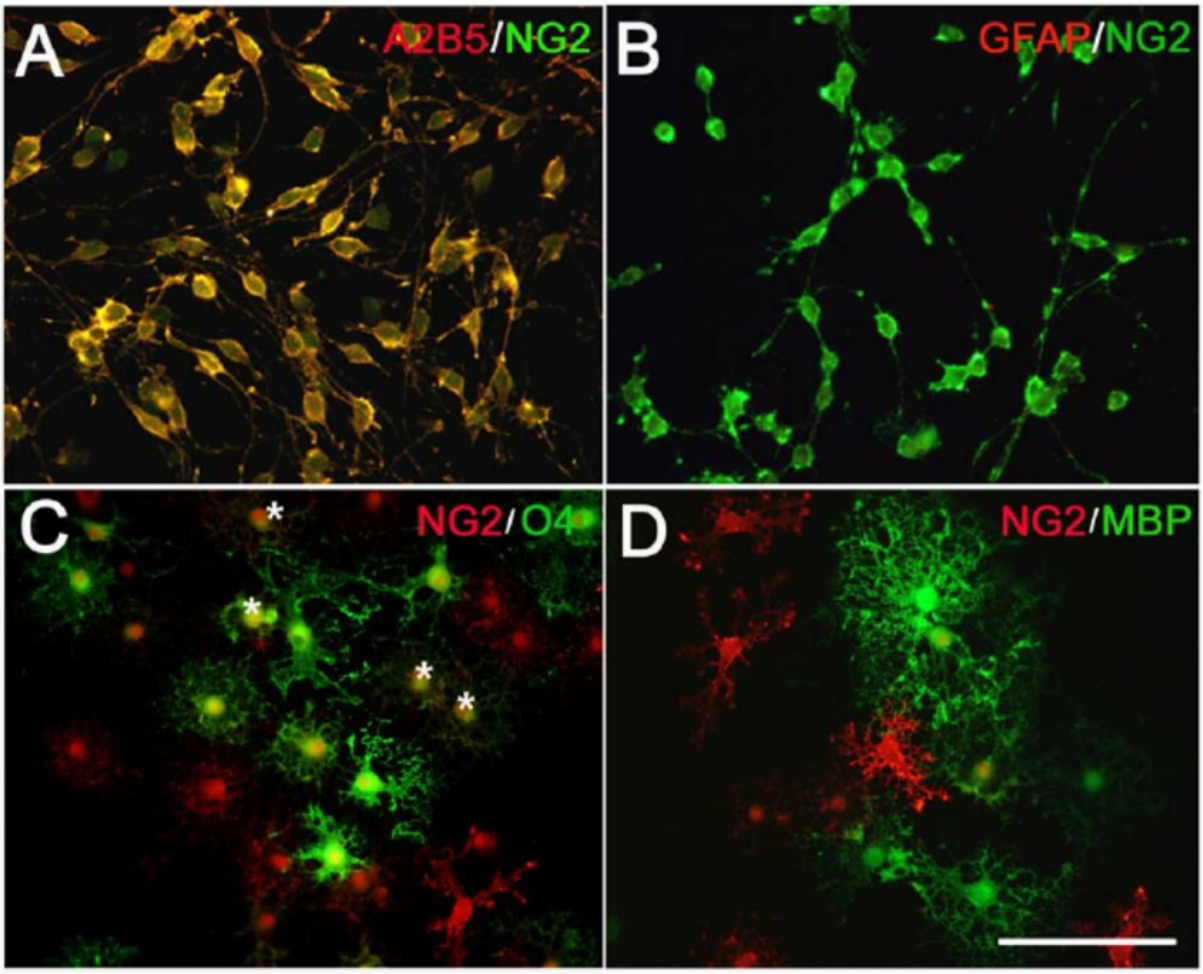

Figure 2: Staining of NG2 glia and co-localization of NG2 proteoglycan with other markers. A: NG2 proteoglycan co-localises with A2B5 antigen. B: GFAP and NG2 do not co-localise. C: Marker of immature oligodendrocytes O4 is sometimes present on NG2 positive cells; co-localization marked by asterisks. D: NG2 and marker of mature oligodendrocytes, MBP, do not co-localise. Taken from (Wang *et al.*, 2011). **Abbreviations**: GFAP - Glial fibrillary acidic protein; NG2 – Nerve/glial antigen 2; MBP – Myelin basic protein.

NG2 proteoglycan in rats is a protein consisting of one long extracellular domain, one transmembrane and one short intracellular domain, with total length of 2325 amino acids. Molecular weight of NG2 proteoglycan is 251 kDa (Nishiyama *et al.*, 1991) and this proteoglycan has multiple functions, such as inducing reorganization of cytoskeleton and cell migration (Fang *et al.*, 1999), binding to and spreading on the collagen VI (Tillet *et al.*, 2002) or modulating long term potentiation (LTP) of *N*-methyl-D-aspartate (NMDA) receptors in communication with neurons (Sakry *et al.*, 2014).

Another widely used marker is α receptor of platelet-derived grow factor (PDGFαR), which can help distinguish NG2 glia from pericytes, since pericytes only express β receptor of platelet-derived grow factor (PDGFβR) (Hart *et al.*, 1989; Lindahl *et al.*, 1997). Cells labelled

with PDGFαR are also NG2 positive (Nishiyama *et al.*, 1996) and PDGFαR co-localizes with markers of immature oligodendrocytes, but not with markers of mature oligodendrocytes (Ellison and de Vellis, 1994). Another antigen used as NG2 glia marker is A2B5 antigen (**Figure 2**). Cells labelled with this antigen are positive for NG2 in 95 % (Stallcup and Beasley, 1987).

Apart from immunolabelling, NG2 glia can be identified by employing transgenic animals, in which the gene for a fluorescent protein (like enhanced green fluorescent protein, EGFP, or yellow fluorescent protein, YFP) is added to the coding sequence of the gene of a specific marker, like *ng2* (Zhu *et al.*, 2008). Another method is the use of Cre recombinase, the gene of which is added to the coding sequence of a specific marker, and which, after expression, induces recombination in a locus with ubiquitous expression, like ROSA26 locus (Rivers *et al.*, 2008).

2.4.3 Function and properties of NG2 glia

NG2 glia exhibit many types of ion channels and neurotransmitter receptors and the activation of those can affect the activity of this cell type. Resting membrane potential (V_M) of NG2 glia is different in grey and white matter. In grey matter V_M reaches values from -70 mV (Kukley *et al.*, 2008) to -90 mV (Clarke *et al.*, 2012), while in white matter it is around -70 mV (Chittajallu *et al.*, 2004). However, the value of V_M can change with age and location. Na^+ channels contribute to this value, permeability for Na^+ ions being three times higher in NG2 glia than in astrocytes (Xie *et al.*, 2007). This was further proved by ribonucleic acid (RNA) sequencing, which found presence of *Nalcn* RNA encoding non-specific Na^+ leak channel (Zhang *et al.*, 2014). Inward rectifying K^+ channels contribute vastly to the value of V_M (Djukic *et al.*, 2007) and it was observed that K_{IR} 4.1 is also participating in communication with neurons, since it is a sensor of K^+ concentration changes caused by neuronal activity (Maldonado *et al.*, 2013). Contribution of chloride ions to V_M is negligible (Xie *et al.*, 2007).

NG2 glia also possess voltage-gated Na^+ channels (De Biase *et al.*, 2010), which can react to depolarization with single spikes (Chittajallu *et al.*, 2004) and these spikes can resemble an action potential, however, they do not meet the criteria normally used to define an AP generation (De Biase *et al.*, 2010).

NG2 glia express many types of K^+ channels, including delayed outwardly rectifying K^+ channel (K_{DR}), A-type K^+ channel (K_A), shaker family K^+ channels, two-pore domain K^+ channels (K2P) and calcium-activated K^+ channels (K_{Ca}) (Zhang *et al.*, 2014). K^+ channels

play an important role in several NG2 glia functions, e.g., their proliferation and cell cycle (Chittajallu *et al.*, 2002; Vautier *et al.*, 2004).

Other voltage gated channels present on NG2 glia are L, T, P/Q and N type Ca^{2+} channels (Zhang *et al.*, 2014). L-type Ca^{2+} channels seem to have a role in NG2 glia differentiation towards mature oligodendrocytes and NG2 glia migration (Paez *et al.*, 2007; Cheli *et al.*, 2015).

NG2 glia form synapses with neurons and can receive both excitatory and inhibitory inputs (Káradóttir *et al.*, 2008). These cells receive glutamatergic synaptic input in various regions of the CNS, such as the hippocampus (Bergles *et al.*, 2000), corpus callosum (Ziskin *et al.*, 2007), cerebral (Chittajallu *et al.*, 2004) and cerebellar cortex (Lin *et al.*, 2005), and are capable of LTP (Ge *et al.*, 2006).

Glutamatergic signalling can affect differentiation of certain subpopulation of NG2 glia towards myelinating oligodendrocytes. Glutamatergic synapses form between demyelinated axons and NG2 glia, and α-amino-3-hydroxy-5-methyl-4-isoxazolepropionic acid (AMPA) receptors play a role in this signalling, however, NMDA receptors take over this role later after the injury (Gautier *et al.*, 2015). Furthermore, activation of NMDA receptors of NG2 glia causes their migration (Xiao *et al.*, 2013) and differentiation to oligodendrocytes (Li *et al.*, 2013). NG2 glia also possess metabotropic glutamatergic receptors that play a role in NG2 glia injury, which is induced by oxygen – glucose deprivation (Deng *et al.*, 2004). This finding suggests a possible role of NG2 glia and their synapses with neurons in ischemic injury.

NG2 glia also receive GABAergic input in several regions, e.g., the hippocampus and neocortex (Kukley *et al.*, 2008; Ge *et al.*, 2009) and these synapses can be maintained after cell division. Activation of $GABA_A$ receptors leads to decreased proliferation and increased differentiation of NG2 glia and helps to ameliorate the effects of hypoxia (Zonouzi *et al.*, 2015). Stimulation of GABA receptors also leads to increased expression of BDNF after ischemic injury. This suggests a role of GABA-induced depolarization of NG2 glia in post-ischemic repair, also supported by behavioural tests (Tanaka *et al.*, 2009).

Moreover, NG2 glia express other types of receptors for neurotransmitters, like cholinergic or purinergic receptors and again, these receptors play a role in regulating their proliferation, differentiation and migration (Othman *et al.*, 2003; Deshmukh *et al.*, 2013). Taken together, we can conclude that NG2 glia synapses with neurons might have roles in physiological as well as pathophysiological states of the CNS.

2.4.4 Development of NG2 glia

First NG2 glia in the developing mouse spinal cord emerge in the ventral ventricular zone at 12.5 days of embryonic age (E12.5) from $Olig2^+$ motor neuron progenitors as migrating cells (Lu *et al.*, 2002). At E13.5, many NG2 glia ($Olig1^+$ $Olig2^+$ OPCs) already migrated out of the ventral ventricular zone. At E14.5, NG2 glia arise in the dorsal ventricular zone (Cai *et al.*, 2005). In the ventral spinal cord, Olig expression is dependent on Sonic hedgehog (Shh) signalling. This morphogen is present in the ventral spinal cord prior to NG2 glia, and these cells do not emerge if the Shh signalling is neutralized (Orentas *et al.*, 1999). In contrast, generation of NG2 glia in the dorsal spinal cord is not affected by the absence of Shh signalling (Cai *et al.*, 2005).

In the mouse brain, NG2 glia arise in three waves from three different neuronal precursors. The first NG2 glia emerge in the medial ganglionic eminence (MGE) and anterior entopeduncular area (AEP), derived from NK2 homeobox 2.1 (Nkx2.1) positive precursors, at E11.5-12.5 and they spread throughout the embryonic telencephalon in a 'ventral-to-dorsal manner'. MGE and AEP regions are main sources of NG2 glia and oligodendrocytes of the embryonic forebrain, but at E16.5 NG2 glia originating from outside of the MGE and AEP regions arise in the embryonic forebrain. However, most of the NG2 cells originating from these areas are later eliminated. The second wave of NG2 glia derived from glutathione synthetase 2 positive precursors emerges in lateral and caudal ganglionic eminence (LGE and CGE). These cells populate the cortex later than MGE and AEP originating cells, but majority of NG2 glia in postnatal telencephalon arises here. Third wave of NG2 glia arises directly from the cortex around birth from empty spiracles homeobox 1 positive precursors and NG2 glia emerging here do not contribute to population of other areas. Cells of oligodendrocyte lineage originating from these areas are functionally equivalent (Kessaris *et al.*, 2006). In the adult brain, NG2 glia can arise in the subventricular zone (SVZ) from the type B cells and migrate to other brain regions (Menn *et al.*, 2006).

3 Differentiation potential of NG2 glia

3.1 Proliferation of NG2 glia

NG2 glia are the major proliferating cell type in the adult rodent brain under physiological conditions. Bromodeoxyuridine (BrdU) incorporation revealed that NG2 glia represent 70 – 75 % of proliferating cells in the cerebral cortex, hippocampus and corpus

callosum, and 1 – 4 % of all $NG2^+$ cells in the observed regions are proliferating NG2 glia. This number decreases with age from 77 % to 38 % in the cerebral cortex (Dawson *et al.*, 2003). Cell cycle time of NG2 glia shows opposite tendency. Cell cycle time is less than two days in early postnatal age (6 days of postnatal age, P6) but increases as the organism gets older to approximately 70 days at P540 in the corpus callosum. In the cortex, cell cycle time increases to 150 days at the same period, cell cycle duration thus depends on brain region and is generally longer in the grey matter (Psachoulia *et al.*, 2009; Young *et al.*, 2013). The duration of cell cycle of NG2 glia is determined by the length of its G1 phase. The length of G1 phase can be a subject to regulation under certain conditions like acute injury (Simon *et al.*, 2011).

By clonal analysis 'StarTrack' it was demonstrated that clone clusters produced from single NG2 glia increase in size with age. In younger animals, NG2 glia give rise to fewer cells, but number of cells derived from one NG2 glia increases with age, growing exponentially between P120 and P240; however, the time needed to double the population increases with age (García-Marqués *et al.*, 2014).

3.2 Differentiation of NG2 glia

3.2.1 Differentiation to oligodendrocytes

One of the first publications concerning NG2 glia described these cells not as $NG2^+$ cells, but as $A2B5^+$ glial progenitors that have capability to give rise to oligodendrocytes and type 2 astrocytes (Raff *et al.*, 1983). Later, it was demonstrated that A2B5 and NG2 can stain the same cells and it was concluded that these cells are indeed NG2 glia (Stallcup and Beasley, 1987). Therefore, NG2 glia are linked to oligodendrocyte lineage since their discovery. To prove such link was a difficult task, because markers of NG2 glia are downregulated in mature oligodendrocytes. However, some cells in the white matter stain weakly for both myelin basic protein (MBP) and NG2 (Nishiyama *et al.*, 1996). Another sign that NG2 glia can differentiate to oligodendrocytes is the co-localization of PDGFαR with markers of immature oligodendrocytes O4 and G_{D3} in tissue slices of the rat brain (Ellison and de Vellis, 1994). Moreover, NG2 glia also express basic helix loop helix transcription factor Olig2, which is required for development of cells of oligodendrocyte lineage and is expressed in oligodendrocyte progenitors (Ligon *et al.*, 2006). The role of NG2 glia in oligodendrocyte lineage was further proved by BrdU labelling. Most of the $BrdU^+$ cells were also positive for NG2, but $NG2^+$ $BrdU^+$ cells declined with age, while number of $BrdU^+$ oligodendrocytes

increased, suggesting differentiation of NG2 glia to oligodendrocytes (Bu *et al.*, 2004). The most recent proof has emerged from *in vivo* fate-mapping experiments in which double transgenic mice expressing Cre recombinase in NG2 glia were employed. Cre recombinase was added under the promoter of the gene encoding NG2 proteoglycan and upon Cre–mediated excision, EGFP was expressed in NG2 cells and cells derived therefrom. This fluorescent protein was expressed in the cells with a typical oligodendrocyte morphology and staining for oligodendrocyte marker adenomatous polyposis coli (APC). EGFP was also present in myelinating processes of the oligodendrocytes (Zhu *et al.*, 2008). Similar method was used with PDGFαR promoter mediated Cre recombinase and YFP in ROSA26 locus and provided similar results. NG2 glia gave rise to cells that no longer expressed PDGFαR, but were positive for mature myelinating oligodendrocyte markers MBP and 2',3'-cyclic-nucleotide 3'-phosphodiesterase (CNP). Differentiation to oligodendrocytes was observed both in the grey and the white matter (Rivers *et al.*, 2008). Generation of oligodendrocytes from NG2 glia and myelination also appears in the adult brain, but the proportion of oligodendrocytes generated from NG2 glia decreases with age (Zhu *et al.*, 2011). After induced demyelinating injury, other cell type capable of giving rise to myelinating oligodendrocytes were neural precursor cells from the SVZ. Myelin created by these cells was thicker compared to that of myelinating oligodendrocytes originating from NG2 glia (Xing *et al.*, 2014). The position of NG2 glia in the oligodendrocyte lineage is summarized in **Figure 3**.

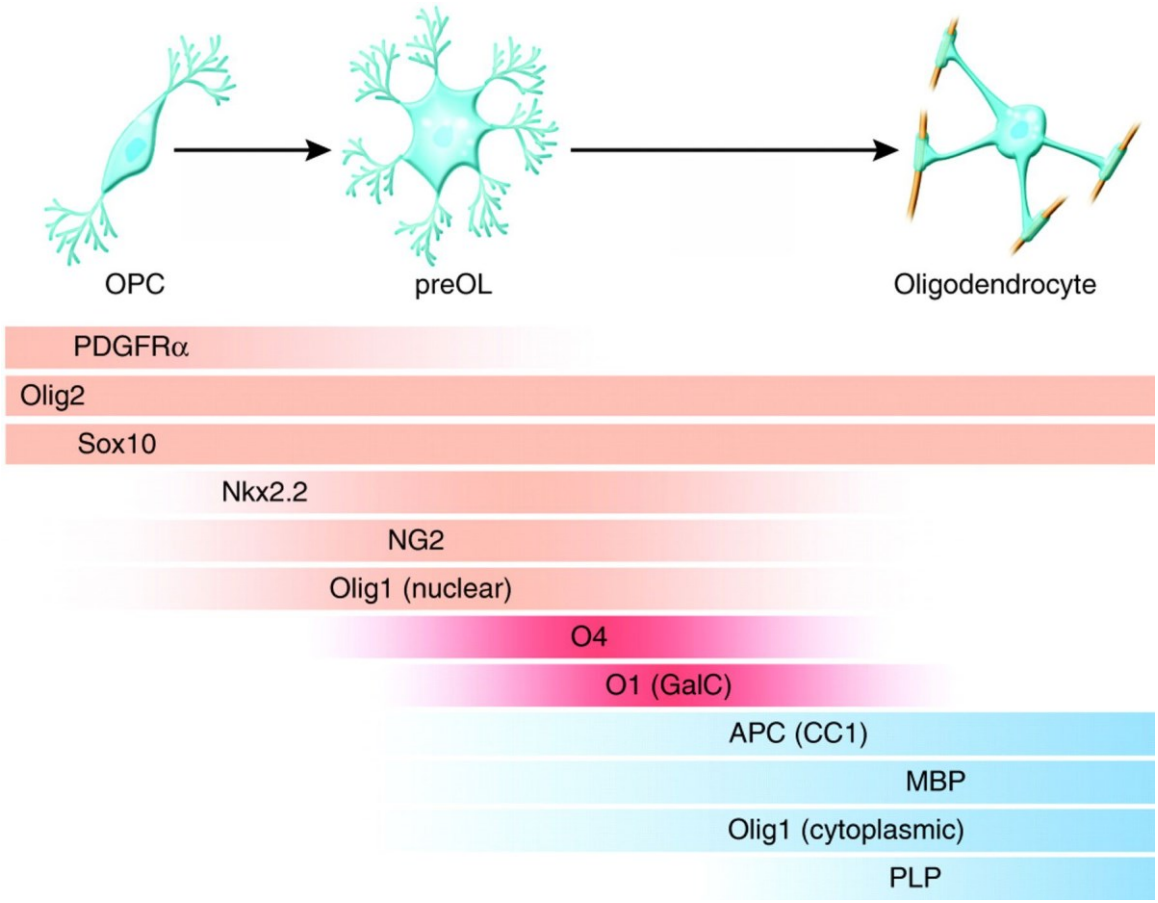

Figure 3: Different markers and their presence in the cells of oligodendrocyte lineage. All cells throughout the lineage are positive for Olig2 and Sox10, while only OPCs and immature oligodendrocytes are positive for NG2, nuclear Olig1, Nkx2.2 and PDGFαR. Immature oligodendrocytes are positive for O4 and O1 and mature oligodendrocytes are positive for APC, MBP, cytoplasmic Olig1 and PLP. Edited from Silbereis *et al.*, 2010. **Abbreviations:** APC – Adenomatous polyposis coli; MBP - Myelin basic protein; NG2 – Nerve/glial antigen 2; Nkx2.2 – NK2 homeobox 2.1; OPC – Oligodendrocyte precursor cell; PDGFRα – Platelet-derived grow factor receptor α; PLP – Proteolipid protein; preOL – Immature oligodendrocyte; Sox10 – Sex region Y related high mobility group box 10.

3.2.2 Differentiation to astrocytes

The question whether NG2 glia can give rise to astrocytes has been asked since their discovery. As mentioned earlier, NG2 glia were also called O-2A progenitors, because they can differentiate to oligodendrocytes and type 2 astrocytes *in vitro*. Differentiation to astrocytes, however, occurred only when progenitor cells were cultured with foetal calf serum (FCS) (Raff *et al.*, 1983). In the organotypic cultures of cerebellar slices isolated from 12 days old mice, NG2 glia started to express GFAP protein after two days of cultivation, suggesting their potential to give rise to astrocytes under such conditions (Leoni *et al.*, 2009). Weak overlap of NG2 positive and GFAP positive cells was also observed in hippocampal slices (Matthias *et al.*, 2003) and in the respiratory network of brainstem slices (Grass *et al.*, 2004).

Fate mapping of cells purified from the perinatal brain showed differentiation of NG2 glia into astrocytes. *In vivo* fate mapping of cells in the brain of P14 old mice revealed that protoplasmic astrocytes in the forebrain grey matter originate from NG2 glia and similar results were observed in P60 mice. In the white matter, differentiation to astrocytes was not observed (Zhu *et al.*, 2008). However, in another fate mapping experiment, no astrocyte production from NG2 glia was observed either in the white or grey matter (Rivers *et al.*, 2008). The difference between these two experiments possibly dwells in employment of transgenic mice with constitutively active Cre recombinase and therefore, the detected differentiation to astrocytes might have occurred only during the embryonic development of the brain (Zhu *et al.*, 2008). This possibility is supported by another fate mapping experiment that follows the fate of NG2 glia both in the embryonic and postnatal mouse brain (Zhu *et al.*, 2011). During development, NG2 glia express Olig2, an essential regulator of oligodendrocyte progenitor, oligodendrocyte and motoneuron development. This regulator is, however, downregulated in astrocytes that differentiated from NG2 glia during development, while it remains expressed in oligodendrocytes. Knockout of Olig2 led to an increase in astrocytes in the dorsal forebrain, but not in the ventral forebrain or the spinal cord. Simultaneously, oligodendrocyte reduction and hypomyelination occurred. Knockout of Olig2 leads to differentiation of NG2 glia also in the early postnatal brain (Zhu *et al.*, 2012). Thus, astrocytes seem to be generated from NG2 glia only during embryonic development.

3.2.3 Differentiation to neurons

Frequently asked question is whether NG2 glia can give rise to neurons. This possibility is tempting, taken that some authors describe that NG2 glia form functional synapses with neurons (Bergles *et al.*, 2000) and have the ability to create single spikes slightly resembling AP generation (De Biase *et al.*, 2010). *In vitro* NG2 glia were observed to give rise to neuronal specific nuclear protein (NeuN) positive neurons that were electrically excitable, so they could generate APs. *In vivo* immunohistochemistry then revealed that some immature neurons in the adult dentate gyrus are $NG2^+$, while mature $NeuN^+$ neurons are not (Belachew *et al.*, 2003). Fate mapping of NG2 glia also addressed this possibility, but showed quite conflicting results. Fate mapping experiments employing transgenic mice with constitutive expression of red fluorescent protein DsRed specifically in NG2 cells (NG2DsRedBac) showed DsRed cells dispersed among $NeuN^+$ neurons, but there was no overlap of these cells in P30 brain. NG2 cells did not differentiate to neurons *in vitro* in neurogenesis supporting medium, which suggests that NG2 glia are not capable of

differentiation to adult neurons in the adult brain (Zhu *et al.*, 2008). This finding is also supported by examination of NG2 glia distribution in the SVZ where NG2 glia are less abundant than in non-neurogenic brain parenchyma and are different from neurogenic cells of the SVZ. Employment of double transgenic mice also showed that NG2 glia in the olfactory bulb do not differentiate to neurons (Komitova *et al.*, 2009), while usage of double transgenic mice with inducible Cre recombinase expression revealed very few NG2 glia-derived neurons. However, this was only observed at P30 and P60 and it was attributed to sporadic neuronal expression of NG2 or Cre in older mice. Employment of other transgenic mice strain did not show this result (Zhu *et al.*, 2011). In contrast to these findings is another fate mapping study, employing double transgenic mice Pdgfra-creER^{T2}/Rosa26-YFP, in which expression of Cre recombinase is inducible by tamoxifen in PDGFαR^{+} cells and leads to the expression of YFP. This study described co-localization of YFP and NeuN in the adult forebrain. These neurons had the appearance of projection neurons and number of these cells increased between 28 and 210 days post tamoxifen injection (Rivers *et al.*, 2008). Another study observed cells positive for both doublecortin (DCX) and NG2 in the cortex, suggesting neurogenesis from NG2 glia. Moreover, usage of transgenic mice showed that NG2 glia differentiate to NeuN^{+} cells in the piriform cortex and accumulation of neurons originating from NG2 glia correlated with a decrease in NG2 glia themselves, suggesting that neurons are continuously generated from NG2 glia in the young adult brain (Guo *et al.*, 2010). Genetic fate mapping using inducible Cre recombinase expression under the NG2 promoter showed that NG2 glia in the hypothalamus give rise to a NeuN^{+} neurons. Identity of these cells was also supported by their electrophysiological properties, identifying them as immature neurons (Robins *et al.*, 2013). Taken together, it seems that neuronal fate of NG2 glia is not yet resolved.

3.2.4 NG2 glia in CNS disorders

NG2 glia respond to various types of CNS injuries. When cortical stab wound was induced, a transient increase in anti-NG2 immunoreactivity appeared, beginning 24 hours after injury and reaching a maximum at 7 days post-lesion. Proliferation of these cells was observed using ^{3}H-thymidine incorporation, which suggests that NG2 glia also belong to reactive cell types responding to injury (Levine, 1994). After spinal cord injury, NG2 glia proliferation was elevated and increased proliferation continued for 4 weeks after injury. However, number of NG2 glia did not increase, suggesting either their cell death or differentiation to another cellular type (McTigue *et al.*, 2001). After the induction of ischemia

followed by reperfusion, number of NG2 glia increased in the peri-infarct area 2 weeks after reperfusion, but decreased in the infarct core (Tanaka *et al.*, 2001). Tracking of nestin positive neural stem cells after ischemia revealed that after occlusion of the middle cerebral artery (MCAO) NG2 glia originating from neural stem/progenitor cells (NS/PCs) were present in the injured area and penumbra (ischemic but viable tissue surrounding the infarct core). However, ischemic injury itself did not induce differentiation towards oligodendrocytes (Li *et al.*, 2010). On the contrary, another group revealed that oligodendrocytes arise from nestin positive NS/PCs after ischemia (Zhang *et al.*, 2012). While NG2 glia in the adult brain striatum decreased after ischemia at 24 hour and 3 days after MCAO, their numbers were elevated in the juvenile brain at the same time interval, suggesting age differences in response to ischemia. Numbers of NG2 glia of both adult and juvenile brain were elevated 7 days post-ischemia, suggesting their ability to respond to the injury by proliferation (Ahrendsen *et al.*, 2016). Moreover, NG2 glia can also react with changes in their morphology. One week after reperfusion, somas of NG2 glia were enlarged and processes stained with increased intensity. Two weeks after reperfusion, soma enlargement was even more striking (Tanaka *et al.*, 2001) and similar changes were observed after cortical stab wound (Levine, 1994). NG2 glia not only proliferate in the lesion, they also extend processes to the lesion site and migrate within several weeks following injury, thus participating on the formation of the glial scar (Hughes *et al.*, 2013).

The role of NG2 glia in the glial scar was elucidated in the spinal cord injury. NG2 glia were found in the glial scar and their association with regenerating axons was inspected. NG2 glia that were also positive for vimentin, were interacting with damaged axons. When co-cultured with dorsal root ganglion neurons, these cells provided a bridge for the neurons, allowing their axons to grow farther (Busch *et al.*, 2010). However, this is in contrast to the finding that NG2 proteoglycan has inhibitory effect on the growth of axons (Dou and Levine, 1994). The same result was obtained with membrane assay that used NG2 glia membranes as a surface for axon growth (Chen *et al.*, 2002), while another study stated that NG2 glia are not inhibitory for growing axons, *in vitro* growth of axons is supported by NG2 glia and alteration of NG2 proteoglycan levels on NG2 glia surface do not alter their supportive role (Yang *et al.*, 2006). NG2 knockout after spinal cord injury revealed that the presence of NG2 glia in the glial scar is necessary for axon stabilization. *In vitro* observation also confirmed that axons seem to grow preferentially on the surface of $NG2^{+}$ cells, but laminin and fibronectin, molecules that are present on the surface of the NG2 glia, also play a role in axon growth

(Filous *et al.*, 2014). Together, these findings indicate that it is not yet clear whether the presence of NG2 glia in the glial scar helps or inhibits axon growth after injury.

As mentioned before, NG2 glia exhibit high differentiation potential in the healthy and developing brain. Their differentiation potential was also inspected after cortical stab wound. Fate mapping of NG2 glia revealed that predominantly, oligodendrogenesis occurs after injury and only small portion of NG2 glia give rise to cells that exhibit weak GFAP expression, however these cells are morphologically distinct from reactive astrocytes (Komitova *et al.*, 2011). In contrast to this, another study describes differentiation of NG2 glia 7 days after MCAO to cells that are positive for GFAP and morphologically resemble reactive astrocytes. Surprisingly, also differentiation to cells positive for marker of neuronal precursors and immature neurons, DCX, was observed 7 days after MCAO (Honsa *et al.*, 2012). Differentiation of NG2 glia after injury is therefore not clearly resolved and needs further investigation.

4 Ischemia

4.1 Ischemia and other types of brain damage

In 2015, stroke was the second leading cause of death worldwide, according to World Health Organization statistics, with over 6 million (WHO.Int., 2016). Stroke is caused either by disruption of cerebral blood flow (cerebral ischemia or ischemic stroke) or by intracerebral bleeding (haemorrhagic stroke). In the United States, ischemic stroke accounts for 87 % of occurring strokes, while haemorrhagic stroke accounts for the rest. Ischemia is defined as a reduction in blood flow that is sufficient to alter normal functions of cells. Brain tissue is especially sensitive to ischemia, even brief ischemic periods can lead to serious damage and cellular death (reviewed in Woodruff et al. 2011). Ischemic stroke is a result of a reduction of cerebral blood flow, either transient or permanent, and it is usually caused by the occlusion of a cerebral artery by an embolus or local thrombosis. Ischemia then leads to a sequence of pathophysiological events, such as excitotoxicity, peri-infarct depolarization, inflammation and cellular death (reviewed in Dirnagl et al. 1999).

Disruption of blood flow leads to deficit of glucose and oxygen and thus to impairment of cellular energetic metabolism. Under these conditions, oxidative phosphorylation and ATP production are weakened, causing damage to energetics required for maintenance of ionic gradients, ultimately leading to loss of membrane potential and depolarization of glia and neurons (Martin *et al.*, 1994). This also affects processes that

participate in glutamate homeostasis maintenance at synapses, and thus ionotropic and metabotropic glutamate receptors are being activated, leading to increased intracellular concentrations of Ca^{2+}. Glutamate overactivation also leads to influx of Na^{+} and Cl^{-}, which is followed by passive influx of water and oedema formation (Dirnagl *et al.*, 1999). High intracellular concentrations of Ca^{2+} lead to activation of phospholipase A_2 and cyclooxygenase, which induces production of reactive oxygen species (ROS). They can react with deoxyribonucleic acid (DNA), proteins and lipids, leading to membrane damage, lipid peroxidation and varying degrees of dysfunction. ROS play an important role in ischemic damage, since treatment with scavengers, even when applied with a delay, can be effective in focal cerebral ischemia (Folbergrova *et al.*, 1995). Mitochondria represent one of the main targets of ROS. Radicals can induce disruption of the inner mitochondrial membrane and damage the oxidation of proteins mediating electron transport and ATP production. Mitochondrial membrane becomes leaky, they swell and pro-apoptotic cytochrome c is released (Fujimura *et al.*, 1998; Kristián and Siesjö, 1998). On the other hand, oxidative stress may have a beneficial effect through the activation of neuroprotective transcription factors, such as nuclear factor-κB (NFκB) or hypoxia-inducible factor 1 (HIF1) (Rothwell and Hopkins, 1995). Increased levels of intracellular Ca^{2+} also lead to activation of neuronal nitric oxide synthase (nNOS), which produces nitric oxide (NO) from L-arginine. NO then reacts with superoxide to form peroxynitrite, which belongs to highly reactive species causing tissue damage. However, increased NO production can lead to improvement of microvascular flow in the early stages of ischemia, and so it also has a beneficial effect (reviewed in Iadecola, 1997).

In the ischemic core, depolarization of the cells is permanent, while in the penumbra, cells can repolarize. Repetitive depolarization can occur in response to increased K^{+} and glutamate levels in the extracellular space. This process is called peri-infarct depolarization or repetitive depolarization (Hossmann, 1996). These depolarizations have a damaging effect on the cells and with increasing number of depolarizations, infarct size grows (Dijkhuizen *et al.*, 1999).

Processes occurring after ischemic stroke, like an increase in ROS or hypoxia, trigger the expression of various proinflammatory genes by inducing synthesis of transcription factors, e.g. NFκB or HIF1 (O'Neill and Kaltschmidt, 1997; Ruscher *et al.*, 1998). This leads to a production of mediators of inflammation, such as tumour necrosis factor α (TNFα) and interleukin 1β (IL-1β) (Rothwell and Hopkins, 1995). Glial cells, especially microglia, but also astrocytes, play an important role in the process of inflammation, producing various

proinflammatory cytokines and neuroprotective factors, but also toxic metabolites and enzymes (del Zoppo *et al.*, 2007; Gelderblom *et al.*, 2009). The blood brain barrier, responsible for separation of circulating blood from the brain and its extracellular fluid, is also damaged after ischemic stroke. Its permeability is increased, and barrier function diminished; moreover, the basal lamina of the vessels is being degraded. Due to loosening of the tight junctions, increased permeability occurs for fluids and plasma elements as large as 360 kDa (del Zoppo and Hallenbeck, 2000). Days to weeks after ischemic stroke, leukocytes respond to injury, infiltrate the CNS by binding to adhesion molecules on the endothelial cells. Leukocytes release inflammatory cytokines such as TNFα, IL-1β and interleukin 6 (IL-6) and their adhesion to the endothelium can reduce the flow of erythrocytes through the microvasculature, release proteases, ROS and lead to further impairment (Kim *et al.*, 2016).

Another important process following CNS injuries is formation of the glial scar. The glial scar is a structure that develops and changes in time, consisting of different cells at different times. Macrophages and activated microglia appear within hours after the injury and few days after the injury, NG2 glia emerge from the surrounding tissue, reaching peak at 7 days. Permanent glial scar consists mainly of astrocytes and those situated close to the lesion express markers of proliferation (vimentin and nestin). The glial scar also contains microglia and several oligodendrocytes that have survived neurodegeneration and myelin damage (reviewed in Fawcett and Asher, 1999). Glial scar formation is a common process that occurs not only in experimental animal models of CNS injuries, but also in humans (Huang *et al.*, 2014).

4.2 Animal models of ischemic stroke

Animal models of stroke are a key tool in understanding stroke and their usage can potentially lead to a development of a better medical approach to ischemic stroke in humans. Human ischemic stroke is very diverse in manifestation, localization and causes, while an experimental stroke is reproducible and standardized. Investigations of stroke also require invasive methods that damage brain tissue. *In vitro* models are not suitable since perfusion and microvasculature, important factors in stroke, cannot be modelled *in vitro* and must be examined in a living organism (reviewed in Fluri *et al.*, 2015). Both large and small animals can be employed as ischemic stroke models. The advantages of using large animals, like dogs, cats or monkeys, is that new regional imaging techniques and measurements of regional cerebral blood flow and metabolism are easier to perform on large animals. Moreover, they are gyrencephalic, like humans. However, large animals are very costly, manipulation is

harder and infarct size is very variable. Small animal models, especially mice and rats, are cheaper to maintain, genetically homogenous and genetic modifications can be easily made. However, brains of these animals are not gyrencephalic and some methods, like physiological monitoring and concurrent measurements over time, are difficult or sometimes impossible to perform on them (Traystman, 2003). Models of cerebral ischemia can be either global or focal.

Global cerebral ischemia is characterised by lack of blood flow to all areas of the brain. In humans, global ischemia occurs after cardiac arrest or asphyxia (Woodruff *et al.*, 2011). One of the easiest methods to achieve global cerebral ischemia without reperfusion is decapitation (Lowry *et al.*, 1964). Frequent methods of global ischemia are four vessel occlusion in the rat, two vessel occlusion combined with hypotension in the rat, two vessel occlusion in the gerbil, and two vessel occlusion in the mouse (Woodruff *et al.*, 2011).

Focal cerebral ischemia (FCI) can be either transient or permanent. Blood flow in FCI is usually higher than in global cerebral ischemia and there is significant gradation of ischemia from the core to its outer boundaries. FCI is usually performed by MCAO, because it is a common case of stroke in humans (Woodruff *et al.*, 2011).

To achieve temporary occlusion, a nylon structure can be inserted into the carotid artery, past the branching of the MCA. However, properties of the nylon filament can influence variability of the outcome. To improve this method, paraffin-coated nylon can be used. After the occlusion period, nylon is removed and reperfusion takes place (Zuo *et al.*, 2012).

For permanent MCAO, the MCA can be surgically approached and electrocoagulated (Taguchi *et al.*, 2010). A model with close resemblance to the human ischemic stroke is the thromboembolic model. The formation of the blood cloth can be triggered using murine thrombin (Orset *et al.*, 2007), or the blood cloth can be injected to the common carotid artery directly, or via a retrograde catheter placed in an external carotid artery (Kaneko *et al.*, 1985).

5 Morphogens

Morphogens, such as Shhs and Wnts are defined as substances that influence development of organisms. They form a gradient of concentration and through this gradient they instruct cells about their location. This leads to formation of complex patterns of gene expression and spatial position of cells. However, morphogens also play a role in the adult brain, where their signalization also occurs (reviewed in Lai *et al.*, 2003; Jagasia *et al.*, 2006).

5.1 Sonic hedgehog signalling

Sonic hedgehog belongs to the family of Hedgehog morphogens with other homologues of Drosophila gene hedgehog. The Shh signalling pathway is a major pathway in developmental processes. Shh protein is synthetized as a 45 kDa precursor, but this protein needs to undergo several modifications before taking its function. This includes proteolysis, addition of a cholesterol moiety and palmitoylation. These modifications improve functionality of Shh. Activation of the Shh signalling pathway requires binding of Shh to the receptor complex consisting of Patched receptor (Ptch) and Smoothened receptor (Smo). Activation of this receptor complex by binding of Shh to Ptch then leads to downstream signalization. When Shh binds to Ptch, Smo is stabilized and activated. Smo is a Class Frizzled G protein-coupled receptor and induces downstream signalling through regulation of several protein kinases that activate transcription factors (TFs) cubitus interruptus proteins (Ci) and glioblastoma proteins (Gli 1-3), inducing transcription changes (**Figure 4**; reviewed in Choudhry *et al.*, 2014).

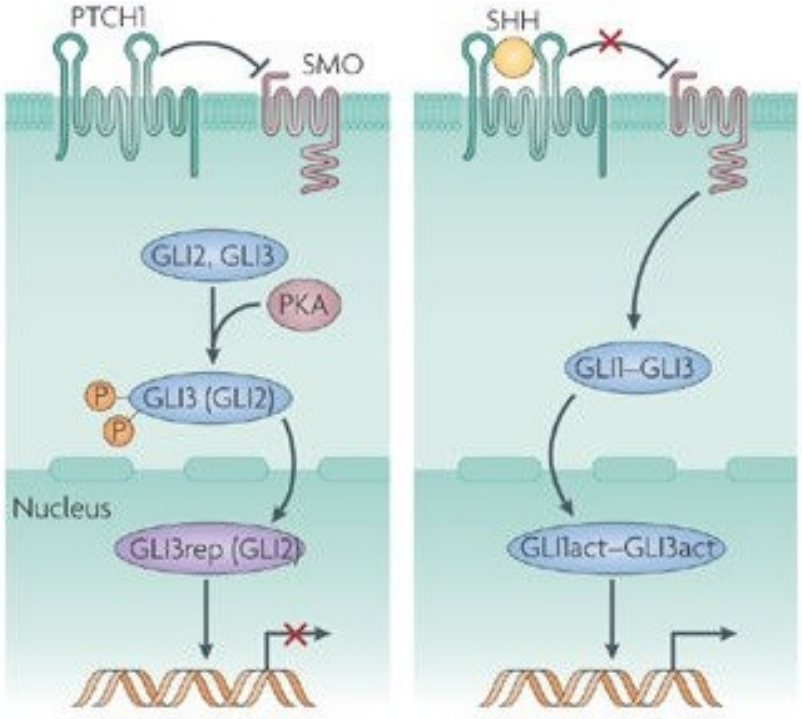

Figure 4: Overview of the Shh signalling pathway. (left) In the absence of Shh, Ptch inhibits Smo and transcription factors (TFs) Gli are phosphorylated and thus, they do not activate transcription of the target genes. (right) In the presence of Shh, inhibition of Smo by Ptch is released,TFs Gli are not phosphorylated and they can activate transcription of the target genes in the nucleus. Edited from (Crompton *et al.*, 2007). **Abbreviations**: Gli – Glioblastoma protein; PKA – Protein kinase A; PTCH – Patched receptor; SHH – Sonic hedgehog; SMO – Smoothened receptor.

In development, Shh plays a major role in definition of neural fates in the ventral CNS along the anterior-posterior axis. Signalling by a Shh gradient leads to the expression of a set of homeodomain proteins divided in two classes. Class I proteins are synthetized by neuronal progenitors in the absence of Shh, while class II proteins are produced upon exposure to Shh. This creates five progenitor domains in the ventral neural tube, defined by the levels of TFs induced by Shh. Moreover, Shh expression is high in the regions, where oligodendrocyte precursors arise during development and Shh is both sufficient and necessary for specification of oligodendrocyte precursors in the mouse spinal cord and forebrain. Shh also seems to play a role in the dorsal CNS, because Shh synthesis appears in these regions during late development and adulthood and functions as a mitogenic signal to expand the granule cell progenitor population in the outer part of the external germinal layer (reviewed in Martí and Bovolenta, 2002).

In the adult brain, Shh also plays an important role. Long-term fate mapping revealed that this morphogen can influence proliferation of neural stem cells in the SVZ and the subgranular zone (SGZ), two main regions of neurogenesis in the adult brain (Ahn and Joyner, 2005). *In vitro*, Shh was observed to affect NS/PCs. A decrease in incidence of cells with neuronal current pattern and promotion of proliferation were observed in the Shh transduced cells (Prajerova *et al.*, 2010). Administration of Shh leads to higher differentiation of NG2 glia to astrocytes, while blocking the Shh signalling pathway lowers the differentiation of NG2 glia to astrocytes after ischemia (Honsa *et al.*, 2016).

5.2 Wingless/Int signalling

Wnt molecules are named after Drosophila segment polarity gene *wingless* and vertebrate homologue *integrated*. These proteins regulate a large scale of cellular processes in development, including cell fate determination, primary axis formation, and organogenesis and play a key role in embryogenesis. Wnt ligands are cysteine-rich glycoproteins that are approximately 350-400 amino acids long. In mammals there are 19 different Wnt ligands. Wnt ligands need to be modified before they take place in signalling, for example Wnt3a is N-glycosylated, which is required for its secretion, then undergoes lipid modifications consisting of the addition of palmitate and palmitoleoyl. Receptors responsible for Wnt signalling are Frizzled (Frz) family receptors. These receptors are topologically homologous with G-protein coupled receptors and have 7 transmembrane domains. However, in addition to Frz receptors, co-receptors are needed; for example, low density lipoprotein related protein 5 and 6 (LRP5/6) is required for the canonical Wnt signalling pathway. There are three main Wnt

signalling pathways: canonical, planar cell polarity and Wnt/Ca^{2+} pathway (reviewed in Komiya and Habas, 2008; MacDonald *et al.*, 2009).

5.2.1 The canonical Wnt signalling pathway

The key element of the canonical Wnt signalling pathway is β-catenin, a molecule that can influence gene transcription and cell adhesion (Logan and Nusse, 2004; Nager *et al.*, 2012). The canonical Wnt signalling pathway begins with binding Wnt ligand to Frz receptor, which is required for multiple Wnt signalling pathways, and LRP5/6 receptor, which is specifically required for β-catenin signalling pathway (He *et al.*, 2004). The essence of canonical Wnt signalling is regulation of β-catenin degradation, which is triggered by β-catenin phosphorylation by glutamine synthase kinase 3 (GSK3) and casein kinase 1α (CK1α), leading to ubiquitination. Interactions of β-catenin, GSK3 and CK1α are supported and coordinated by scaffolding protein Axin, which also interacts with APC, another protein capable of binding β-catenin. Binding of Wnt ligand to its receptors prevents the phosphorylation and degradation of β-catenin through Dishevelled (Dsh) protein, which causes a disruption of the β-catenin degradation complex. Stabilization of β-catenin leads to increased levels of this protein in the cell nucleus, where, in cooperation with DNA-binding transcription factors T-cell factor/lymphoid enhancer factor (TCF/LEF), it induces gene expression (**Figure 5**; reviewed in MacDonald *et al.*, 2009).

The canonical Wnt signalling pathway can be inhibited by several different classes of molecules. Dickkopf 1 (Dkk1) molecule has the capability to inhibit Wnt signalling without interacting with Wnt ligands of Frz receptor. Inhibition of Wnt signalling is achieved by binding to LRP6 co-receptor and disrupting formation of Frz-LRP6 receptor complex. This inhibition is considered specific for canonical Wnt signalling pathway (Semënov *et al.*, 2001). Sclerostin also inhibits canonical Wnt signalling pathway in this way (Semënov *et al.*, 2005). Another way to inhibit Wnt signalling is by binding to Wnt ligands. This mechanism is used by Wnt inhibitory factors (WIFs) like WIF1, which binds to *Xenopus* XWnt8 and *Drosophila* Wg. Wnt antagonist Cerberus acts in similar way. Secreted Frizzled related proteins also inhibit Wnt signalling by binding to Wnt ligands, however, this mechanism of inhibition is not specific for canonical Wnt signalling pathway (Kawano and Kypta, 2003).

5.2.2 The planar cell polarity pathway

The noncanonical planar cell polarity Wnt signalling pathway begins by activation of Frz receptor. Co-receptors functioning in this pathway are not clearly defined, but presumably

neurotrophin receptor homolog 1, receptor-like tyrosine kinase (Ryk), protein tyrosine kinase and receptor tyrosine kinase-like orphan receptor 2 (ROR2) can take on this role. The signal is then transduced to Dsh, where the pathway divides. Small guanosine triphosphate (GTP) hydrolases (GTPases) Rho and Rac are activated through two domains of Dsh. Rho GTPase is activated through activation of dishevelled associated activator of morphogenesis 1 (Daam1) protein that interacts with Dsh. Rho then activates Rho-associated kinase and myosin, which triggers modification of the actin cytoskeleton. Daam1 also activates Profilin, actin binding protein that can also cause cytoskeletal changes. Rac GTPase activation requires DEP domain of Dsh and leads to activation of c-Jun N-terminal kinase (JNK)(**Figure 5**; Komiya and Habas, 2008; Sugimura and Li, 2010).

5.2.3 Wnt/Ca^{2+} pathway

Some Wnt ligands (e.g. Wnt5a) can induce intracellular Ca^{2+} release without affecting β-catenin stabilization. This leads to activation of protein kinase C (PKC) and Ca^{2+}/calmodulin-dependent protein kinase II (CamKII) (Kühl *et al.*, 2000). CamKII can influence diverse transcription factors and kinases (**Figure 5**), such as nuclear factor of activated T-cells (NFAT) or Nemo-like kinase (NLK), to influence processes in the cell (Komiya and Habas, 2008).

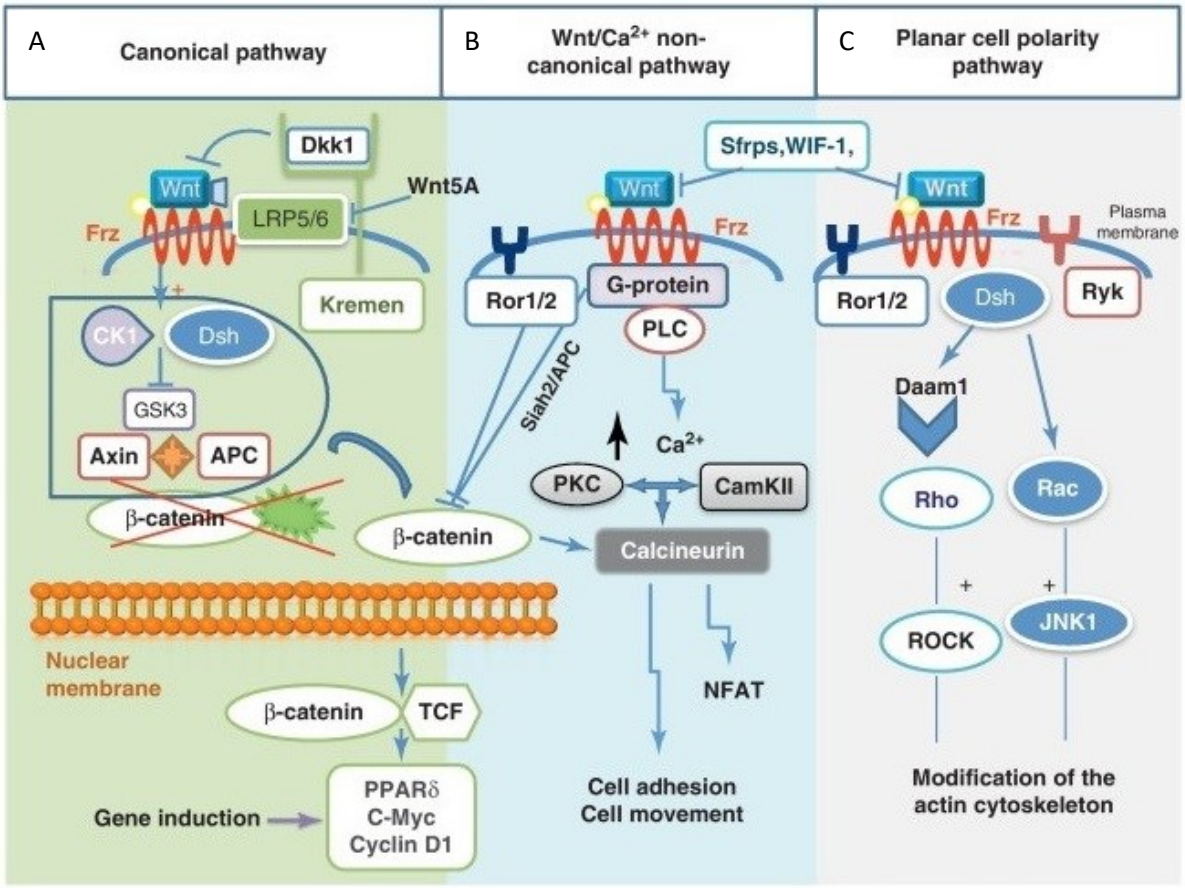

Figure 5: Overview of Wnt signalling pathways. A: The canonical Wnt signalling pathway starts with binding of Wnt ligand to Frz receptor and LRP5/6 co-receptor. Wnt ligands can be inhibited by Dkk1, LRP5/6 can be inhibited by Wnt5A. Binding of a Wnt ligand leads to activation of Dsh and CK1, which causes inhibition of the molecules of the degradation complex (GSK3, Axin and APC). Thus β-catenin is not marked for degradation and can induce transcription of Wnt signalling target genes by binding to TCF TF. B: The Wnt/Ca^{2+} pathway begins with binding of a Wnt ligand to Frz receptor, which leads to G-protein mediated activation of PLC. PLC causes an increase in intracellular concentration of Ca^{2+}, which activates PKC and CamKII. Through these proteins, signalling is transmitted to other kinases or transcription factors and cell function is regulated. C: Planar cell polarity pathway starts with binding of a Wnt ligand to Frz. This activates Dsh, which leads to activation of JNK through Rac. This pathway also activates Rho GTPase through Daam1, which activates ROCK. Edited from (Marinou *et al.*, 2012). **Abbreviations**: APC – Adenomatous polyposis coli; CamK – Ca^{2+}/calmodulin-dependent protein kinase II; CK1 – Casein kinase 1; C-Myc – Myelocytomatosis cellular oncogene; Daam – Dishevelled associated activator of morphogenesis ; Dkk1 – Dickkopf 1; Dsh – Dishevelled; Frz – Frizzled; GSK3 – Glutamine synthase kinase 3; JNK – c-Jun N-terminal kinase; Lrp5/6 – Low density lipoprotein related protein 5 and 6; NFAT – Nuclear factor of activated T-cells; PKC – Protein kinase C; PLC – Phospholipase C; PPAR – peroxisome proliferator-activated receptor; ROCK – Rho associated kinase; ROR – receptor tyrosine kinase-like orphan receptor; Ryk – Receptor-like tyrosine kinase; Sfrp – Secreted frizzled-related protein; TF – Transcription factor; TCF – T-cell factor; WIF – Wnt inhibitory factors; Wnt – Wingless/Int.

5.2.4 The role of Wnt signalling

Wnt signalling plays a major role in early development. The expression of genes for several Wnt ligands is observable in the primitive streak from the onset of gastrulation. Wnt3 is a part of signalling network that regulates gastrulation and formation of anterior-posterior axis. Wnt signalling is required for proper posterior patterning and must be supressed anteriorly for proper patterning of anterior epiblast. After gastrulation, Wnt3 is downregulated, but Wnt signalling remains active in the primitive streak and its derivative, tail bud, and is required for maintenance and function of the primitive streak. Determination of left-right axis is also influenced by Wnt signalling. Non-canonical Wnt signalling has an effect on neural tube closure and formation of limbs (reviewed in Wang *et al.*, 2012).

Apart from its developmental functions, Wnt signalling also influences various processes in the adult CNS. Investigation of β-catenin target genes in the thalamus revealed that in thalamic neurons, genes for GABA receptor, calretinin and two ion channels are regulated by this molecule. These proteins participate in modulating neuronal excitability and thus Wnt signalling can have an influence activity in thalamocortical circuit (Wisniewska *et al.*, 2012). In hippocampal neurons, some effect of Wnt signalling on electrophysiological properties is also observable. Applications of Wnt5a produced a dose-dependent increase in field excitatory postsynaptic potential (fEPSP), which is probably linked to activation of the Wnt/Ca^{2+} pathway. Similarly, glutamatergic transmission in cultured hippocampal neurons is affected by Wnt5a signalling (Varela-Nallar *et al.*, 2010). Furthermore, the Wnt/Ca^{2+} pathway in hippocampal neurons influences the insertion and clustering of $GABA_A$ receptors and induces rapid recycling of $GABA_A$ receptors (Cuitino *et al.*, 2010). In glial cells, Wnt3a application increases expression of BDNF, suggesting a role of Wnt signalling in modulating synaptic plasticity (Yi *et al.*, 2012). Moreover, Wnt signalling seems to play a role in regulating adult hippocampal neurogenesis by affecting both maintenance and differentiation of progenitor cells (Lie *et al.*, 2005; Wexler *et al.*, 2009). Application of Wnt7a to neonatal NS/PCs resulted in increased number of cells expressing neuronal markers and decreased gliogenesis (Prajerova *et al.*, 2010). Genetic modification of Wnt signalling in neonatal NP/SCs resulted in increased expression of neuronal marker β III tubulin and decreased expression of astrocytic marker GFAP in the case of activation of the pathway, while in the case of its suppression, incidence of GFAP positive cells increased (Kriska *et al.*, 2016).

Activity of Wnt signalling pathway has also an impact on NG2 glia. Anti-inflammatory drug Aspirin can inhibit the Wnt signalling pathway by increasing

β-catenin phosphorylation and, subsequently, its degradation, which results in an increase in the number of oligodendrocytes observed *in vitro* as well as *in vivo* (Huang *et al.*, 2016). An increase in Wnt signalling through the β-catenin pathway in NG2 glia was observed after SCI. Inhibition of β-catenin signalling reduces NG2 glia proliferation and accumulation of these cells in the tissue around the injury. Moreover, inflammation and reactive astrogliosis is decreased in response to inhibition of the canonical Wnt signalling pathway. In contrast, stimulation of the Wnt signalling pathway leads to increased NG2 glia proliferation. Reducing of β-catenin signalling in NG2 glia after optic nerve crush injury leads to higher permeability to axons (Rodriguez *et al.*, 2014).

6 Methods

6.1 Transgenic animals

All procedures involving the use of laboratory mice were performed in accordance with the European Communities Council Directive 24 November 1986 (86/609/EEC) and animal care guidelines approved by the Institute of Experimental Medicine, Academy of Sciences of the Czech Republic (Animal Care Committee; approval numbers 146/2013, 91/2016, 62/2017).

We used transgenic mouse strains that allowed us to visualize NG2 glia and cells that arise from them and manipulate the Wnt signalling pathway in mouse brains. To achieve this, we crossbred CSPG4-CreER^{T2} strain with Rosa26-tdTomato strain, which allowed us to visualize NG2 glia and their offspring due to expression of tdTomato fluorescent protein, with Rosa26-Dkk1 or Catnb$^{lox(ex3)}$ mice, which enabled us to manipulate the Wnt signalling pathway. This resulted in the following mouse strains CSPG4-CreERT2/Rosa26-tdTomato-Dkk1 (further referred to as Dkk1), and CSPG4-CreERT2/Rosa26-tdTomato/Catnb$^{lox(ex3)}$ (further referred to as Ex3). Rosa26-Dkk1 mice (Wu *et al.*, 2008) can produce Wnt pathway inhibitor Dkk1 upon Cre-mediated excision of transcriptional blocker. Catnb$^{lox(ex3)}$ mice (Harada *et al.*, 1999) allow to delete the sequence of β-catenin gene encoding the part of the protein that can be marked to induce degradation of the protein, therefore Cre-mediated excision of this sequence leads to stabilization of β-catenin protein and hyper-activation of Wnt signalling pathway. To induce recombination, tamoxifen dissolved in corn oil (20 mg/ml) was administered intraperitoneally in two doses (10 μl/g of body mass) at P59-69.

6.2 Middle cerebral artery occlusion

Focal cerebral ischemia was induced at P75-85 by MCAO. Mice were anesthetized with 1.5% isoflurane (Abbot, IL, USA) and maintained in 1% isoflurane using a vaporizer (Tec-3, Cyprane Ltd., UK?). Skin was cut between the orbit and the external auditory meatus. A hole with 1-2 mm in diameter was drilled through the frontal bone ~-1.5 mm from bregma and 3.5 mm ventral to the dorsal surface of the brain. Dura mater was opened and gently removed. The MCA was then occluded by a short coagulation induced by bipolar tweezers (SMT, Czech Republic) at a proximal location, followed by transection of the vessel to ensure permanent occlusion. To maintain the body temperature at 37 ± 1 °C, heating pad was used. For visualization of ischemic region, we used 2% 2,3,5-Triphenyltetrazolium chloride (TTC) at 37°C for 20 minutes. The MCAO model results in an infarct localized only in the cortical region (**Figure 6**). After the surgery, the animals were treated with antibiotics and analgesics

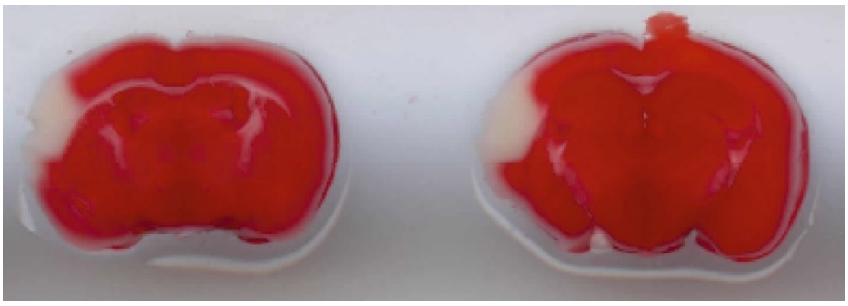

Figure 6: 2,3,5-Triphenyltetrazolium chloride staining of the injured mouse brains. White region represents cortical area damaged by ischemia induced by middle cerebral artery occlusion.

6.3 Cell culture preparation

Cells for cultures were isolated from adult transgenic mouse brains. Mice were anesthetized using pentobarbital (PTB, 100 mg/kg, i.p.; Sigma-Aldrich, St. Louis, MO, USA) and then transcardially perfused with 4 °C artificial cerebrospinal fluid containing (in mM): 110 NMDG-Cl, 2.5 KCl ,24.5 $NaHCO_3$, 1.25 Na_2HPO_4, 0.5 $CaCl_2$, 7 $MgCl_2$ and 20 glucose, osmolality 290 ± 3 mOsmol/kg, after decapitation. Brains were quickly dissected out and sliced. The neocortex from unoperated mice or the ischemic hemisphere of operated mice (ipsilateral to the site of MCAO) was then cut out and mechanically dissociated with a razor. Tissue was then dissociated chemically in 1 ml of papain (20U/ml) and 50 µl DNAse (Worthington, Lakewood, NJ) for 40 minutes at 37 °C. After dissociation, papain was inhibited with 1 ml of trypsin inhibitor (Sigma-Aldrich, St. Louis, MO, USA) and cells were centrifuged at 1020×g for 3 minutes, while 100 µl of the cell suspension was used to count cells in the hemocytometer. Pellet was resuspended in 1 ml of isolation medium containing

advanced Dulbecco's Modified Eagle Medium/Nutrient Mixture F-12 (DMEM/F12) (Life Technologies, Carlsbad, CA, USA) supplemented with Penicillin-Streptomycin-Amphotericin B solution (PSA) (10 µl/ml; Sigma-Aldrich, St. Louis, MO, USA), foetal bovine serum (150 µl/ml; HyClone, GE Healthcare Life Sciences, UK), glutamine (5 µl/ml; Sigma-Aldrich, St. Louis, MO, USA) and PDGFα (0.2 µl/ml, PeproTech, Rocky Hill, NJ, USA). Cells were placed in a 24-well plate on poly-L-lysine (PLL; Sigma-Aldrich, St. Louis, MO, USA) coated coverslips, cell density being $6*10^4$ cells/well, and cultivated at 37 °C and 5 % CO_2. After one day of cultivation, the medium was exchanged for differentiation medium containing DMEM supplemented with PSA (10 µl/ml), B27 (20 µl/ml; Life Technologies, Waltham, MA, USA), glutamine (5 µl/ml; Sigma-Aldrich, St. Louis, MO, USA) and PDGFα (0.2 µl/ml). After two days, differentiation medium was exchanged and next two days patch-clamp recordings were performed.

6.4 Immunocytochemistry

Primary cultures attached to PLL-coated coverslips were fixed in 4% paraformaldehyde solution in 0.2 M phosphate buffer (PB) (pH 7.4) for 9 minutes and kept in 10 mM phosphate-buffered saline (PBS) at 4°C for further processing. The coverslips were incubated in a blocking solution containing 5% Chemiblocker (Millipore, Billerica, MA, USA), and 0.5% Triton X-100 (Sigma-Aldrich, St. Louis, MO, USA) in 10 mM PBS, at 4°C for 2 hours. Next, they were incubated overnight at 4°C with primary antibodies in PBS, containing 0.2% Triton X-100. After the overnight incubation, three 10-minute washes with PBS were performed, followed by incubation with secondary antibodies for two hours at 4°C. The following primary antibodies were used: GFAP (1:800, Sigma-Aldrich, St. Louis, MO, USA), DCX (1:1000; Abcam, Cambridge, UK), microtubule-associated protein 2 (MAP2) (1:800; Merck Millipore, Billerica, MA, USA), NG2 (1:400; Merck Millipore, Billerica, MA, USA), PDGFαR (1:200; Santa Cruz, Dallas, TX, USA). Secondary antibodies were goat anti-mouse/rabbit IgG conjugated with Alexa Fluor 488/594/660 (1:200; Molecular Probes, Carlsbad, CA, USA).

Afterwards, the coverslips were washed in PBS three times for 10 minutes. Then the coverslips were incubated with 300 nM 4′,6-diamidino-2-phenylindole (DAPI; Molecular Probes, Carlsbad, CA, USA) in PBS for 5 minutes at room temperature to visualize cell nuclei. Finally, the coverslips were mounted using Aqua Poly/Mount (Polysciences Inc., Eppelheim, Germany). An LSM 5 DUO spectral confocal microscope (Zeiss, Gottingen, Germany), equipped with an Arg/HeNe laser was used for immunochemical analyses.

6.5 Patch-clamp recordings

Cell membrane currents were recorded 3-4 days after the onset of differentiation, using the patch-clamp technique in the whole-cell configuration. Recording pipettes with a tip resistance of 8–12 MΩ were produced from borosilicate capillaries (Sutter Instruments, Novato, CA, USA), using a P-97 Brown-Flaming micropipette puller (Sutter Instruments, Novato, CA, USA). Recording pipettes were loaded with intracellular solution containing (in mM): 130 KCl, 0.5 $CaCl_2$, 2 $MgCl_2$, 5 Ethylene glycol-bis(2-aminoethylether)-N,N,N′,N′-tetraacetic acid (EGTA), 10 2-[4-(2-hydroxyethyl)piperazin-1-yl]ethanesulfonic acid (HEPES) (pH 7.2).

All recordings were performed in artificial cerebrospinal fluid (aCSF), containing (in mM): 122 NaCl, 3 KCl, 1.5 $CaCl_2$, 1.3 $MgCl_2$, 1.25 Na_2HPO_4, 28 $NaHCO_3$, and 10 D-glucose (osmolality 300 ± 5 mmol/kg). The solution was continuously gassed with 5% CO_2, to keep a final pH of 7.4. All recordings were made on coverslips perfused with aCSF at room temperature. Electrophysiological data were measured with a 10 kHz sample frequency, using an EPC9 amplifier, controlled by PatchMaster software (HEKA Elektronik, Lambrecht/Pfalz, Germany), and filtered by a Bessel filter. The coverslips with cells were transferred to the recording chamber of an upright Axioscop microscope (Zeiss, Gottingen, Germany), equipped with electronic micromanipulators (Luigs & Neumann, Ratingen, Germany) and a high-resolution AxioCam HR digital camera (Zeiss, Gottingen, Germany).

V_M was measured in the current clamp mode of the amplifier. Membrane input resistance (IR) was calculated with FitMaster software (HEKA Elektronik, Lambrecht/Pfalz, Germany) from the current value of 40 ms after the onset of the depolarizing 10 mV pulse, from the holding potential, of -70 mV to -60 mV for 50 ms. Membrane capacitance (C_M) was determined automatically from the Lock-in protocol by PatchMaster. Current patterns were obtained by depolarizing and hyperpolarizing the cell membrane from the holding potential of -70 mV to the values ranging from -160 mV to +40 mV, at 10 mV intervals. Pulse duration was 50 ms. To isolate K_{DR} current components, a voltage step from -70 to -60 mV was used to subtract the time- and voltage-independent currents, as described previously (Anderova *et al.*, 2006; Neprasova *et al.*, 2007). To activate K_{DR} currents only, the cells were held at -50 mV, and the amplitude of K_{DR} currents was measured at 40 mV, at the end of the pulse. Inwardly rectifying K^+ currents were determined at -160 mV, at the end of the pulse. A-type of K^+ currents were isolated by subtracting the current traces, clamped at -110 mV from those clamped at -50 mV, and its amplitude was measured at the peak value. Current densities were

calculated by dividing the maximum current amplitudes by the size of the corresponding cell, indicated by C_m values, for each individual cell. The amplitudes of sodium current evoked by membrane depolarization were measured at the peak value. To measure the action potentials current clamp mode was used. Current values ranged from 50 pA to 1 nA, at 50 pA intervals. Pulse duration was 300 ms.

After recording, the coverslips were fixed in PB (0.2 M; pH 7.4), containing 4% paraformaldehyde for 9 minutes, and then transferred to PBS (10 mM; pH 7.2), for post-recording identification using immunocytochemistry.

6.6 Data Analysis

Four founder mice were used for each treatment to derive NG2 glia for the experiments. Data are presented as mean or as mean ± standard error of the mean (S.E.M.) for n cells or animals, unless otherwise stated. Kruskal-Wallis version of non-parametric unpaired ANOVA with Dunn's multiple comparison correction was used to evaluate significant differences in individual electrophysiological parameters and unpaired parametric ANOVA with Dunnet's multiple comparison correction was used to determine significant differences in incidence among experimental groups. Values of *$p < 0.05$ were considered significant, **$p < 0.01$ very significant and *** $p < 0.001$ extremely significant.

7 Aims of the study

- To assess the impact of ischemic injury on differentiation of NG2 glia
- To examine the impact of Wnt signalling on differentiation of NG2 glia in the healthy brain
- To identify the role of Wnt signalling in differentiation of NG2 glia in mice with ischemic injury

8 Results

To examine the differentiation potential of NG2 glia, we characterized electrophysiological properties of cells isolated from the cortex of adult male mice. In total, 810 cells were recorded and categorized into 27 groups, based on the treatment (CTRL, D3, D7), employed transgenic mouse strain (CT, Ex3, Dkk1), and current profile (cells with passive, complex and outwardly rectifying current profiles).

Current profiles were distinguished according to several electrophysiological properties. The most important criterion was the appearance of the specific current pattern (**Figure 7C, 8C and 9C**). Using the patch-clamp technique in the whole-cell configuration, 3 distinct current patterns were identified in tdTomato positive NG2 cells and their offspring: a passive current pattern represented by symmetrical, time- and voltage-independent passive currents (mainly carried by K^+), a complex current pattern represented by inwardly and outwardly rectifying K^+ currents (K_{IR}, K_A and K_{DR}) together with Na^+ currents, and an outwardly rectifying current pattern (also termed neuron-like) represented by outwardly rectifying K^+ currents (K_A and K_{DR}) and Na^+ currents. Cells displaying complex and passive current patterns were characterized by more negative V_M than those with an outwardly rectifying current pattern. Cells with a neuron-like current pattern possessed high IR, usually higher than 400 MΩ and high amplitudes of K_A and K_{DR} currents. Cells with a complex current profile had IR ranging between 100 and 400 MΩ, while those with a passive current profile had low values of IR, completely lacked K_A currents and the amplitudes of K_{IR} and K_{DR} currents were relatively low. Average values of V_M and IR of cells displaying passive, complex and outwardly rectifying current patterns are summarized in **Table 1**. Furthermore, two cells with a time- and voltage-independent K^+ currents decaying during the duration of the voltage pulse, a typical current profile of mature oligodendrocytes, were found, but they were not included in further analysis.

In our previously performed study, it was found that cells with a passive current profile were positive for markers of astrocytes, while cells with an outwardly rectifying current profile were positive for markers of neuronal precursors. Cells with a complex current profile were positive for markers of NG2 glia (Prajerova *et al.*, 2010; Honsa *et al.*, 2012, 2016; Kriska *et al.*, 2016). Results of immunocytochemistry were not quantified in present study.

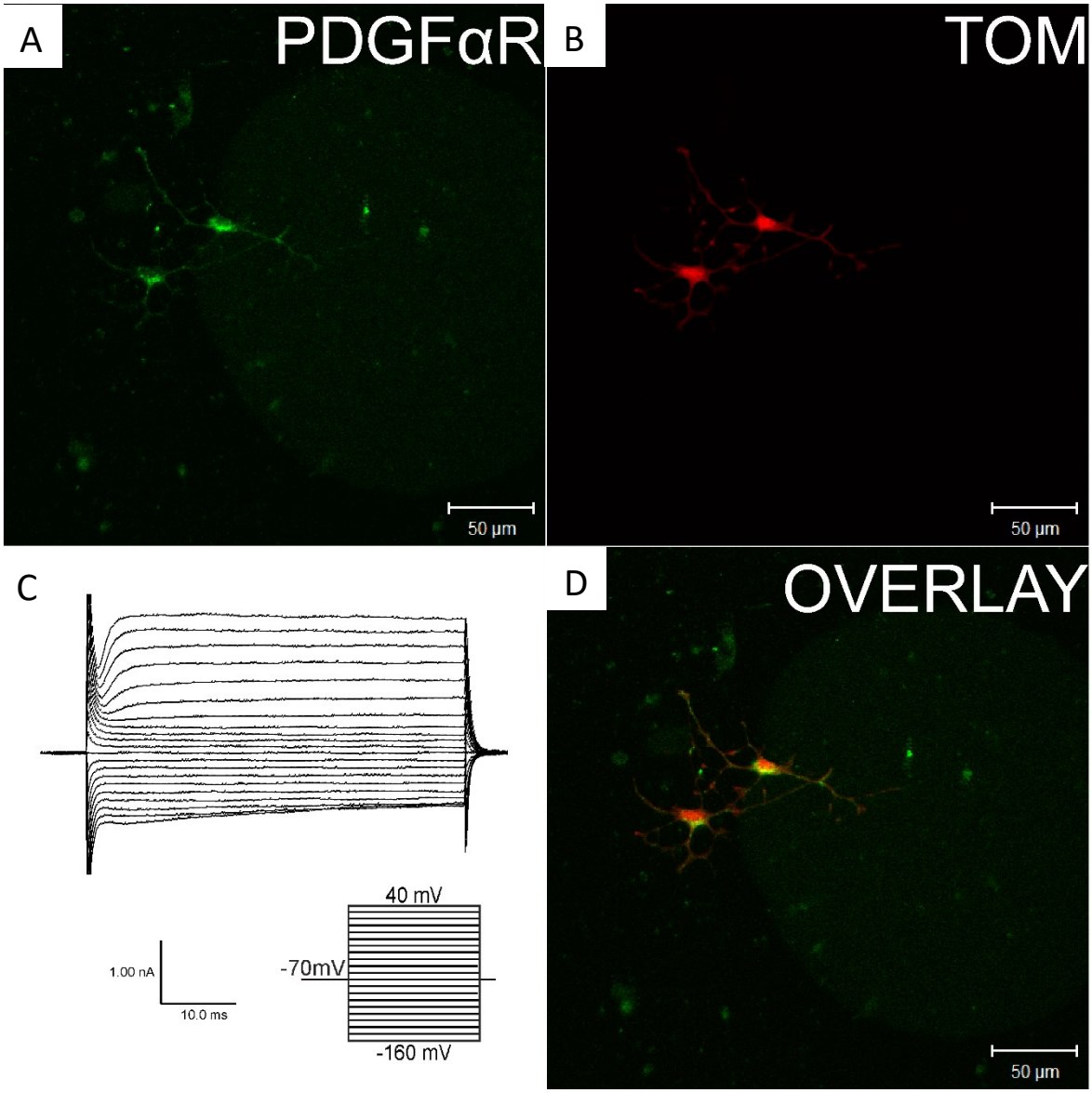

Figure 7: tdTomato positive cells that are also positive for PDGFαR, and a typical current pattern of such cells. A – Cells positive for PDGFαR, typical marker of NG2 cells. B – Cells expressing tdTomato fluorescent protein controlled by *Cspg4* promoter. C - A typical complex current profile characterized by inwardly and outwardly rectifying K^+ currents, measured after depolarizing the cell membrane from a holding potential of -70 mV to +40 mV and hyperpolarizing to -160 mV (see the inset, bottom). Such current pattern is typical for NG2 cells that did not differentiate. D – Cells staining with PDGFαR are also cells expressing tdTomato fluorescent protein. **Abbreviations**: Cspg4 – Chondroitin sulphate proteoglycan 4; PDGFαR - Platelet-derived grow factor receptor α; TOM – tdTomato fluorescent protein.

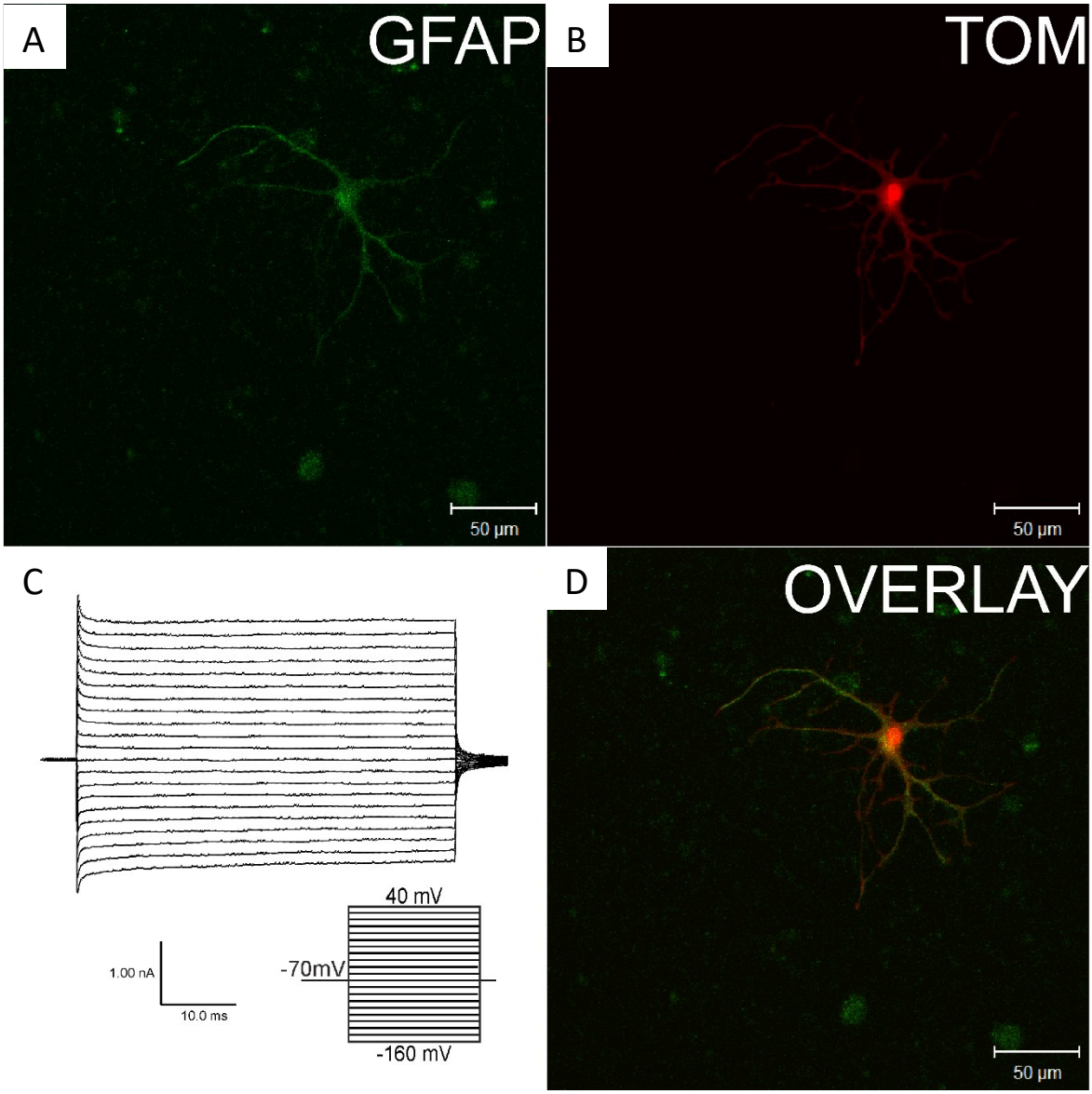

Figure 8: tdTomato positive cell that is also positive for GFAP, and a typical current pattern of such cells. A – Cell positive for GFAP, typical marker of astrocytes. B – Cell expressing tdTomato fluorescent protein controlled by *Cspg4* promoter. C - A typical passive current profile characterized by symmetrical, time- and voltage-independent passive currents, measured after depolarizing the cell membrane from a holding potential of -70 mV to +40 mV and hyperpolarizing to -160 mV (see the inset, bottom). Such current pattern is typical for cells expressing astrocytic markers. D – Cells staining with GFAP are also cells expressing tdTomato fluorescent protein. **Abbreviations**: Cspg4 – Chondroitin sulphate proteoglycan 4; GFAP – Glial fibrillary acidic protein; TOM – tdTomato fluorescent protein.

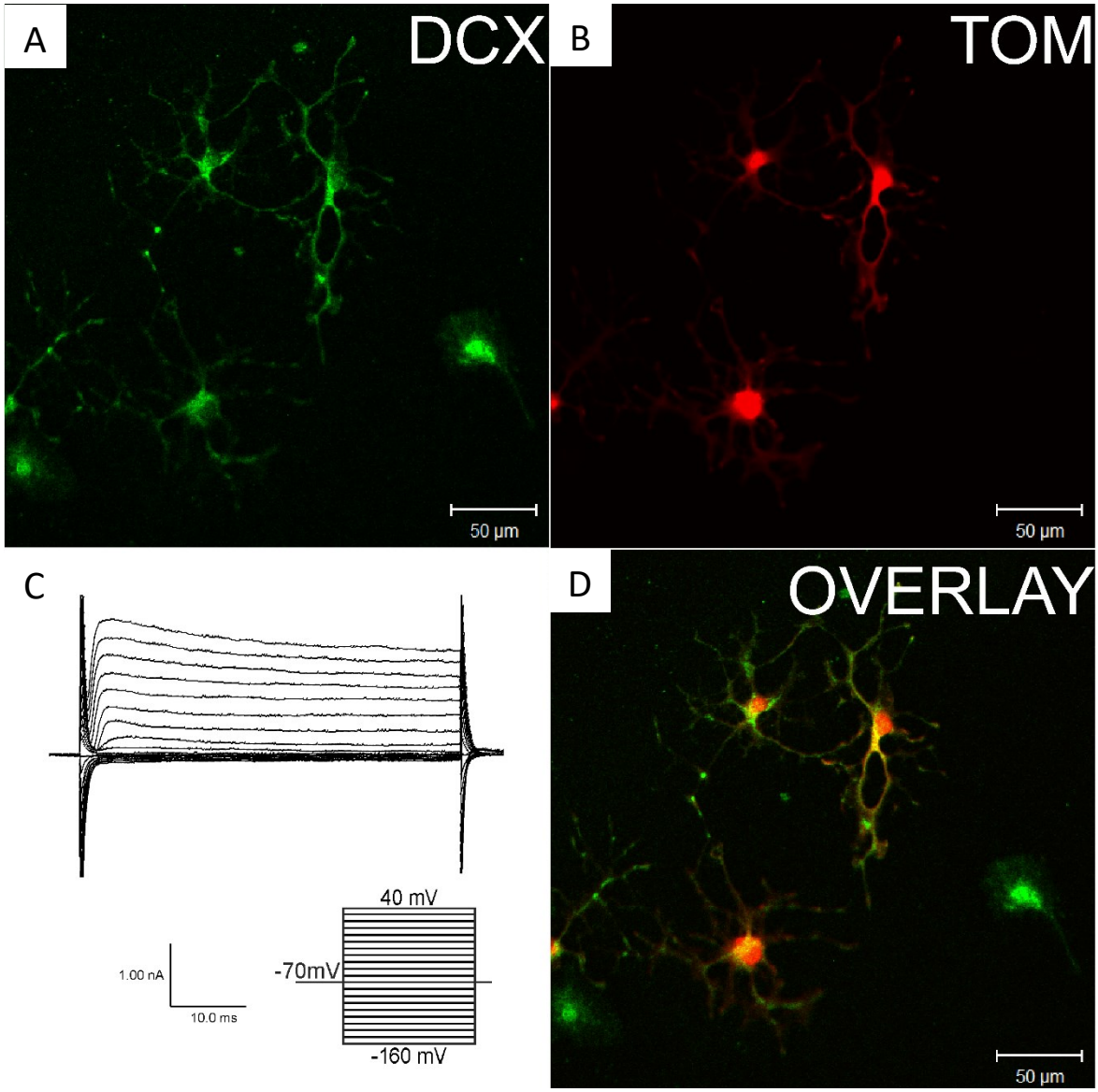

Figure 9: tdTomato positive cells that are also positive for DCX, and a typical current pattern of such cells. A – Cells positive for DCX, typical marker of immature neurons. B – Cells expressing tdTomato fluorescent protein controlled by Cspg4 promoter. C - A typical outwardly rectifying current profile characterized by outwardly rectifying K^+ currents (K_A and K_{DR} currents), measured after depolarizing the cell membrane from a holding potential of -70 mV to +40 mV and hyperpolarizing to -160 mV (see the inset, bottom). Such current pattern is typical for cells expressing markers of cells committed to neuronal lineage. D – Cells staining with DCX are also cells expressing tdTomato fluorescent protein. **Abbreviations**: Cspg4 – Chondroitin sulphate proteoglycan 4; DCX – Doublecortin; TOM – tdTomato fluorescent protein.

Table 1: Average values of V_M and IR of 3 distinct cell types.

Cell type	Average V_M	Average IR	N
Cells with a complex current pattern	-84.90±0.76	169.12±31.33	89
Cells with a passive current pattern	-79.80±3.98	54.97±7.98	5
Cells with an outwardly rectifying current pattern	-65.67±6.12	583.18±71.51	3

The values in the table are presented as mean ± S.E.M. **Abbreviations**: IR – Input resistance; N – Number of cells; S.E.M. – Standard error of the mean; V_M – Resting membrane potential.

8.1 The impact of ischemia on electrophysiological properties of NG2 cells *in vitro*

To assess the impact of ischemia on NG2 cells in mice without modified Wnt signalling, mouse strain CSPG4-CreERT2/Rosa26-tdTomato (further referred to as CT mouse strain) was employed. This strain conditionally expressed gene for tdTomato fluorescent protein after administration of tamoxifen, but there was no manipulation of Wnt signalling. We compared electrophysiological properties of NG2 cells isolated from mice that did not undergo MCAO (labelled as CT-CTRL) with those obtained from cells isolated 3 or 7 days after MCAO (labelled as CT-D3 and CT-D7, respectively). There were 4 animals in each group.

8.1.1 Incidence of distinct cell types did not change after MCAO

First, we compared incidence of individual cell types in 3 types of cell cultures; cells isolated from brains of non-operated mice and those isolated from brains of post-ischemic mice, 3 or 7 days following ischemia. NG2 cells obtained from CT-CTRL mice mainly showed a complex current pattern (91.83 ± 1.61 %). Only minority of cells exhibited a passive (5.13 ± 1.87 %) or an outwardly rectifying (3.04 ± 1.92 %) current profile. In cells isolated from CT-D3 mice, majority of cells also displayed a complex current profile (80.00 ± 4.91 %). Cells with a passive current profile comprised 7.15 ± 3.16 % of all measured cells and cells with an outwardly rectifying current pattern comprised 12.85 ± 6.84 % of cells. Differences between these two groups were not significant. In CT-D7 mice, most of the measured cells exhibited a complex current pattern (79.75 ± 6.09 %), while the occurrence of those displaying a passive current pattern was rather rare (3.56 ± 2.62 %). Cells expressing an outwardly rectifying current pattern comprised 16.69 ± 3.91 %.

Taken together, the induction of FCI caused no changes in incidence of 3 distinct cell types. The results are summarized in **Figure 10**.

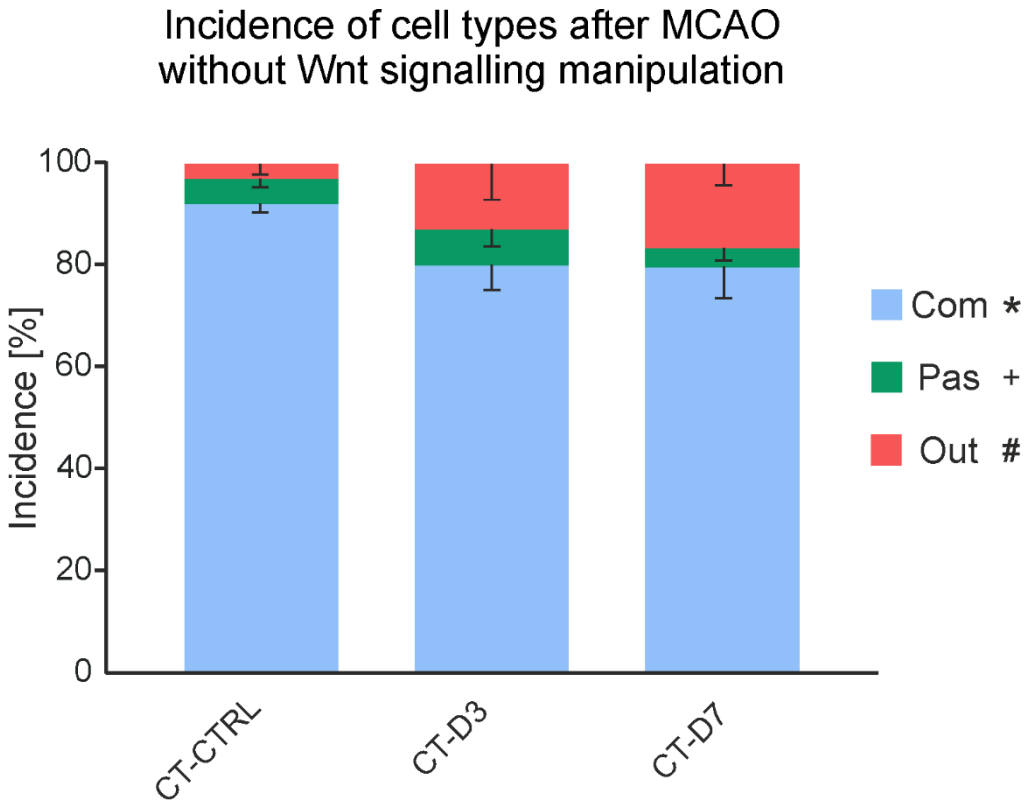

Figure 10: Incidence of 3 distinct cell types and its change after MCAO in mice without Wnt signalling manipulation. **Abbreviations**: Com – Cells with a complex current pattern; CT – Mouse strain without manipulated Wnt signalling; CTRL – Non-operated mice; D3 – 3 days after MCAO; D7 – 7 days after MCAO; MCAO – Middle cerebral artery occlusion; Out – Cells with an outwardly rectifying current pattern; Pas – Cells with a passive current pattern; Wnt – Wingless/Int; * - Significant changes in incidence of cells with a complex current pattern; + - Significant changes in incidence of cells with a passive current pattern; # - Significant changes in incidence of cells with an outwardly rectifying current pattern.

8.1.2 Changes in passive membrane properties induced by ischemia

To further investigate differences after MCAO in mice without Wnt signalling manipulation, we inspected their passive membrane properties, specifically V_M, IR and C_M. Since some of these properties contributed to the classification of the current profiles, we only compared differences within individual cell types.

No changes in V_M and IR were detected in any of the cell types, but we observed a significant increase in C_M of cells with a complex current pattern both 3 days (from 21.14 pF to 33.01 pF) and 7 days (to 25.58 pF) after MCAO. In cells with a passive and an outwardly rectifying current pattern no significant changes occurred. Complete results are summarized in **Table 2** for all the 3 cell types.

Table 2: Passive membrane properties of 3 distinct cell types and their changes after MCAO in mice without Wnt signalling manipulation.

		CT			N		
		CTRL	D3	D7	CTRL	D3	D7
Com	V_M [mV]	-84.90±0.76	-84.45±0.71	-86.50±0.57	89	78	86
	IR [MΩ]	169.12±31.33	127.71±8.69	145.03±8.36	89	78	86
	C_M [pF]	21.14±0.97	**33.01±2.14**	25.58±1.21	89	78	86
Pas	V_M [mV]	-79.80±3.98	-83.50±1.74	-82.00±4.38	5	8	4
	IR [MΩ]	54.97±7.98	70.67±11.16	40.92±8.23	5	8	4
	C_M [pF]	29.96±0.82	27.61±4.28	44.61±7.42	5	8	4
Out	V_M [mV]	-65.67±6.12	-80.23±2.49	-79.33±2.30	3	13	18
	IR [MΩ]	583.18±71.51	585.64±128.94	475.99±83.02	3	13	18
	C_M [pF]	22.49±4.66	24.15±3.29	24.61±2.78	3	13	18

p<0.05	p<0.01	**p<0.001**

The values in the table are presented as mean ± S.E.M. **Abbreviations:** C_M – Membrane capacitance; Com – Cells with a complex current pattern; CT – Mouse strain without manipulated Wnt signalling; CTRL – Non-operated mice; D3 – 3 days after MCAO; D7 – 7 days after MCAO; IR – Input resistance; MCAO – Middle cerebral artery occlusion; N – Number of measured cells; Out – Cells with an outwardly rectifying current pattern; Pas – Cells with a passive current pattern; S.E.M. – Standard error of the mean; V_M – Resting membrane potential; Wnt – Wingless/Int.

8.1.3 K^+ and Na^+ currents in NG2 glia following MCAO

To investigate the impact of MCAO on membrane properties of NG2 cells, we also compared the amplitudes and densities of K_{IR}, K_{DR}, K_A, and Na^+ currents of cells isolated from non-operated and post-ischemic brains of CT mice. The current density was calculated by dividing the amplitude by the C_M value of the corresponding cell.

The amplitude of K_{IR} current did not change significantly in cells with a complex and a passive current profile, nevertheless, changes in the density of K_{IR} currents after MCAO were significant in cells with a complex current profile, where a decrease was observed both 3 (from 11.72 pA/pF to 7.63 pA/pF) and 7 days (to 8.08 pA/pF) following ischemia. The density of K_{IR} currents did not change significantly in cells with a passive current pattern (**Tables 3, 4**).

The amplitude of K_{DR} current increased in cells with a complex current pattern 7 days after MCAO (from 794.88 to 1130.80). Since a very small number of cells with a passive

current profile exhibited K_{DR} current, we were unable to perform statistical data processing. In cells with an outwardly rectifying current pattern, the amplitude of K_{DR} currents did not change following ischemic injury. The density of K_{DR} currents in cells with a complex current pattern significantly decreased only 3 days after MCAO (from 44.00 to 30.17), while their density 7 days after ischemic injury was comparable with that observed in cell cultures isolated from non-operated mice. The number of cells with a passive current profile exhibiting K_{DR} currents was again too low to be analysed. We did not observe any significant changes in the density of this current in cells with an outwardly rectifying current pattern (**Tables 3, 4, 5**).

The amplitude and the density of K_A currents were not changed after MCAO in cells with a complex current pattern and in cells with an outwardly rectifying current pattern (**Tables 3, 5)**.

The amplitude of Na^+ currents in cells with a complex current pattern did not change after MCAO. In non-injured CT mice, only one cell with Na^+ currents was observed among cells with an outwardly rectifying current pattern and thus we were not able to evaluate whether the changes in this cell type were significant. The density of Na^+ currents decreased significantly in NG2 cells displaying a complex current profile 3 days (from 22.37 to 10.44), but not 7 days after MCAO. Complete results are summarized in **Table 3** for cells with a complex current profile, **Table 4** for cells with a passive current profile and **Table 5** for cells with an outwardly rectifying current profile.

Table 3: K^+ and Na^+ currents in cells with a complex current pattern and their changes after MCAO in mice without Wnt signalling manipulation.

Com	CT			N		
	CTRL	D3	D7	CTRL	D3	D7
K_{IR} [pA]	216.66±14.84	208.55±10.33	185.21±8.55	89	76	86
K_{IR}/C_M [pA/pF]	11.72±1.00	**7.63±0.53**	8.08±0.43	89	76	86
K_{DR} [pA]	794.88±49.46	848.23±56.75	**1130.80±67.79**	84	78	86
K_{DR}/C_M [pA/pF]	44.00±3.07	30.17±2.18	48.80±3.23	84	78	86
K_A [pA]	587.72±47.76	568.83±61.23	824.81±79.53	67	52	64
K_A/C_M [pA/pF]	34.57±3.79	23.35±3.06	37.09±3.84	67	52	64
Na^+ [pA]	324.32±21.58	365.38±57.30	363.19±55.77	20	9	13
Na^+/C_M [pA/pF]	22.37±2.92	10.44±1.50	16.51±2.38	20	9	13

p<0.05	p<0.01	**p<0.001**

The values in the table are presented as mean ± S.E.M. **Abbreviations**: Com – Cells with a complex current pattern; CT – Mouse strain without manipulated Wnt signalling; CTRL – Non-operated mice; D3 – 3 days after MCAO; D7 – 7 days after MCAO; K_A – A-type K^+ current amplitude; K_A/C_M – A-type K^+ current density; K_{DR} – Delayed outwardly rectifying K^+ current amplitude; K_{DR}/C_M – Delayed outwardly rectifying K^+ current density; K_{IR} – Inwardly rectifying K^+ current amplitude; K_{IR}/C_M – Inwardly rectifying K^+ current density; MCAO – Middle cerebral artery occlusion; N – Number of measured cells; Na^+ – Na^+ current amplitude; Na^+/C_M – Na^+ current density; S.E.M. – Standard error of the mean; Wnt – Wingless/Int.

Table 4: K^+ and Na^+ currents in cells with a passive current pattern and their changes after MCAO in mice without Wnt signalling manipulation.

Pas	CT			N		
	CTRL	D3	D7	CTRL	D3	D7
K_{IR} [pA]	153.57±65.83	123.31±22.95	272.20	4	7	1
K_{IR}/C_M [pA/pF]	5.17±2.24	5.49±1.83	9.19	4	7	1
K_{DR} [pA]	434.00	155.80±107.30	144.00	1	2	1
K_{DR}/C_M [pA/pF]	14.04	5.89±4.56	2.22	1	2	1

p<0.05	p<0.01	**p<0.001**

The values in the table are presented as mean ± S.E.M. **Abbreviations**: CT – Mouse strain without manipulated Wnt signalling; CTRL – Non-operated mice; D3 – 3 days after MCAO; D7 – 7 days after MCAO; K_{DR} – Delayed outwardly rectifying K^+ current amplitude; K_{DR}/C_M – Delayed outwardly rectifying K^+ current density; K_{IR} – Inwardly rectifying K^+ current amplitude; K_{IR}/C_M – Inwardly rectifying K^+ current density; MCAO – Middle cerebral artery occlusion; N – Number of measured cells; Pas – Cells with a passive current pattern; S.E.M. – Standard error of the mean; Wnt – Wingless/Int.

Table 5: K^+ and Na^+ currents in cells with an outwardly rectifying current pattern and their changes after MCAO in mice without Wnt signalling manipulation.

Out	CT			N		
	CTRL	D3	D7	CTRL	D3	D7
K_{DR} [pA]	1408.55±440.72	1592.63±139.87	1744.56±132.59	3	13	18
K_{DR}/C_M [pA/pF]	71.63±26.36	75.80±7.70	79.74±6.24	3	13	18
K_A [pA]	862.77±146.24	953.18±175.16	1130.08±223.39	2	13	18
K_A/C_M [pA/pF]	51.77±24.48	47.68±8.33	59.90±13.65	2	13	18
Na^+ [pA]	200.44	240.72±28.98	313.18±29.51	1	5	4
Na^+/C_M [pA/pF]	15.10	12.13±2.09	13.10±2.33	1	5	4

p<0.05	p<0.01	**p<0.001**

The values in the table are presented as mean ± S.E.M. **Abbreviations**: CT – Mouse strain without manipulated Wnt signalling; CTRL – Non-operated mice; D3 – 3 days after MCAO; D7 – 7 days after MCAO; K_A – A-type K^+ current amplitude; K_A/C_M – A-type K^+ current density; K_{DR} – Delayed outwardly rectifying K^+ current amplitude; K_{DR}/C_M – Delayed outwardly rectifying K^+ current density; MCAO – Middle cerebral artery occlusion; N – Number of measured cells; Na^+ – Na^+ current amplitude; Na^+/C_M – Na^+ current density; Out – Cells with an outwardly rectifying current pattern; S.E.M. – Standard error of the mean; Wnt – Wingless/Int.

Taken together, there were no changes in electrophysiological properties of cells displaying a passive or an outwardly rectifying current pattern. However, in cells having a complex current pattern ischemia resulted in enlargement of cell surface (C_M) and therefore, in a decrease in K_{IR}, K_{DR} and Na^+ current densities. Interestingly, there was an increase in K_{DR} current amplitude observed in these cells 7 days following ischemia.

8.2 Manipulating Wnt signalling pathway under physiological conditions.

To examine the impact of Wnt signalling on NG2 cells differentiation under physiological conditions, we compared data obtained in cell cultures from non-operated mice, in which Wnt signalling was not manipulated (CT-CTRL) with those found in non-operated mice with hyper-activated (Ex3-CTRL) or inhibited (Dkk1-CTRL) Wnt signalling.

8.2.1 Incidence of distinct cell types

Cells with a complex current pattern were the most abundant cell type in all 3 mouse strains. In CT-CTRL mice cells with a complex current pattern constituted 91.83 ± 1.61 % of

all cells. In Ex3-CTRL mice, where the Wnt signalling pathway was activated, 66.61 ± 3.78 % of cells showed a complex current pattern. This value was significantly lower than in CT-CTRL mice. When Wnt signalling was inhibited (Dkk1-CTRL strain), cells with a complex current pattern constituted 87.43 ± 2.53 % of all measured cells, and this value was not significantly different from that found in cultured cells from CT-CTRL mice. Cells with a passive current pattern made only 5.13 ± 1.87 % of the measured cells in CT-CTRL mice, while their incidence in Ex3-CTRL mice was significantly higher, constituting almost a quarter of all cells measured in this mouse strain (23.57 ± 3.70 %). In Dkk1-CTRL mice, cells with a passive current profile made 5.83 ± 3.44 % of the measured cells and this value was not significantly different from incidence of this cell type in CT-CTRL mice. As for cells with an outwardly rectifying current profile, no significant differences in incidence among the 3 strains were observed. Moreover, this cell type constituted only a small percentage of all measured cells (3.04 ± 1.92 % in CT-CTRL mice, 9.82 ± 4.17 % in Ex3 mice and 6.73 ± 3.53 % in Dkk1 mice). There were 4 animals in each experimental group.

Collectively, changes in the occurrence of cells with complex and passive current patterns were observed only after Wnt signalling pathway activation, while its inhibition caused no alterations (**Figure 11**).

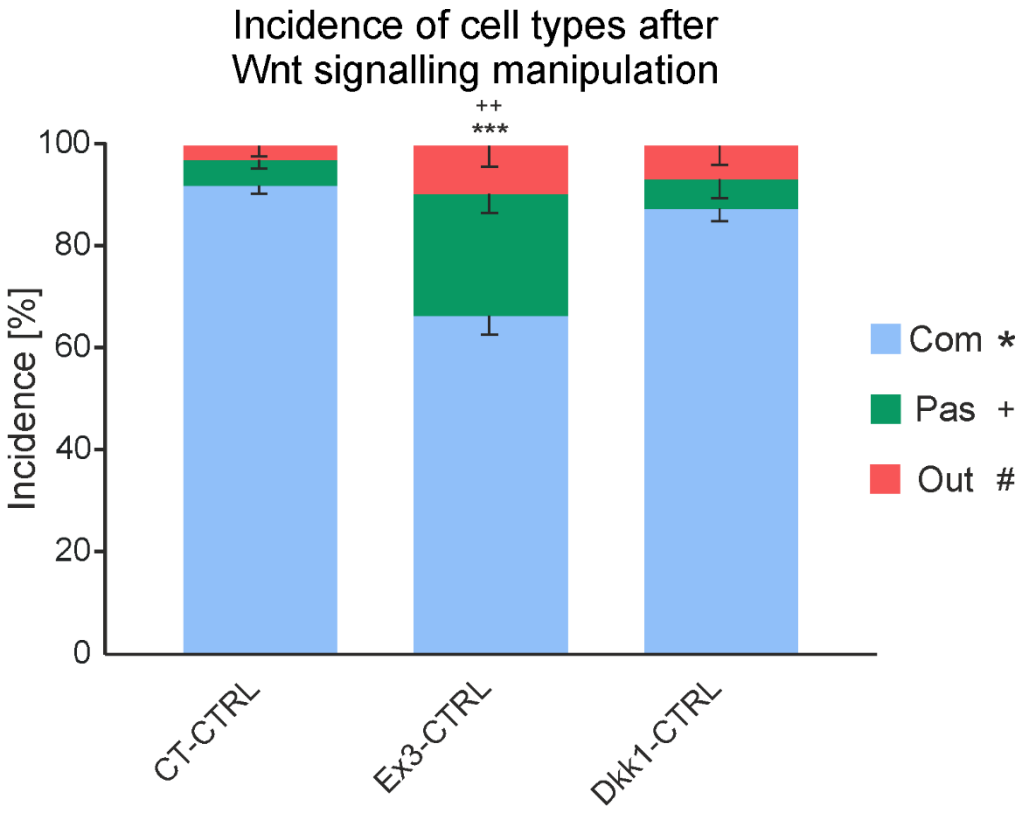

Figure 11: Incidence of the cell types in non-operated mice and its changes when Wnt signalling is manipulated. **Abbreviations**: Com – Cells with a complex current pattern; CT – Mouse strain without manipulated Wnt signalling; CTRL – Non-operated mice; Dkk1 – Mouse strain with inhibited Wnt signalling; Ex3 – Mouse strain with activated Wnt signalling; Pas – Cells with a passive current pattern; Out – Cells with an outwardly rectifying current pattern; Wnt – Wingless/Int ; * – Significant changes in incidence of cells with a complex current pattern; *** – $p<0.001$; + – Significant changes in incidence of cells with a passive current pattern; ++ – $p<0.01$; # – Significant changes in incidence of cells with an outwardly rectifying current pattern.

8.2.2 Passive membrane properties of NG2 cells after Wnt signalling manipulation

In cells with a complex current profile, an average value of V_M was -84.90 mV and we observed significant hyperpolarization when the Wnt signalling pathway was activated (to -90.17 mV). Similarly, hyperpolarization of cells with a complex current profile was observed in Dkk1 mice (to -88.60 mV). In cells with a passive current profile Wnt signalling activation resulted in a significant shift in V_M to more a negative value (from -79.80 mV to -90.84 mV), while after Wnt signalling inhibition no changes in V_M occurred. Cells with an outwardly rectifying current pattern had an average value of V_M -65.67 mV and neither activation nor inhibition of this pathway had any impact on it (**Table 6**).

As for IR, cells with a complex current profile isolated from CT-CTRL mice exhibited an average IR value of 169.12 MΩ and this value was lower in cells from Ex3-CTRL mice

(92.31 MΩ) but was not significantly different in Dkk1-CTRL mice. Significant differences in IR were also observed in cells with a passive current profile, where IR lowered after Wnt signalling activation (from 54.97 MΩ to 37.95 MΩ). Nevertheless, activation or inhibition of this pathway led to no IR changes in cells with an outwardly rectifying current pattern (**Table 6**).

Wnt signalling manipulation had no impact on C_M. Complete results summarizing passive membrane properties of cells with a complex current profile, a passive current profile and an outwardly rectifying current profile are in **Table 6**.

Table 6: Passive membrane properties of 3 distinct cell types and their changes after manipulation of the Wnt signalling pathway in non-operated mice.

		CTRL			N		
		CT	Ex3	Dkk1	CT	Ex3	Dkk1
Com	V_M [mV]	-84.90±0.76	**-90.17±0.35**	**-88.60±0.59**	89	66	58
	IR [MΩ]	169.12±31.33	**92.31±7.49**	136.85±27.77	89	66	58
	C_M [pF]	21.14±0.97	22.10±0.88	18.09±0.78	89	66	58
Pas	V_M [mV]	-79.80±3.98	-90.84±0.34	-83.00±2.16	5	25	4
	IR [MΩ]	54.97±7.98	37.95±2.39	81.84±12.56	5	25	4
	C_M [pF]	29.96±0.82	40.67±2.38	21.49±3.68	5	25	4
Out	V_M [mV]	-65.67±6.12	-75.00±6.14	-86.00±3.67	3	9	4
	IR [MΩ]	583.18±71.51	647.02±103.49	275.95±22.15	3	9	4
	C_M [pF]	22.49±4.66	19.21±3.04	12.57±2.21	3	9	4

p<0.05	p<0.01	**p<0.001**

The values in the table are presented as mean ± S.E.M. **Abbreviations**: C_M – Membrane capacitance; Com – Cells with a complex current pattern; CT – Mouse strain without manipulated Wnt signalling; CTRL – Non-operated mice; Dkk1 – Mouse strain with inhibited Wnt signalling; Ex3 – Mouse strain with activated Wnt signalling; IR – Input resistance; N – Number of measured cells; Out – Cells with an outwardly rectifying current pattern; Pas – Cells with a passive current pattern; S.E.M. – Standard error of the mean; V_M – Resting membrane potential; Wnt – Wingless/Int.

8.2.3 K^+ and Na^+ currents in NG2 glia after Wnt signalling manipulation

Surprisingly, the only significant changes were detected in cells with complex currents. In these cells Wnt signalling activation caused an increase in the amplitude of K_{DR} currents. An average K_{DR} current amplitude in this cell type isolated from CT-CTRL mice with intact Wnt signalling was 794.88 pA and it was significantly higher in the mice with

activated Wnt signalling (1030.30 pA). The density of this current also increased after Wnt signalling inhibition (from 44.00 pA/pF to 58.35 pA/pF). However, such increase in K_{DR} current density is probably an indirect effect of a slight C_M decrease. The manipulation of Wnt signalling did not affect K_{IR}, K_A and Na^+ currents (summarized in **Table 7** for cells with a complex current profile, **Table 8** for cells with a passive current profile and **Table 9** for cells with an outwardly rectifying current profile).

Table 7: K^+ and Na^+ currents in cells with a complex current pattern and their changes after manipulation of the Wnt signalling pathway in non-operated mice.

Com	CTRL			N		
	CT	Ex3	Dkk1	CT	Ex3	Dkk1
K_{IR} [pA]	216.66±14.84	188.63±10.51	186.15±13.53	89	67	57
K_{IR}/C_M [pA/pF]	11.72±1.00	9.08±0.55	11.25±1.00	89	67	57
K_{DR} [pA]	794.88±49.46	1030.30±74.99	938.50±54.72	84	67	58
K_{DR}/C_M [pA/pF]	44.00±3.07	51.57±4.25	58.35±4.30	84	67	58
K_A [pA]	587.72±47.76	615.56±51.03	659.49±73.56	67	22	55
K_A/C_M [pA/pF]	34.57±3.79	34.48±4.16	43.11±5.38	67	22	55
Na^+ [pA]	324.32±21.58	344.95±70.44	230.97±33.91	20	4	7
Na^+/C_M [pA/pF]	22.37±2.92	18.72±3.42	17.61±3.21	20	4	7

p<0.05	p<0.01	**p<0.001**

The values in the table are presented as mean ± S.E.M. **Abbreviations**: Com – Cells with a complex current pattern; CT – Mouse strain without manipulated Wnt signalling; CTRL – Non-operated mice; Dkk1 – Mouse strain with inhibited Wnt signalling; Ex3 – Mouse strain with activated Wnt signalling; K_A – A-type K^+ current amplitude; K_A/C_M – A-type K^+ current density; K_{DR} – Delayed outwardly rectifying K^+ current amplitude; K_{DR}/C_M – Delayed outwardly rectifying K^+ current density; K_{IR} – Inwardly rectifying K^+ current amplitude; K_{IR}/C_M – Inwardly rectifying K^+ current density; N – Number of measured cells; Na^+– Na^+ current amplitude; Na^+/C_M – Na^+ current density; S.E.M. – Standard error of the mean; Wnt – Wingless/Int.

Table 8: K^+ and Na^+ currents in cells with a passive current pattern and their changes after manipulation of the Wnt signalling pathway in non-operated mice.

Pas	CTRL			N		
	CT	Ex3	Dkk1	CT	Ex3	Dkk1
K_{IR} [pA]	153.57±65.83	123.70±14.29	58.06±11.32	4	15	4
K_{IR}/C_M [pA/pF]	5.17±2.24	3.38±0.43	2.89±0.72	4	15	4
K_{DR} [pA]	434.00	231.42±55.49	91.76±16.53	1	15	4
K_{DR}/C_M [pA/pF]	14.04	6.44±1.58	4.97±1.52	1	15	4

p<0.05	p<0.01	**p<0.001**

The values in the table are presented as mean ± S.E.M. **Abbreviations**: CT – Mouse strain without manipulated Wnt signalling; CTRL – Non-operated mice; Dkk1 – Mouse strain with inhibited Wnt signalling; Ex3 – Mouse strain with activated Wnt signalling; K_{DR} – Delayed outwardly rectifying K^+ current amplitude; K_{DR}/C_M – Delayed outwardly rectifying K^+ current density; K_{IR} – Inwardly rectifying K^+ current amplitude; K_{IR}/C_M – Inwardly rectifying K^+ current density; N – Number of measured cells; Pas – Cells with a passive current pattern; S.E.M. – Standard error of the mean; Wnt – Wingless/Int.

Table 9: K^+ and Na^+ currents in cells with an outwardly rectifying current pattern and their changes after manipulation of the Wnt signalling pathway in non-operated mice.

Out	CTRL			N		
	CT	Ex3	Dkk1	CT	Ex3	Dkk1
K_{DR} [pA]	1408.55±440.72	1492.13±247.25	1521.15±198.05	3	9	4
K_{DR}/C_M [pA/pF]	71.63±26.36	85.00±12.96	125.41±11.52	3	9	4
K_A [pA]	862.77±146.24	842.46±270.83	820.45±103.33	2	6	4
K_A/C_M [pA/pF]	51.77±24.48	77.35±30.33	74.55±19.11	2	6	4
Na^+ [pA]	200.44	354.20±183.76	179.95±61.60	1	3	3
Na^+/C_M [pA/pF]	15.10	17.45±3.77	15.28±5.10	1	3	3

p<0.05	p<0.01	**p<0.001**

The values in the table are presented as mean ± S.E.M. **Abbreviations**: CT – Mouse strain without manipulated Wnt signalling; CTRL – Non-operated mice; Dkk1 – Mouse strain with inhibited Wnt signalling; Ex3 – Mouse strain with activated Wnt signalling; K_A – A-type K^+ current amplitude; K_A/C_M – A-type K^+ current density; K_{DR} – Delayed outwardly rectifying K^+ current amplitude; K_{DR}/C_M – Delayed outwardly rectifying K^+ current density; N – Number of measured cells; Na^+– Na^+ current amplitude; Na^+/C_M – Na^+ current density; Out – Cells with an outwardly rectifying current pattern; S.E.M. – Standard error of the mean; Wnt – Wingless/Int.

Collectively, no changes were observed in cells displaying outwardly rectifying currents, while several shifts in electrophysiological properties were detected in the other 2 cell types. Activation of Wnt signalling led to more hyperpolarized membranes in cells with

complex and passive currents, while inhibition of this signalling caused hyperpolarization only in cells with a complex current profile. Furthermore, activation of the Wnt signalling pathway caused shift in IR to lower values in cells displaying passive and complex currents, while inhibition of Wnt signalling did not have any effect on IR. Additionally, an increase in K_{DR} current amplitude was observed in cells exhibiting a complex current pattern, in which Wnt signalling was activated, while inhibition of this pathway in these cells caused an increase in K_{DR} current density, which can be attributed to a slight C_M decrease. The manipulation of Wnt signalling did not significantly affect K_{IR}, K_A and Na^+ currents.

8.3 Wnt signalling manipulation at early post-ischemic phase

Since we had observed an impact of Wnt signalling on some electrophysiological properties of NG2 glia in non-operated mice, we aimed to examine whether there was any influence on the changes induced by ischemia. Here we focus specifically on early post-ischemic phase, in which a marked proliferation of NG2 glia occurs and is accompanied by microglia and astrocyte activation (Pivonkova *et al.*, 2010; Anderova *et al.*, 2011). To achieve this goal, we employed mice, in which Wnt signalling was inhibited or activated and these mice were sacrificed 3 days after MCAO, therefore called Dkk1-D3 and Ex3-D3 mice, respectively. As a control, we used mice, in which Wnt signalling is not affected by tamoxifen application and NG2 cells from these mice were isolated 3 days after the induction of ischemic injury (labelled as CT-D3 mice).

8.3.1 Incidence of distinct cell types

NG2 cells isolated from mice 3 days after MCAO (CT-D3) consisted predominantly of cells with a complex current pattern, which made 80.00 ± 4.91 % of cells. Cells with a passive current profile made 7.15 ± 3.16 % and cells with an outwardly rectifying current pattern constituted 12.85 ± 6.84 % of all measured cells.

In Dkk1-D3 mice, where Wnt signalling is inhibited, we did not observe any differences in incidence of cell types; however, we observed differences in Ex3-D3 mice. Mice with activated Wnt signalling exhibited a significantly lower incidence of cells with a complex current pattern. These cells constituted only 44.05 ± 10.52 % of the measured cells. Incidence of cells with a passive current profile did not change significantly (15,05 ± 7,47 %), but we observed a significant increase in incidence of cells with an outwardly rectifying current profile. Incidence of this cell type raised to 40.89 ± 8.43 %. These changes are presented in **Figure 12**.

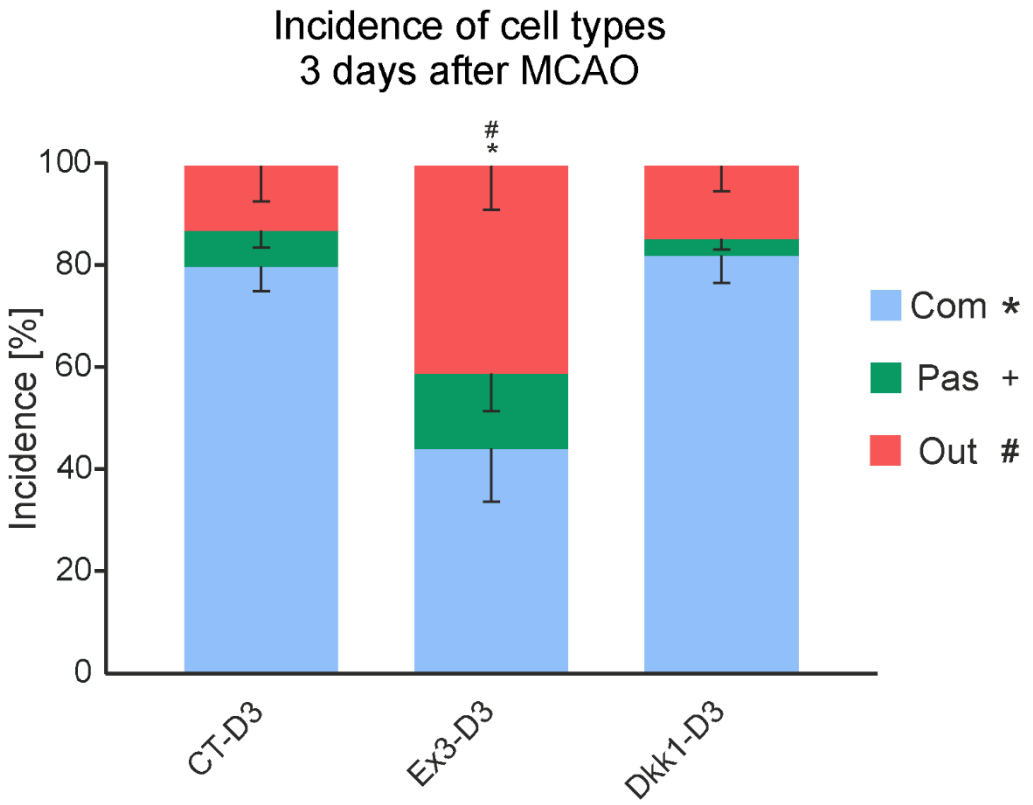

Figure 12: Incidence of cell types 3 days after MCAO in mice with manipulated Wnt signalling. **Abbreviations**: Com – Cells with a complex current pattern; CT – Mouse strain without manipulated Wnt signalling; Dkk1 – Mouse strain with inhibited Wnt signalling; D3 – 3 days after MCAO; Ex3 – Mouse strain with activated Wnt signalling; Out – Cells with an outwardly rectifying current pattern; Pas – Cells with a passive current pattern; Wnt – Wingless/Int ; * – Significant changes in incidence of cells with a complex current pattern, $p<0.05$; + – Significant changes in incidence of cells with a passive current pattern; # – Significant changes in incidence of cells with an outwardly rectifying current pattern, $p<0.05$.

8.3.2 The impact of Wnt signalling manipulation on passive membrane properties in post-ischemic NG2 cells

In cells with a complex current profile isolated from the CT-D3 mice, V_M was -84.45 mV. This value was significantly hyperpolarized in the mouse strain with activated Wnt signalling, reaching -88.11 mV. Smaller, but also significant hyperpolarization was observed in Dkk1-D3 mice, shifting V_M to -86.66 mV. In cells with a passive current profile isolated from CT-D3 mice, V_M was -83.50 mV and this value was not significantly changed by Wnt signalling manipulation. In cells with an outwardly rectifying current pattern, V_M was -80.23 mV in CT-D3 mice and significantly depolarized cells of this cell type were observed in the Ex3-D3 mice, where V_M was -53.97 mV. Inhibition of Wnt signalling caused no changes of V_M in these cells (**Table 10**).

No significant changes in IR were observed in any of the cells types, control values being 127.71 MΩ for cells with a complex current pattern, 70.67 MΩ for cells with a passive current profile, and 585.64 MΩ for cells with an outwardly rectifying current profile (**Table 10**).

As for C_M, the average value measured in cells with a complex current profile was 33.01 pF and it did not change significantly after any Wnt signalling manipulation. Similarly, no significant change was observed in cells with a passive current profile, where the control value was 27.61 pF. However, in cells with an outwardly rectifying current profile, C_M changed from 24.15 pF in CT-D3 to 15.79 pF in the strain with activated Wnt signalling pathway. Complete results are summarized in **Table 10** for all 3 cell types.

Table 10: Passive membrane properties of 3 distinct cell types and their changes after manipulation of the Wnt signalling pathway in mice 3 days after MCAO.

		D3			N		
		CT	Ex3	Dkk1	CT	Ex3	Dkk1
Com	V_M [mV]	-84.45±0.71	**-88.11±0.86**	-86.66±0.61	78	36	82
	IR [MΩ]	127.71±8.69	113.77±12.36	152.58±25.61	78	36	82
	C_M [pF]	33.01±2.14	26.22±1.76	28.52±1.50	78	36	82
Pas	V_M [mV]	-83.50±1.74	-81.82±3.46	-80.33±3.84	8	11	3
	IR [MΩ]	70.67±11.16	43.72±4.94	121.52±43.53	8	11	3
	C_M [pF]	27.61±4.28	41.78±5.32	23.33±5.69	8	11	3
Out	V_M [mV]	-80.23±2.49	**-53.97±2.45**	-75.38±4.18	13	36	13
	IR [MΩ]	585.64±128.94	823.07±98.91	482.31±45.68	13	36	13
	C_M [pF]	24.15±3.29	15.79±1.57	19.28±2.98	13	36	13

p<0.05	p<0.01	**p<0.001**

The values in the table are presented as mean ± S.E.M. **Abbreviations**: C_M – Membrane capacitance; Com – Cells with a complex current pattern; CT – Mouse strain without manipulated Wnt signalling; Dkk1 – Mouse strain with inhibited Wnt signalling; D3 – 3 days after MCAO; Ex3 – Mouse strain with activated Wnt signalling; IR – Input resistance; MCAO – Middle cerebral artery occlusion; N – Number of measured cells; Out – Cells with an outwardly rectifying current pattern; Pas – Cells with a passive current pattern; V_M – Resting membrane potential; S.E.M. – Standard error of the mean; Wnt – Wingless/Int.

8.3.3 The effect of Wnt signalling manipulation on K^+ and Na^+ currents

In cells displaying passive currents no changes in electrophysiological properties occurred in response to Wnt signalling manipulation. Additionally, K_{IR} current amplitude and density did not change in any of the cell types (**Tables 11, 12**).

The values of K_{DR} current amplitude did not change in cells with complex as well as passive current profiles, but the amplitude of this current was significantly lower in cells with an outwardly rectifying current profile isolated from Ex3-D3 mice (904.23 pA) than in those isolated from CT-D3 mice (1592.63 pA). Interestingly, no K_{DR} currents were detected in cells with a passive current profile when isolated from the Dkk1-D3 mice. Despite the fact that no increase in K_{DR} current amplitude was detected in cells with complex currents, increased density of K_{DR} currents was observed in both strains with manipulated Wnt signalling. The value was 30.17 pA/pF in the CT-D3 strain, but it rose to 49.21 pA/pF in Ex3-D3 mice and to 40.46 pA/pF in Dkk1-D3 mice. No significant change in density of K_{DR} currents was observed in cells with a passive or an outwardly rectifying current pattern (**Tables 11, 12, 13**).

Inhibition of the Wnt signalling pathway also induced a rise of K_A current amplitude in cells with a complex current pattern. The control value of K_A current amplitude in this cell type was 568.83 pA and it rose to 828.19 pA in Dkk1-D3 mice. Activation of Wnt signalling did not have any significant impact on K_A current amplitude in this cell type. In cells with outwardly rectifying currents, the amplitude was not different from the value recorded in cells isolated from CT-D3 mice (953.18 pA). As for the density of this current, a significant increase was observed in cells with a complex current pattern isolated from both mouse strains with manipulated Wnt signalling. Its value in cells from CT-D3 mice was 23.35 pA/pF, but it reached 38.60 pA/pF in Ex3-D3 mice and 37.01 pA/pF in Dkk1-D3 mice. A significant increase in K_A current density was also observed in Dkk1-D3 mice in cells with an outwardly rectifying current profile. In this cell type, K_A current density almost doubled, increasing from 47.68 pA/pF to 89.41 pA/pF (**Tables 11, 13**).

While we did not observe any significant change in Na^+ current amplitude in cells with complex currents and cells with outwardly rectifying currents, we observed a significant increase in Na^+ current density in cells with a complex current pattern isolated from Ex3-D3 mice. This value rose from 10.44 pA/pF to 22.69 pA/pF. No significant changes were observed in cells with an outwardly rectifying current profile with respect to Na^+ current density. Complete results are summarized in **Table 11** for cells with a complex current

profile, **Table 12** for cells with a passive current profile and **Table 13** for cells with an outwardly rectifying current profile.

Table 11: K^+ and Na^+ currents in cells with a complex current pattern and their changes after manipulation of the Wnt signalling pathway in mice 3 days after MCAO.

Com	D3			N		
	CT	Ex3	Dkk1	CT	Ex3	Dkk1
K_{IR} [pA]	208.55±10.33	207.01±18.71	196.91±9.82	76	36	82
K_{IR}/C_M [pA/pF]	7.63±0.53	8.73±0.76	7.86±0.42	76	36	82
K_{DR} [pA]	848.23±56.75	1110.75±100.71	1039.81±64.44	78	36	82
K_{DR}/C_M [pA/pF]	30.17±2.18	49.21±5.20	40.46±2.38	78	36	82
K_A [pA]	568.83±61.23	842.38±112.04	828.19±77.55	52	28	64
K_A/C_M [pA/pF]	23.35±3.06	38.60±5.94	37.01±4.35	52	28	64
Na^+ [pA]	365.38±57.30	540.38±98.71	270.05±30.66	9	4	12
Na^+/C_M [pA/pF]	10.44±1.50	22.69±4.82	14.56±2.18	9	4	12

p<0.05	p<0.01	**p<0.001**

The values in the table are presented as mean ± S.E.M. **Abbreviations**: Com – Cells with a complex current pattern; CT – Mouse strain without manipulated Wnt signalling; Dkk1 – Mouse strain with inhibited Wnt signalling; D3 – 3 days after MCAO; Ex3 – Mouse strain with activated Wnt signalling; K_A – A-type K^+ current amplitude; K_A/C_M – A-type K^+ current density; K_{DR} – Delayed outwardly rectifying K^+ current amplitude; K_{DR}/C_M – Delayed outwardly rectifying K^+ current density; K_{IR} – Inwardly rectifying K^+ current amplitude; K_{IR}/C_M – Inwardly rectifying K^+ current density; MCAO – Middle cerebral artery occlusion; N – Number of measured cells; Na^+– Na^+ current amplitude; Na^+/C_M – Na^+ current density; S.E.M. – Standard error of the mean; Wnt – Wingless/Int.

Table 12: K^+ and Na^+ currents in cells with a passive current pattern and their changes after manipulation of the Wnt signalling pathway in mice 3 days after MCAO.

Pas	D3			N		
	CT	Ex3	Dkk1	CT	Ex3	Dkk1
K_{IR} [pA]	123.31±22.95	168.96±25.35	72.07±39.85	7	8	3
K_{IR}/C_M [pA/pF]	5.49±1.83	4.31±0.73	2.68±0.86	7	8	3
K_{DR} [pA]	155.80±107.30	112.68±25.93	-	2	5	0
K_{DR}/C_M [pA/pF]	5.89±4.56	2.89±0.44	-	2	5	0

p<0.05	p<0.01	**p<0.001**

The values in the table are presented as mean ± S.E.M. **Abbreviations**: CT – Mouse strain without manipulated Wnt signalling; Dkk1 – Mouse strain with inhibited Wnt signalling; D3 – 3 days after MCAO; Ex3 – Mouse strain with activated Wnt signalling; K_{DR} – Delayed outwardly rectifying K^+ current amplitude; K_{DR}/C_M – Delayed outwardly rectifying K^+ current density; K_{IR} – Inwardly rectifying K^+ current amplitude; K_{IR}/C_M – Inwardly rectifying K^+ current density; MCAO – Middle cerebral artery occlusion; N – Number of measured cells; Pas – Cells with a passive current pattern; S.E.M. – Standard error of the mean; Wnt – Wingless/Int.

Table 13: K^+ and Na^+ currents in cells with an outwardly rectifying current pattern and their changes after manipulation of the Wnt signalling pathway in mice 3 days after MCAO.

Out	D3			N		
	CT	Ex3	Dkk1	CT	Ex3	Dkk1
K_{DR} [pA]	1592.63±139.87	**904.23±95.41**	1534.00±129.99	13	36	13
K_{DR}/C_M [pA/pF]	75.80±7.70	61.31±5.23	91.10±8.21	13	36	13
K_A [pA]	953.18±175.16	981.32±87.08	1281.36±167.68	13	32	13
K_A/C_M [pA/pF]	47.68±8.33	73.03±6.60	89.41±14.59	13	32	13
Na^+ [pA]	240.72±28.98	358.28±136.19	246.81±42.72	5	8	8
Na^+/C_M [pA/pF]	12.13±2.09	18.58±3.78	14.78±3.38	5	8	8

p<0.05	p<0.01	**p<0.001**

The values in the table are presented as mean ± S.E.M. **Abbreviations**: CT – Mouse strain without manipulated Wnt signalling; Dkk1 – Mouse strain with inhibited Wnt signalling; D3 – 3 days after MCAO; Ex3 – Mouse strain with activated Wnt signalling; K_A – A-type K^+ current amplitude; K_A/C_M – A-type K^+ current density; K_{DR} – Delayed outwardly rectifying K^+ current amplitude; K_{DR}/C_M – Delayed outwardly rectifying K^+ current density; MCAO – Middle cerebral artery occlusion; N – Number of measured cells; Na^+– Na^+ current amplitude; Na^+/C_M – Na^+ current density; Out – Cells with an outwardly rectifying current pattern; S.E.M. – Standard error of the mean; Wnt – Wingless/Int.

Taken together, neither Wnt signalling activation nor its inhibition caused changes in electrophysiological properties of cells with a passive current profile and their incidence. Both activation and inhibition of Wnt signalling led to a shift in V_M to more negative values in cells with complex currents, while in cells with an outwardly rectifying current pattern, activation of this pathway caused depolarization of cell membrane and a decrease in its surface. Cells with outwardly rectifying currents displayed lower K_{DR} current amplitudes after Wnt signalling activation. Density of this current type was raised in cells with a complex current pattern, which can be attributed to a slight increase in the amplitudes of this current combined with a slight decrease in C_M. The amplitude of K_A current was higher after Wnt signalling inhibition in cells with complex currents, while its density was higher after both inhibition and activation of this pathway. At the same time, we observed an increase in K_A current density after inhibition of Wnt signalling in cells with an outwardly rectifying current profile. Additionally, density of Na^+ currents was increased in cells with a complex current profile after Wnt signalling activation.

8.4 Wnt signalling manipulation at later post-ischemic phase

To examine whether Wnt signalling manipulation affects changes occurring later after ischemic injury, when permanent glial scar is formed and the proliferative activity of NG2 glia declines, we studied electrophysiological properties of cells isolated 7 days after MCAO from mice of all 3 strains, either with activated or inhibited Wnt signalling, namely Ex3-D7 and Dkk1-D7 mice, respectively. As a control we used cells isolated 7 days after MCAO from mice, in which Wnt signalling was not manipulated (CT-D7).

8.4.1 The impact of the Wnt signalling manipulation on incidence of distinct cell types

Cells isolated from CT-D7 mice consisted predominantly of cells with a complex current pattern, which made 79.75 ± 6.09 % of cells. Cells with a passive current profile made 3.56 ± 2.62 % and cells with an outwardly rectifying current pattern constituted 16.69 ± 3.91 % of all measured cells. We found changes in incidence of cells with a complex and a passive current profile in cultures from Ex3-D7 mice. Incidence of cells with a complex current profile was significantly lower in Ex3-D7 mice (44.45 ± 2.69 %), while incidence of cells with a passive current profile was significantly higher in this mouse strain (24.40 ± 8.71 %). No significant change was observed in cells with an outwardly rectifying

current pattern. Inhibition of Wnt signalling did not lead to any changes in the occurrence of cell types.

Taken together, activation of Wnt signalling caused increased incidence of cells with a passive current pattern and decreased incidence of cells with a complex current pattern. These results are summarized in **Figure 13**.

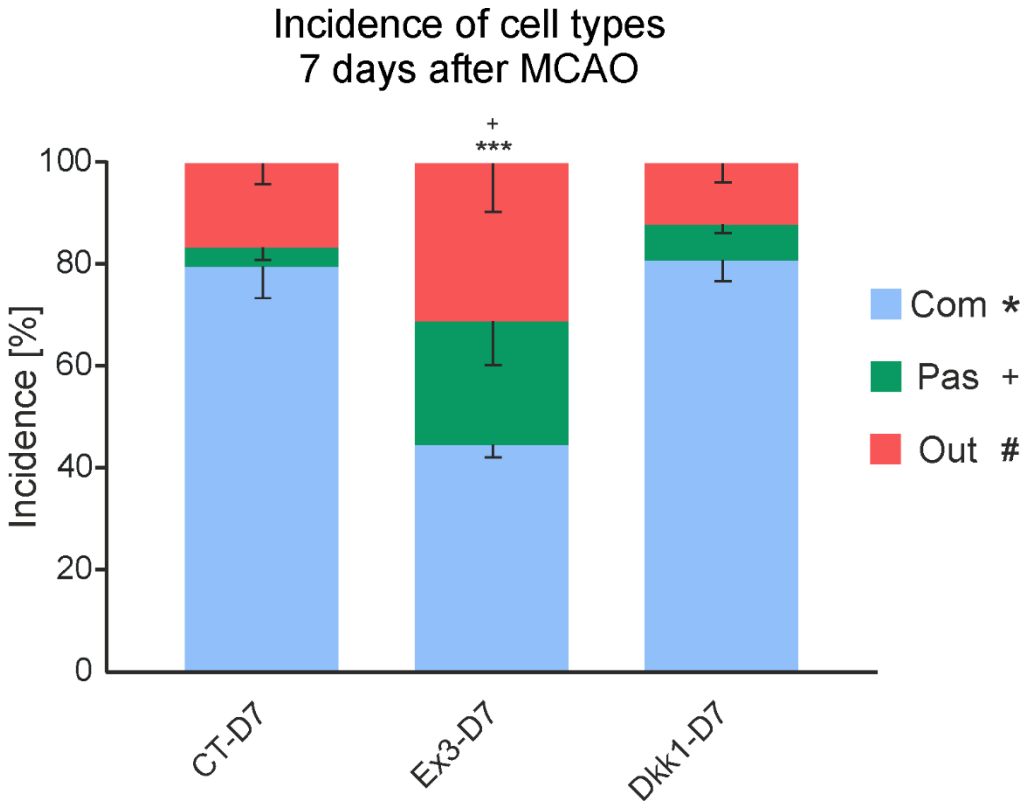

Figure 13: Incidence of cell types 7 days after MCAO and its changes in mice with manipulated Wnt signalling. **Abbreviations**: Com – Cells with a complex current pattern; CT – Mouse strain without manipulated Wnt signalling; Dkk1 – Mouse strain with inhibited Wnt signalling; D7 – 7 days after MCAO; Ex3 – Mouse strain with activated Wnt signalling; Out – Cells with an outwardly rectifying current pattern; Pas – Cells with a passive current pattern; Wnt – Wingless/Int ; * – Significant changes in incidence of cells with a complex current pattern; *** – $p<0.001$; + – Significant changes in incidence of cells with a passive current pattern, $p<0.05$; # – Significant changes in incidence of cells with an outwardly rectifying current pattern.

8.4.2 Changes of passive membrane properties of NG2 cells induced by the Wnt signalling manipulation 7 days after MCAO

No significant changes in V_M were observed in cells with a complex or a passive current profile, but a depolarization was observed in cells displaying outwardly rectifying currents in response to Wnt signalling activation. The resting membrane potential in these cells shifted from -79.33 mV to -67.09 mV (**Table 14**).

The input resistance in cells with a complex current pattern was 145.03 MΩ and it was lowered in both Ex3-D7 and Dkk1-D7 mouse strains. In Ex3-D7 mice, its value reached 112.23 MΩ, and in Dkk1-D7 mice it reached 116.96 MΩ. In cells with a passive current profile or with outwardly rectifying currents we did not observe any significant changes in IR (**Table 14**).

No significant changes in C_M occurred in any of the cell types in response to Wnt signalling manipulation. Complete results are summarized in **Table 14**.

Table14: Passive membrane properties of 3 distinct cell types and their changes after manipulation of the Wnt signalling pathway in mice 7 days after MCAO.

		D7			N		
		CT	Ex3	Dkk1	CT	Ex3	Dkk1
Com	V_M [mV]	-86.50±0.57	-82.52±2.35	-86.76±0.63	86	33	79
	IR [MΩ]	145.03±8.36	112.23±13.35	116.96±6.99	86	33	79
	C_M [pF]	25.58±1.21	24.67±1.43	24.48±1.09	86	33	79
Pas	V_M [mV]	-82.00±4.38	-88.39±0.59	-87.17±1.45	4	18	6
	IR [MΩ]	40.92±8.23	46.76±4.29	51.56±7.20	4	18	6
	C_M [pF]	44.61±7.42	39.03±3.37	45.47±11.93	4	18	6
Out	V_M [mV]	-79.33±2.30	-67.09±3.30	-81.64±2.88	18	23	11
	IR [MΩ]	475.99±83.02	738.15±111.05	347.68±39.22	18	23	11
	C_M [pF]	24.61±2.78	19.24±1.21	21.88±2.73	18	23	11

p<0.05	p<0.01	**p<0.001**

The values in the table are presented as mean ± S.E.M. **Abbreviations**: C_M – Membrane capacitance; Com – Cells with a complex current pattern; CT – Mouse strain without manipulated Wnt signalling; Dkk1 – Mouse strain with inhibited Wnt signalling; D7 – 7 days after MCAO; Ex3 – Mouse strain with activated Wnt signalling; IR – Input resistance; MCAO – Middle cerebral artery occlusion; N – Number of measured cells; Out – Cells with an outwardly rectifying current pattern; Pas – Cells with a passive current pattern; V_M – Resting membrane potential; S.E.M. – Standard error of the mean; Wnt – Wingless/Int.

8.4.3 The effect of Wnt signalling on voltage-dependent K^+ and Na^+ currents in NG2 cells

No significant changes in K_{IR} current amplitude and current density were observed in any of the cell types. As for cells with a passive current profile, we observed only one cell with K_{IR} currents in the control group, therefore we were not able to analyse changes in this cell type (**Tables 15, 16**).

The average value of K_{DR} current amplitude in cells with a complex current profile from CT-D7 mice was 1130.80 pA and it was significantly lower in both mouse strains enabling Wnt signalling manipulation. In Ex3-D7 mice, it decreased to 795.72 pA and in Dkk1-D7 mice to 847.05 pA. In cells with an outwardly rectifying current profile, K_{DR} current amplitude was not significantly different from the value obtained from CT-D7 mice (1744.56 pA). Again, properties of K_{DR} currents were not analysable in cells with passive currents, since only one of these cells exhibited this type of current. As for K_{DR} current density, we observed significantly lower values in cells with a complex current pattern isolated from Ex3-D7 mice. Current density decreased from 48.80 pA/pF to 32.91 pA/pF. In cells with an outwardly rectifying current pattern, K_{DR} current density did not change significantly after Wnt signalling manipulation (**Tables 15, 16, 17**).

The amplitude of K_A currents only changed in cells with complex currents, where it decreased from 824.81 pA to 399.41 pA in Ex3-D7 mice. The density of K_A currents measured in CT-D7 mice was 37.09 pA/pF and it decreased to 17.28 pA/pF in Ex3-D7 mice. In cells with an outwardly rectifying current pattern, no significant changes in K_A density were observed (**Tables 15, 17**).

Examination of Na^+ currents revealed that no significant change occurred in the amplitude or the density in any of the cell types. Complete results are summarized in **Table 15** for cells with a complex current profile, **Table 16** for cells with a passive current profile and **Table 17** for cells with an outwardly rectifying current profile.

Table 15: K^+ and Na^+ currents in cells with a complex current pattern and their changes after manipulation of the Wnt signalling pathway in mice 7 days after MCAO.

Com	D7			N		
	CT	Ex3	Dkk1	CT	Ex3	Dkk1
K_{IR} [pA]	185.21±8.55	151.71±13.24	196.35±9.66	86	33	79
K_{IR}/C_M [pA/pF]	8.08±0.43	6.41±0.52	8.82±0.52	86	33	78
K_{DR} [pA]	1130.80±67.79	795.72±92.34	847.05±51.02	86	33	76
K_{DR}/C_M [pA/pF]	48.80±3.23	32.91±3.36	40.69±2.90	86	33	76
K_A [pA]	824.81±79.53	**399.41±82.77**	668.48±52.94	64	22	64
K_A/C_M [pA/pF]	37.09±3.84	17.28±3.51	33.80±3.30	64	22	64
Na^+ [pA]	363.19±55.77	345.69±27.72	391.49±43.78	13	7	9
Na^+/C_M [pA/pF]	16.51±2.38	14.50±1.44	19.14±2.72	13	7	9

p<0.05	p<0.01	**p<0.001**

The values in the table are presented as mean ± S.E.M. **Abbreviations**: Com – Cells with a complex current pattern; CT – Mouse strain without manipulated Wnt signalling; Dkk1 – Mouse strain with inhibited Wnt signalling; D7 – 7 days after MCAO; Ex3 – Mouse strain with activated Wnt signalling; K_A – A-type K^+ current amplitude; K_A/C_M – A-type K^+ current density; K_{DR} – Delayed outwardly rectifying K^+ current amplitude; K_{DR}/C_M – Delayed outwardly rectifying K^+ current density; K_{IR} – Inwardly rectifying K^+ current amplitude; K_{IR}/C_M – Inwardly rectifying K^+ current density; MCAO – Middle cerebral artery occlusion; N – Number of measured cells; Na^+– Na^+ current amplitude; Na^+/C_M – Na^+ current density; S.E.M. – Standard error of the mean; Wnt – Wingless/Int.

Table 16: K^+ and Na^+ currents in cells with a passive current pattern and their changes after manipulation of the Wnt signalling pathway in mice 7 days after MCAO.

Pas	D7			N		
	CT	Ex3	Dkk1	CT	Ex3	Dkk1
K_{IR} [pA]	272.20	136.84±18.82	184.98±20.58	1	14	5
K_{IR}/C_M [pA/pF]	9.19	3.77±0.48	5.88±2.02	1	14	5
K_{DR} [pA]	144.00	170.86±41.24	98.80±9.90	1	8	2
K_{DR}/C_M [pA/pF]	2.22	4.63±0.77	1.65±0.52	1	8	2

p<0.05	p<0.01	**p<0.001**

The values in the table are presented as mean ± S.E.M. **Abbreviations**: CT – Mouse strain without manipulated Wnt signalling; Dkk1 – Mouse strain with inhibited Wnt signalling; D7 – 7 days after MCAO; Ex3 – Mouse strain with activated Wnt signalling; K_{DR} – Delayed outwardly rectifying K^+ current amplitude; K_{DR}/C_M – Delayed outwardly rectifying K^+ current density; K_{IR} – Inwardly rectifying K^+ current amplitude; K_{IR}/C_M – Inwardly rectifying K^+ current density; MCAO – Middle cerebral artery occlusion; N – Number of measured cells; Pas – Cells with a passive current pattern; S.E.M. – Standard error of the mean; Wnt – Wingless/Int.

Table 17: K^+ and Na^+ currents in cells with an outwardly rectifying current pattern and their changes after manipulation of the Wnt signalling pathway in mice 7 days after MCAO.

Out	D7			N		
	CT	Ex3	Dkk1	CT	Ex3	Dkk1
K_{DR} [pA]	1744.56±132.59	1490.50±133.04	1409.41±199.12	18	24	11
K_{DR}/C_M [pA/pF]	79.74±6.24	81.71±8.29	66.96±7.44	18	24	11
K_A [pA]	1130.08±223.39	830.32±101.77	1009.06±174.94	18	20	10
K_A/C_M [pA/pF]	59.90±13.65	51.37±9.34	55.92±10.63	18	20	10
Na^+ [pA]	313.18±29.51	389.36±61.87	475.78±51.37	4	10	5
Na^+/C_M [pA/pF]	13.10±2.33	22.73±3.50	20.32±4.46	4	10	5

p<0.05	p<0.01	**p<0.001**

The values in the table are presented as mean ± S.E.M. **Abbreviations**: CT – Mouse strain without manipulated Wnt signalling; Dkk1 – Mouse strain with inhibited Wnt signalling; D7 – 7 days after MCAO; Ex3 – Mouse strain with activated Wnt signalling; K_A – A-type K^+ current amplitude; K_A/C_M – A-type K^+ current density; K_{DR} – Delayed outwardly rectifying K^+ current amplitude; K_{DR}/C_M – Delayed outwardly rectifying K^+ current density; MCAO – Middle cerebral artery occlusion; N – Number of measured cells; Na^+– Na^+ current amplitude; Na^+/C_M – Na^+ current density; Out – Cells with an outwardly rectifying current pattern; S.E.M. – Standard error of the mean; Wnt – Wingless/Int.

Collectively, the only change of electrophysiological properties observed in cells with an outwardly rectifying current profile was depolarization of the cell membrane after Wnt signalling activation. Electrophysiological properties of cells with a complex current pattern were more affected by the Wnt signalling pathway manipulations. Both inhibition and activation of this pathway caused a decrease in IR and a decrease in K_{DR} current amplitude. Furthermore, activation of Wnt signalling led to a decrease in K_{DR} current density and to a decrease in both the density and the amplitude of K_A current.

9 Discussion

In the present study, we employed transgenic mouse strains that allow tamoxifen-induced Cre-mediated recombination and in which Cre recombinase is driven by *Cspg4* promoter. Three different mouse strains were used: CT mice, in which recombination induced the expression of tdTomato fluorescent dye in NG2 glia, but did not affect Wnt signalling, Ex3 mice, in which Wnt signalling was activated in addition to tdTomato protein expression in NG2 cells, and Dkk1 mice, in which tamoxifen administration initiated inhibition of Wnt signalling and tdTomato expression in NG2 glia. This type of glial cells is generally accepted as a proliferative cell type and an oligodendrocyte precursor *in vivo* but has also shown multipotency *in vitro*. NG2 cells also play a role in CNS tissue regeneration after various types of injury. Recent publications have shown that some properties of adult brain cells, including NG2 glia, are regulated by Wnt signalling. Therefore, our goal was to elucidate the role of this signalling in NG2 glia differentiation after ischemic brain injury.

To inspect changes in electrophysiological properties of NG2 cells and their differentiation following ischemic injury and Wnt signalling manipulation, we used the patch-clamp technique in the whole-cell configuration. Ischemic injury was induced by MCAO, a reproducible model of permanent FCI (Taguchi *et al.*, 2010). This produced a cortical injury visible with the naked eye on brain slices.

We demonstrated that mainly Wnt signalling activation has an impact on the differentiation potential of NG2 cells and that this effect changes with time following ischemia. We also found that both ischemia and Wnt signalling influence various electrophysiological properties of NG2 cells and their offspring.

9.1 NG2 glia differentiation does not changed following ischemia

We isolated the adult mouse cortex from the injured hemisphere 3 or 7 days after MCAO, or from both hemispheres from non-operated mice, and analysed electrophysiological properties of NG2 glia after 3 or 4 days of *in vitro* differentiation by the patch-clamp technique. To distinguish differentiated cells from non-differentiated NG2 glia, we divided the cells, based on their current profile, to 3 categories: cells with complex, passive and outwardly rectifying current patterns. This classification reflects the differentiation state of NG2 glia – undifferentiated (cells with complex currents), or differentiated either to astrocytes (cell with a passive current pattern) or to neuronal precursors (cells with an outwardly

rectifying current pattern) and is also supported by immunocytochemistry (Prajerova *et al.*, 2010; Honsa *et al.*, 2012, 2016).

To examine the impact of ischemia on NG2 glia, we calculated incidence of these 3 cell types in non-operated CT mice and compared it with incidence in CT mice 3 and 7 days after MCAO. We found that no significant changes occurred, implying that NG2 cell differentiation is not affected by ischemia. These results were unexpected and in conflict with our previous findings. Data obtained from transgenic mouse strain NG2creBAC:ZEG described a significant increase in $GFAP^+$ and DCX^+ cells originating from NG2 glia 7 days after MCAO, implicating astrogliogenesis and neurogenesis, respectively (Honsa *et al.*, 2012). Such conflicting results might be caused by the use of different mouse strains and thus by a different approach to NG2 glia fate mapping. Honsa and co-authors used NG2creBAC:ZEG mice with constitutive expression of EGFP under the promotor for NG2, while in our study mouse strains with tamoxifen inducible activity of Cre recombinase were employed. The fact that (Honsa *et al.*, 2012) examined differentiation *in situ* while our experiments were performed on cells isolated from the mouse brain and cultivated *in vitro* can also be the cause of discrepancies between above described results.

However, differentiation of NG2 glia to astrocytes after ischemia was also observed *in vitro* after injury in CSPG4-Tomato mice (Honsa *et al.*, 2016). Disagreement with our results might be caused by the length of cultivation of isolated cells. While in our experiment cells were kept in differentiation medium for only 3 or 4 days before being analysed, (Honsa *et al.*, 2016) cultivated cells for 7 days.

Another study that employed NG2creBAC:ZEG mice did not observe generation of reactive astrocytes from NG2 glia after injury, similarly to our results; however, differentiation of these cells to oligodendrocytes was observed (Komitova *et al.*, 2011). Throughout our experiments, only two differentiated oligodendrocytes were found and because of their low number, we did not include these cells to analysis. A different mouse strain and a different type of injury might both be the reason of contrasting results; however, since the major role of NG2 glia is to give rise to oligodendrocytes, we revised our approach. This revealed that combination of short cultivation time with the presence of PDGFα in cultivation medium might be to blame, since PDGFα had been shown to slow down the maturation of oligodendrocytes both *in vivo* and *in vitro* (Bögler *et al.*, 1990; Butt *et al.*, 1997). Another reason for the low numbers of oligodendrocytes in our study might be slow maturation of oligodendrocytes in the adult cortex, even after injury, as reported in (Zhu *et al.*, 2011).

We also observed various changes in individual electrophysiological parameters that are summarized in **Tables 2-5**. Ischemic injury induced no changes in electrophysiological properties of cells with passive and outwardly rectifying currents. However, in cells displaying complex currents K_{IR} current density declined 3 as well as 7 days after MCAO, which might reflect an increased proliferation of these cells evoked by ischemic injury. Similar decline of K_{IR} currents was observed in other types of CNS injuries, such as global cerebral ischemia, stab wound and freeze lesion (Bordey *et al.*, 2001; Anderova *et al.*, 2004; Pivonkova *et al.*, 2010). Nevertheless, Pivonkova and co-authors also detected marked increases in K_A and K_{DR} current densities, which were not observed in our experiments. This discrepancy possibly originates from employing different models of ischemia, which affect diverse brain regions, such as hippocampus and cortex, and moreover, global cerebral ischemia was induced in rats (Pivonkova *et al.*, 2010).

9.2 Wnt signalling activation supports differentiation of NG2 glia to astrocytes in the healthy brain

When we compared incidence of cell types in CT-CTRL mice with incidence obtained from mice with manipulated Wnt signalling, we observed a significant increase in cells with a passive current profile and a decrease in cells with a complex current profile in Ex3-CTRL mice, indicating that Wnt signalling activation results in the differentiation of NG2 cells to astrocytes. No significant change in incidence of cell types was observed after the inhibition of Wnt signalling. Inhibition of Wnt signalling by Aspirin has been shown to promote *in vitro* and *in vivo* oligodendrogliogenesis from NG2 glia (Huang *et al.*, 2016). As stated above, number of observed oligodendrocytes in our study was extremely low and thus we were not able to assess any changes in incidence of this cell type.

Both inhibition and activation of Wnt signalling caused changes in individual electrophysiological parameters and these changes differed among cell types. Interestingly, we observed that Wnt signalling activation caused hyperpolarization of cells with passive currents (presumably NG2 cells–derived astrocytes), suggesting that Wnt signalling activation might affect expression of other ion channels that participate in V_M maintenance, such as two-pore domain K^+ channels that were described in astrocytes (Zhou *et al.*, 2009). Such hyperpolarization was accompanied by an IR decrease. Similar effect of Wnt activation was observed also in cells with a complex current pattern (NG2 cells) that were also shown to express K2P channels (Zhang *et al.*, 2014).

While we observed increased astrogliogenesis after activation of the Wnt signalling pathway in NG2 glia, an opposite impact of this manipulation was observed in NS/PCs, where activation of this pathway caused increased neurogenesis (Kriska *et al.*, 2016). Both these findings support the idea that Wnt signalling plays an important role in regulation of differentiation. While Dkk1 mouse strain had a significant effect on incidence in NS/PCs, we did not observe such phenomenon, probably because of very low incidence of differentiated cells in non-manipulated Wnt signalling. As mentioned above, the presence of PDGFα in cultivation medium can be the cause of low differentiation, however, the presence of this factor is required for NG2 glia survival.

9.3 Wnt signalling activation 3 days after MCAO supports neurogenesis

Our investigation of the impact of Wnt signalling on differentiation of NG2 glia 3 days after ischemic injury revealed that incidence of cells with outwardly rectifying currents was significantly higher when Wnt signalling was active. This suggests that differentiation of NG2 glia after ischemic injury can be regulated by Wnt signalling, activation of which leads to increased number of cells displaying outwardly rectifying currents, i.e. increased neurogenesis. This is also supported by a fact that in response to ischemic injury together with Wnt signalling activation NG2 cells-derived neuroblasts displayed more depolarized $V_{M,}$ a typical feature of immature neuron-committed cells (Prajerova *et al.*, 2010). Another study that examined the role of Wnt signalling in regeneration after ischemic brain injury also described neurogenesis supporting effect of Wnt signalling activation in SVZ and striatum, however, role of NG2 glia in observed neurogenesis was not addressed by this study. Neurogenesis in this study was observable as early as 2 days after ischemic injury (Shruster *et al.*, 2012).

Interestingly, no effect of Wnt signalling inhibition was observed. As mentioned above, since differentiation in CT mice was very low, suppression of differentiation by Wnt signalling inhibition would be difficult to observe. This can be caused by short cultivation time in the combination with PDGFα in cultivation medium. The impact of Wnt signalling inhibition was previously studied by annulment of Wnt signalling in NG2 glia, which lowered glial scarring. However, this study did not inspect whether this effect is also mediated by changes in NG2 glia differentiation toward astrocytes (Rodriguez *et al.*, 2014).

Individual electrophysiological parameters were influenced by Wnt signalling, and interestingly, we observed that inhibition and activation of this signalling pathway caused similar changes in some electrophysiological features, such as V_M of cells with a complex current profile or an increase in the density of K_{DR} a K_A currents in the same cell type. So far, we do not have any explanation for this phenomenon, however we hypothesize that inhibition of Wnt signalling via Dkk1 might expose other signalling pathways that ultimately result in similar impact on functional properties of NG2 cells. An interesting finding was that Na^+ current density, which was attenuated by ischemia itself, was completely recovered when Wnt signalling was active in post-ischemic cells with a complex current profile. An opposite finding was described by Liang and co-authors, who showed a decrease in Na^+ currents in neonatal cardiomyocytes after Wnt3a treatment. However, they performed their experiment under physiological conditions, in which the impact of Wnt signalling activation might differ from that in pathology (Liang *et al.*, 2015).

9.4 Wnt signalling activation leads to astrogliogenesis 7 days after MCAO

Changes in incidence of the 3 cell types showed that 7 days after inducing ischemic injury, cells with a passive current profile were more frequent in Ex3 mice than in mice with non-manipulated Wnt signalling, however their number was not significantly different from that observed in Ex3 mice under physiological conditions. This suggests that Wnt signalling activation leads to differentiation of NG2 cells predominantly towards astrocytes. This is a surprising finding, as it was shown that Wnt signalling activation rather supports neurogenesis (Prajerova *et al.*, 2010), however at late post ischemic stages expression of other factors, such as BDNF (Bejot *et al.*, 2011), Shh (Sirko *et al.*, 2013) and leukemia inhibitory factor (Suzuki *et al.*, 2005) can be initiated and possibly cross-react with this signalling pathway altering the outcome (Valny *et al.*, 2017). In present study, astrogliogenic effect of Wnt signalling activation was also observed in non-operated mice, while Wnt signalling inhibition did not trigger any significant changes in cell incidence.

In cells expressing a complex current pattern a marked decrease in IR and both outwardly rectifying K^+ currents was detected. This possibly reflects shift in NG2 cells towards astrocytes, which also accords well with increasing incidence of cells with passive current profile.

10 Conclusion

In this study we examined the impact of Wnt signalling manipulation on NG2 glia differentiation in ischemic mice and showed that activation of Wnt signalling leads to significant changes in their differentiation. These changes differ 3 and 7 days after the induction of ischemia, suggesting that the effect of Wnt signalling changes in different phases of ischemic injury. In the acute phase of ischemic injury, Wnt signalling activation causes increased neurogenesis, while in the later phase, it supports astrogliogenesis. Interestingly, we did not observe any impact of Wnt signalling inhibition. We also examined the effect of Wnt signalling manipulation under physiological conditions and observed that activation of the Wnt signalling pathway causes increased astrogliogenesis, similarly to the effect appearing after Wnt signalling activation in the later phase of ischemia. In addition, Wnt signalling manipulation has a complex impact on changes of individual electrophysiological properties in both non-operated and ischemic mice (**Figure 14**).

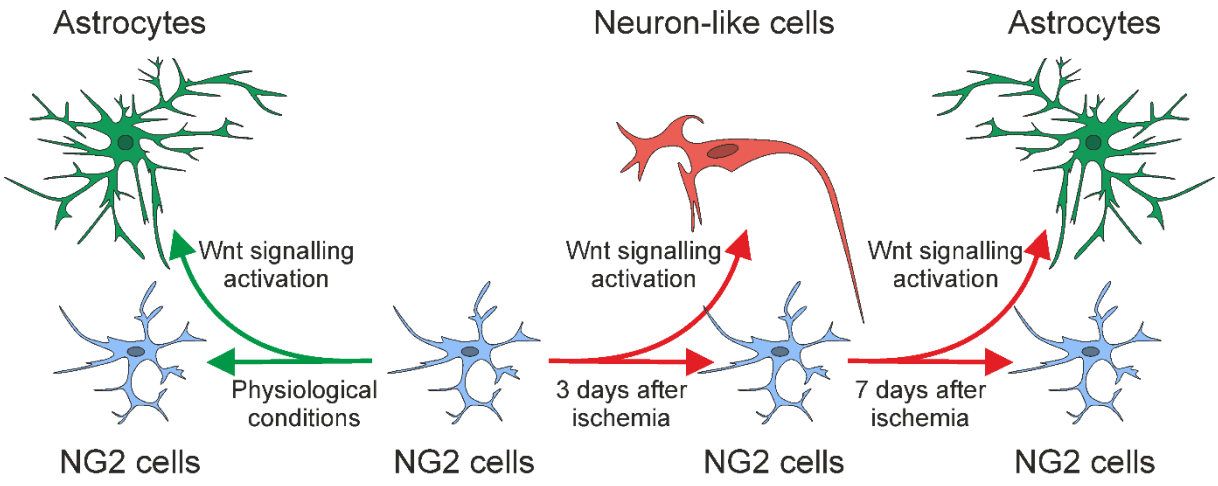

Figure 14: Graphical summary of observed changes in differentiation of NG2 cells. No changes in differentiation occurs after ischemic injury when Wnt signalling is not manipulated. Under physiological conditions, Wnt signalling activation leads to increased differentiation of NG2 cells to astrocytes. The impact of activation of this signalling pathway after ischemia is different in early and late phase of ischemic injury. In early phase, increased differentiation to neuron-like cells occurs when Wnt signalling is activated, while in late phase, Wnt signalling activation leads to increased differentiation of NG2 cells to astrocytes.

11 References

Ahn, S. and Joyner, A. L. (2005) 'In vivo analysis of quiescent adult neural stem cells responding to Sonic hedgehog.', *Nature*, 437(7060), pp. 894–7. doi: 10.1038/nature03994.

Ahrendsen, J. T., Grewal, H. S., Hickey, S. P., Culp, C. M., Gould, E. A., Shimizu, T., Strnad, F. A., Traystman, R. J., Herson, P. S. and Macklin, W. B. (2016) 'Juvenile striatal white matter is resistant to ischemia-induced damage.', *Glia*, 64(11), pp. 1972–86. doi: 10.1002/glia.23036.

Anderova, M., Antonova, T., Petrik, D., Neprasova, H., Chvatal, A. and Sykova, E. (2004) 'Voltage-dependent potassium currents in hypertrophied rat astrocytes after a cortical stab wound', *Glia*, 48(4), pp. 311–326. doi: 10.1002/glia.20076.

Anderova, M., Kubinova, S., Jelitai, M., Neprasova, H., Glogarova, K., Prajerova, I., Urdzikova, L., Chvatal, A. and Sykova, E. (2006) 'Transplantation of embryonic neuroectodermal progenitor cells into the site of a photochemical lesion: Immunohistochemical and electrophysiological analysis', *Journal of Neurobiology*, 66(10), pp. 1084–1100. doi: 10.1002/neu.20278.

Anderova, M., Vorisek, I., Pivonkova, H., Benesova, J., Vargova, L., Cicanic, M., Chvatal, A. and Sykova, E. (2011) 'Cell death/proliferation and alterations in glial morphology contribute to changes in diffusivity in the rat hippocampus after hypoxia-ischemia', *Journal of Cerebral Blood Flow and Metabolism*. Nature Publishing Group, 31(3), pp. 894–907. doi: 10.1038/jcbfm.2010.168.

Bejot, Y., Prigent-Tessier, A., Cachia, C., Giroud, M., Mossiat, C., Bertrand, N., Garnier, P. and Marie, C. (2011) 'Time-dependent contribution of non neuronal cells to BDNF production after ischemic stroke in rats', *Neurochemistry International*. Elsevier Ltd, 58(1), pp. 102–111. doi: 10.1016/j.neuint.2010.10.019.

Belachew, S., Chittajallu, R., Aguirre, A. a., Yuan, X., Kirby, M., Anderson, S. and Gallo, V. (2003) 'Postnatal NG2 proteoglycan-expressing progenitor cells are intrinsically multipotent and generate functional neurons', *Journal of Cell Biology*, 161(1), pp. 169–186. doi: 10.1083/jcb.200210110.

Bergles, D. E., Roberts, J. D., Somogyi, P. and Jahr, C. E. (2000) 'Glutamatergic synapses on oligodendrocyte precursor cells in the hippocampus.', *Nature*, 405(6783), pp. 187–91. doi: 10.1038/35012083.

De Biase, L. M., Nishiyama, A. and Bergles, D. E. (2010) 'Excitability and synaptic communication within the oligodendrocyte lineage.', *The Journal of neuroscience : the*

official journal of the Society for Neuroscience, 30(10), pp. 3600–11. doi: 10.1523/JNEUROSCI.6000-09.2010.

Bögler, O., Wren, D., Barnett, S. C., Land, H. and Noble, M. (1990) 'Cooperation between two growth factors promotes extended self-renewal and inhibits differentiation of oligodendrocyte-type-2 astrocyte (O-2A) progenitor cells.', *Proceedings of the National Academy of Sciences of the United States of America*, 87(16), pp. 6368–72. doi: 10.1073/pnas.87.16.6368.

Bordey, A., Lyons, S. A., Hablitz, J. J. and Sontheimer, H. (2001) 'Electrophysiological characteristics of reactive astrocytes in experimental cortical dysplasia.', *Journal of neurophysiology*, 85(4), pp. 1719–31. doi: 10.1152/jn.2001.85.4.1719.

Bu, J., Akhtar, N. and Nishiyama, A. (2001) 'Transient expression of the NG2 proteoglycan by a subpopulation of activated macrophages in an excitotoxic hippocampal lesion.', *Glia*, 34(4), pp. 296–310. doi: 10.1002/glia.1063.

Bu, J., Banki, A., Wu, Q. and Nishiyama, A. (2004) 'Increased NG2+ glial cell proliferation and oligodendrocyte generation in the hypomyelinating mutant shiverer', *Glia*, 48(1), pp. 51–63. doi: 10.1002/glia.20055.

Busch, S. A., Horn, K. P., Cuascut, F. X., Hawthorne, A. L., Bai, L., Miller, R. H. and Silver, J. (2010) 'Adult NG2+ cells are permissive to neurite outgrowth and stabilize sensory axons during macrophage-induced axonal dieback after spinal cord injury.', *The Journal of neuroscience : the official journal of the Society for Neuroscience*, 30(1), pp. 255–65. doi: 10.1523/JNEUROSCI.3705-09.2010.

Butt, A. M., Hornby, M. F., Kirvell, S. and Berry, M. (1997) 'Platelet-derived growth factor delays oligodendrocyte differentiation and axonal myelination in vivo in the anterior medullary velum of the developing rat', *Journal of Neuroscience Research*, 48(6), pp. 588–596. doi: 10.1002/(SICI)1097-4547(19970615)48:6<588::AID-JNR12>3.0.CO;2-R.

Cahoy, J. D., Emery, B., Kaushal, A., Foo, L. C., Zamanian, J. L., Christopherson, K. S., Xing, Y., Lubischer, J. L., Krieg, P. A., Krupenko, S. A., Thompson, W. J. and Barres, B. A. (2008) 'A Transcriptome Database for Astrocytes, Neurons, and Oligodendrocytes: A New Resource for Understanding Brain Development and Function', *Journal of Neuroscience*, 28(1), pp. 264–278. doi: 10.1523/JNEUROSCI.4178-07.2008.

Cai, J., Qi, Y., Hu, X., Tan, M., Liu, Z., Zhang, J., Li, Q., Sander, M. and Qiu, M. (2005) 'Generation of oligodendrocyte precursor cells from mouse dorsal spinal cord independent of Nkx6 regulation and Shh signaling.', *Neuron*, 45(1), pp. 41–53. doi: 10.1016/j.neuron.2004.12.028.

Cheli, V. T., Santiago González, D. A., Spreuer, V. and Paez, P. M. (2015) 'Voltage-gated Ca^{2+} entry promotes oligodendrocyte progenitor cell maturation and myelination in vitro.', *Experimental neurology*. Elsevier Inc., 265, pp. 69–83. doi: 10.1016/j.expneurol.2014.12.012.

Chen, Z. J., Ughrin, Y. and Levine, J. M. (2002) 'Inhibition of axon growth by oligodendrocyte precursor cells.', *Molecular and cellular neurosciences*, 20(1), pp. 125–39. doi: 10.1006/mcne.2002.1102.

Chittajallu, R., Aguirre, A. and Gallo, V. (2004) 'NG2-positive cells in the mouse white and grey matter display distinct physiological properties.', *The Journal of physiology*, 561(Pt 1), pp. 109–22. doi: 10.1113/jphysiol.2004.074252.

Chittajallu, R., Chen, Y., Wang, H., Yuan, X., Ghiani, C. a, Heckman, T., McBain, C. J. and Gallo, V. (2002) 'Regulation of Kv1 subunit expression in oligodendrocyte progenitor cells and their role in G1/S phase progression of the cell cycle.', *Proceedings of the National Academy of Sciences of the United States of America*, 99(4), pp. 2350–2355. doi: 10.1073/pnas.042698399.

Choudhry, Z., Rikani, A. A., Choudhry, A. M., Tariq, S., Zakaria, F., Asghar, M. W., Sarfraz, M. K., Haider, K., Shafiq, A. A. and Mobassarah, N. J. (2014) 'Sonic hedgehog signalling pathway: a complex network.', *Annals of neurosciences*, 21(1), pp. 28–31. doi: 10.5214/ans.0972.7531.210109.

Clarke, L. E., Young, K. M., Hamilton, N. B., Li, H., Richardson, W. D. and Attwell, D. (2012) 'Properties and Fate of Oligodendrocyte Progenitor Cells in the Corpus Callosum, Motor Cortex, and Piriform Cortex of the Mouse', *Journal of Neuroscience*, 32(24), pp. 8173–8185. doi: 10.1523/JNEUROSCI.0928-12.2012.

Crompton, T., Outram, S. V. and Hager-Theodorides, A. L. (2007) 'Sonic hedgehog signalling in T-cell development and activation.', *Nature reviews. Immunology*, 7(9), pp. 726–35. doi: 10.1038/nri2151.

Cuitino, L., Godoy, J. A., Farías, G. G., Couve, A., Bonansco, C., Fuenzalida, M. and Inestrosa, N. C. (2010) 'Wnt-5a modulates recycling of functional GABAA receptors on hippocampal neurons.', *The Journal of neuroscience : the official journal of the Society for Neuroscience*, 30(25), pp. 8411–20. doi: 10.1523/JNEUROSCI.5736-09.2010.

Dawson, M. R. L., Polito, A., Levine, J. M. and Reynolds, R. (2003) 'NG2-expressing glial progenitor cells: an abundant and widespread population of cycling cells in the adult rat CNS.', *Molecular and cellular neurosciences*, 24(2), pp. 476–88. doi: 10.1016/S1044-7431(03)00210-0.

Deng, W., Wang, H., Rosenberg, P. a, Volpe, J. J. and Jensen, F. E. (2004) 'Role of

metabotropic glutamate receptors in oligodendrocyte excitotoxicity and oxidative stress.', *Proceedings of the National Academy of Sciences of the United States of America*, 101(20), pp. 7751–7756. doi: 10.1073/pnas.0307850101.

Deshmukh, V. A., Tardif, V., Lyssiotis, C. A., Green, C. C., Kerman, B., Kim, H. J., Padmanabhan, K., Swoboda, J. G., Ahmad, I., Kondo, T., Gage, F. H., Theofilopoulos, A. N., Lawson, B. R., Schultz, P. G. and Lairson, L. L. (2013) 'A regenerative approach to the treatment of multiple sclerosis.', *Nature*. Nature Publishing Group, 502(7471), pp. 327–32. doi: 10.1038/nature12647.

Dijkhuizen, R. M., Beekwilder, J. P., van der Worp, H. B., Berkelbach van der Sprenkel, J. W., Tulleken, K. A. F. and Nicolay, K. (1999) 'Correlation between tissue depolarizations and damage in focal ischemic rat brain.', *Brain research*, 840(1–2), pp. 194–205. doi: 10.1016/S0006-8993(99)01769-2.

Dirnagl, U., Iadecola, C. and Moskowitz, M. a (1999) 'Pathobiology of ischaemic stroke: an integrated view.', *Trends in neurosciences*, 22(9), pp. 391–7. doi: 10.1016/S0166-2236(99)01401-0.

Djukic, B., Casper, K. B., Philpot, B. D., Chin, L. and Mccarthy, K. D. (2007) 'Conditional Knock-Out of K ir4.1 Leads to Glial Membrane Depolarization , Inhibition of Potassium and Glutamate Uptake , and Enhanced Short-Term Synaptic Potentiation', *Neuroscience*, 27(42), pp. 11354–11365. doi: 10.1523/JNEUROSCI.0723-07.2007.

Dou, C. L. and Levine, J. M. (1994) 'Inhibition of neurite growth by the NG2 chondroitin sulfate proteoglycan.', *The Journal of neuroscience : the official journal of the Society for Neuroscience*, 14(12), pp. 7616–28. doi: 10.1523/JNEUROSCI.14-12-07616.1994.

Ellison, J. A. and de Vellis, J. (1994) 'Platelet-derived growth factor receptor is expressed by cells in the early oligodendrocyte lineage.', *Journal of neuroscience research*, 37(1), pp. 116–28. doi: 10.1002/jnr.490370116.

Emsley, J. G. and Macklis, J. D. (2006) 'Astroglial heterogeneity closely reflects the neuronal-defined anatomy of the adult murine CNS.', *Neuron glia biology*, 2(3), pp. 175–86. doi: 10.1017/S1740925X06000202.

Fang, X., Burg, M. a, Barritt, D., Dahlin-Huppe, K., Nishiyama, A. and Stallcup, W. B. (1999) 'Cytoskeletal reorganization induced by engagement of the NG2 proteoglycan leads to cell spreading and migration.', *Molecular biology of the cell*, 10(10), pp. 3373–87. doi: 10.1091/mbc.10.10.3373.

Fawcett, J. W. and Asher, R. A. (1999) 'The glial scar and central nervous system repair', *Brain Research Bulletin*, 49(6), pp. 377–391. doi: 10.1016/S0361-9230(99)00072-6.

Filous, A. R., Tran, A., Howell, C. J., Busch, S. A., Evans, T. A., Stallcup, W. B., Kang, S. H., Bergles, D. E., Lee, S., Levine, J. M. and Silver, J. (2014) 'Entrapment via synaptic-like connections between NG2 proteoglycan+ cells and dystrophic axons in the lesion plays a role in regeneration failure after spinal cord injury.', *The Journal of neuroscience : the official journal of the Society for Neuroscience*, 34(49), pp. 16369–84. doi: 10.1523/JNEUROSCI.1309-14.2014.

Fluri, F., Schuhmann, M. K. and Kleinschnitz, C. (2015) 'Animal models of ischemic stroke and their application in clinical research', *Drug Design, Development and Therapy*, 9, pp. 3445–3454. doi: 10.2147/DDDT.S56071.

Folbergrova, J., Zhao, Q., Katsura, K. and Siesjö, B. K. (1995) 'N-tert-butyl-alpha-phenylnitrone improves recovery of brain energy state in rats following transient focal ischemia.', *Proceedings of the National Academy of Sciences of the United States of America*, 92(11), pp. 5057–61. doi: 10.1073/pnas.92.11.5057.

Fujimura, M., Morita-Fujimura, Y., Murakami, K., Kawase, M. and Chan, P. H. (1998) 'Cytosolic redistribution of cytochrome c after transient focal cerebral ischemia in rats.', *Journal of cerebral blood flow and metabolism : official journal of the International Society of Cerebral Blood Flow and Metabolism*, 18(11), pp. 1239–47. doi: 10.1097/00004647-199811000-00010.

García-Marqués, J., Núñez-Llaves, R. and López-Mascaraque, L. (2014) 'NG2-glia from pallial progenitors produce the largest clonal clusters of the brain: time frame of clonal generation in cortex and olfactory bulb.', *The Journal of neuroscience : the official journal of the Society for Neuroscience*, 34(6), pp. 2305–13. doi: 10.1523/JNEUROSCI.3060-13.2014.

Gautier, H. O. B., Evans, K. A., Volbracht, K., James, R., Sitnikov, S., Lundgaard, I., James, F., Lao-Peregrin, C., Reynolds, R., Franklin, R. J. M. and Káradóttir, R. T. (2015) 'Neuronal activity regulates remyelination via glutamate signalling to oligodendrocyte progenitors.', *Nature communications*, 6, p. 8518. doi: 10.1038/ncomms9518.

Ge, W.-P., Yang, X.-J., Zhang, Z., Wang, H.-K., Shen, W., Deng, Q.-D. and Duan, S. (2006) 'Long-term potentiation of neuron-glia synapses mediated by Ca^{2+}-permeable AMPA receptors.', *Science (New York, N.Y.)*, 312(5779), pp. 1533–7. doi: 10.1126/science.1124669.

Ge, W.-P., Zhou, W., Luo, Q., Jan, L. Y. and Jan, Y. N. (2009) 'Dividing glial cells maintain differentiated properties including complex morphology and functional synapses.', *Proceedings of the National Academy of Sciences of the United States of America*, 106(1), pp. 328–33. doi: 10.1073/pnas.0811353106.

Gelderblom, M., Leypoldt, F., Steinbach, K., Behrens, D., Choe, C.-U., Siler, D. A., Arumugam,

T. V., Orthey, E., Gerloff, C., Tolosa, E. and Magnus, T. (2009) 'Temporal and spatial dynamics of cerebral immune cell accumulation in stroke.', *Stroke*, 40(5), pp. 1849–57. doi: 10.1161/STROKEAHA.108.534503.

Grass, D., Pawlowski, P. G., Hirrlinger, J., Papadopoulos, N., Richter, D. W., Kirchhoff, F. and Hülsmann, S. (2004) 'Diversity of functional astroglial properties in the respiratory network.', *The Journal of neuroscience : the official journal of the Society for Neuroscience*, 24(6), pp. 1358–65. doi: 10.1523/JNEUROSCI.4022-03.2004.

Guo, F., Maeda, Y., Ma, J., Xu, J., Horiuchi, M., Miers, L., Vaccarino, F. and Pleasure, D. (2010) 'Pyramidal neurons are generated from oligodendroglial progenitor cells in adult piriform cortex.', *The Journal of neuroscience : the official journal of the Society for Neuroscience*, 30(36), pp. 12036–49. doi: 10.1523/JNEUROSCI.1360-10.2010.

Harada, N., Tamai, Y., Ishikawa, T., Sauer, B., Takaku, K., Oshima, M. and Taketo, M. M. (1999) 'Intestinal polyposis in mice with a dominant stable mutation of the beta-catenin gene.', *The EMBO journal*, 18(21), pp. 5931–42. doi: 10.1093/emboj/18.21.5931.

Hart, I. K., Richardson, W. D., Heldin, C. H., Westermark, B. and Raff, M. C. (1989) 'PDGF receptors on cells of the oligodendrocyte-type-2 astrocyte (O-2A) cell lineage.', *Development (Cambridge, England)*, 105(3), pp. 595–603.

He, X., Semenov, M., Tamai, K. and Zeng, X. (2004) 'LDL receptor-related proteins 5 and 6 in Wnt/beta-catenin signaling: arrows point the way.', *Development (Cambridge, England)*, 131(8), pp. 1663–77. doi: 10.1242/dev.01117.

Honsa, P., Pivonkova, H., Dzamba, D., Filipova, M. and Anderova, M. (2012) 'Polydendrocytes display large lineage plasticity following focal cerebral ischemia.', *PloS one*, 7(5), p. e36816. doi: 10.1371/journal.pone.0036816.

Honsa, P., Valny, M., Kriska, J., Matuskova, H., Harantova, L., Kirdajova, D., Valihrach, L., Androvic, P., Kubista, M. and Anderova, M. (2016) 'Generation of reactive astrocytes from NG2 cells is regulated by sonic hedgehog.', *Glia*, 64(9), pp. 1518–31. doi: 10.1002/glia.23019.

Hossmann, K. A. (1996) 'Periinfarct depolarizations.', *Cerebrovascular and brain metabolism reviews*, 8(3), pp. 195–208.

Huang, L., Wu, Z.-B., Zhuge, Q., Zheng, W., Shao, B., Wang, B., Sun, F. and Jin, K. (2014) 'Glial scar formation occurs in the human brain after ischemic stroke.', *International journal of medical sciences*, 11(4), pp. 344–8. doi: 10.7150/ijms.8140.

Huang, N., Chen, D., Wu, X., Chen, X., Zhang, X., Niu, J., Shen, H. Y. and Xiao, L. (2016) 'Aspirin Promotes Oligodendroglial Differentiation Through Inhibition of Wnt Signaling

Pathway', *Molecular Neurobiology*. Molecular Neurobiology, 53(5), pp. 3258–3266. doi: 10.1007/s12035-015-9241-z.

Hughes, E. G., Kang, S. H., Fukaya, M. and Bergles, D. E. (2013) 'Oligodendrocyte progenitors balance growth with self-repulsion to achieve homeostasis in the adult brain.', *Nature neuroscience*, 16(6), pp. 668–76. doi: 10.1038/nn.3390.

Iadecola, C. (1997) 'Bright and dark sides of nitric oxide in ischemic brain injury.', *Trends in neurosciences*, 20(3), pp. 132–9. doi: S0166-2236(96)10074-6 [pii].

Jagasia, R., Song, H., Gage, F. H. and Lie, D. C. (2006) 'New regulators in adult neurogenesis and their potential role for repair.', *Trends in molecular medicine*, 12(9), pp. 400–5. doi: 10.1016/j.molmed.2006.07.006.

Kaneko, D., Nakamura, N. and Ogawa, T. (1985) 'Cerebral infarction in rats using homologous blood emboli: development of a new experimental model.', *Stroke*, 16(1), pp. 76–84. doi: 10.1161/01.STR.16.1.76.

Káradóttir, R., Hamilton, N. B., Bakiri, Y. and Attwell, D. (2008) 'Spiking and nonspiking classes of oligodendrocyte precursor glia in CNS white matter', *Nature Neuroscience*, 11(4), pp. 450–456. doi: 10.1038/nn2060.

Kasischke, K. A., Vishwasrao, H. D., Fisher, P. J., Zipfel, W. R. and Webb, W. W. (2004) 'Neural activity triggers neuronal oxidative metabolism followed by astrocytic glycolysis.', *Science (New York, N.Y.)*, 305(5680), pp. 99–103. doi: 10.1126/science.1096485.

Kawano, Y. and Kypta, R. (2003) 'Secreted antagonists of the Wnt signalling pathway.', *Journal of cell science*, 116(Pt 13), pp. 2627–34. doi: 10.1242/jcs.00623.

Kessaris, N., Fogarty, M., Iannarelli, P., Grist, M., Wegner, M. and Richardson, W. D. (2006) 'Competing waves of oligodendrocytes in the forebrain and postnatal elimination of an embryonic lineage.', *Nature neuroscience*, 9(2), pp. 173–9. doi: 10.1038/nn1620.

Kim, J. Y., Park, J., Chang, J. Y., Kim, S.-H. and Lee, J. E. (2016) 'Inflammation after Ischemic Stroke: The Role of Leukocytes and Glial Cells.', *Experimental neurobiology*, 25(5), pp. 241–251. doi: 10.5607/en.2016.25.5.241.

Kofuji, P. and Newman, E. A. (2004) 'Potassium buffering in the central nervous system.', *Neuroscience*, 129(4), pp. 1045–56. doi: 10.1016/j.neuroscience.2004.06.008.

Komitova, M., Serwanski, D. R., Lu, Q. R. and Nishiyama, A. (2011) 'NG2 cells are not a major source of reactive astrocytes after neocortical stab wound injury.', *Glia*, 59(5), pp. 800–9. doi: 10.1002/glia.21152.

Komitova, M., Zhu, X., Serwanski, D. R. and Nishiyama, A. (2009) 'NG2 cells are distinct from neurogenic cells in the postnatal mouse subventricular zone', *Journal of Comparative*

Neurology, 512(5), pp. 702–716. doi: 10.1002/cne.21917.

Komiya, Y. and Habas, R. (2008) 'Wnt signal transduction pathways.', *Organogenesis*, 4(2), pp. 68–75.

Kriska, J., Honsa, P., Dzamba, D., Butenko, O., Kolenicova, D., Janeckova, L., Nahacka, Z., Andera, L., Kozmik, Z., Taketo, M. M., Korinek, V. and Anderova, M. (2016) 'Manipulating Wnt signaling at different subcellular levels affects the fate of neonatal neural stem/progenitor cells.', *Brain research*. Elsevier, 1651, pp. 73–87. doi: 10.1016/j.brainres.2016.09.026.

Kristian, T. and Siesjö, B. K. (1998) 'Calcium in ischemic cell death.', *Stroke*, 29(3), pp. 705–18. doi: 10.1161/01.STR.29.3.705.

Kühl, M., Sheldahl, L. C., Malbon, C. C. and Moon, R. T. (2000) 'Ca(2+)/calmodulin-dependent protein kinase II is stimulated by Wnt and Frizzled homologs and promotes ventral cell fates in Xenopus.', *The Journal of biological chemistry*, 275(17), pp. 12701–11. doi: 10.1074/jbc.275.17.12701.

Kukley, M., Kiladze, M., Tognatta, R., Hans, M., Swandulla, D., Schramm, J. and Dietrich, D. (2008) 'Glial cells are born with synapses.', *The FASEB journal : official publication of the Federation of American Societies for Experimental Biology*, pp. 2957–2969. doi: 10.1096/fj.07-090985.

Lai, K., Kaspar, B. K., Gage, F. H. and Schaffer, D. V. (2003) 'Sonic hedgehog regulates adult neural progenitor proliferation in vitro and in vivo.', *Nature neuroscience*, 6(1), pp. 21–7. doi: 10.1038/nn983.

Lee, Y., Morrison, B. M., Li, Y., Lengacher, S., Farah, M. H., Hoffman, P. N., Liu, Y., Tsingalia, A., Jin, L., Zhang, P., Pellerin, L., Magistretti, P. J. and Rothstein, J. D. (2012) 'Oligodendroglia metabolically support axons and contribute to neurodegeneration.', *Nature*, 487(7408), pp. 443–8. doi: 10.1038/nature11314.

Leoni, G., Rattray, M. and Butt, A. M. (2009) 'NG2 cells differentiate into astrocytes in cerebellar slices.', *Molecular and cellular neurosciences*. Elsevier Inc., 42(3), pp. 208–18. doi: 10.1016/j.mcn.2009.07.007.

Levine, J. M. (1994) 'Increased expression of the NG2 chondroitin-sulfate proteoglycan after brain injury.', *The Journal of neuroscience : the official journal of the Society for Neuroscience*, 14(8), pp. 4716–30. doi: 10.1523/JNEUROSCI.14-08-04716.1994.

Li, C., Xiao, L., Liu, X., Yang, W., Shen, W., Hu, C., Yang, G. and He, C. (2013) 'A functional role of NMDA receptor in regulating the differentiation of oligodendrocyte precursor cells and remyelination.', *Glia*, 61(5), pp. 732–49. doi: 10.1002/glia.22469.

Li, L., Harms, K. M., Ventura, P. B., Lagace, D. C., Eisch, A. J. and Cunningham, L. A. (2010)

‘Focal cerebral ischemia induces a multilineage cytogenic response from adult subventricular zone that is predominantly gliogenic.’, *Glia*, 58(13), pp. 1610–9. doi: 10.1002/glia.21033.

Liang, W., Cho, H. C. and Marbán, E. (2015) ‘Wnt signalling suppresses voltage-dependent Na + channel expression in postnatal rat cardiomyocytes’, *The Journal of Physiology*, 593(5), pp. 1147–1157. doi: 10.1113/jphysiol.2014.285551.

Lie, D.-C., Colamarino, S. A., Song, H.-J., Désiré, L., Mira, H., Consiglio, A., Lein, E. S., Jessberger, S., Lansford, H., Dearie, A. R. and Gage, F. H. (2005) ‘Wnt signalling regulates adult hippocampal neurogenesis.’, *Nature*, 437(7063), pp. 1370–5. doi: 10.1038/nature04108.

Ligon, K. L., Kesari, S., Kitada, M., Sun, T., Arnett, H. A., Alberta, J. A., Anderson, D. J., Stiles, C. D. and Rowitch, D. H. (2006) ‘Development of NG2 neural progenitor cells requires Olig gene function.’, *Proceedings of the National Academy of Sciences of the United States of America*, 103(20), pp. 7853–8. doi: 10.1073/pnas.0511001103.

Lin, S.-C., Huck, J. H. J., Roberts, J. D. B., Macklin, W. B., Somogyi, P. and Bergles, D. E. (2005) ‘Climbing fiber innervation of NG2-expressing glia in the mammalian cerebellum.’, *Neuron*, 46(5), pp. 773–85. doi: 10.1016/j.neuron.2005.04.025.

Lindahl, P., Johansson, B. R., Levéen, P. and Betsholtz, C. (1997) ‘Pericyte loss and microaneurysm formation in PDGF-B-deficient mice.’, *Science (New York, N.Y.)*, 277(5323), pp. 242–5. doi: 10.1126/science.277.5323.242.

Logan, C. Y. and Nusse, R. (2004) ‘The Wnt signaling pathway in development and disease.’, *Annual review of cell and developmental biology*, 20(1), pp. 781–810. doi: 10.1146/annurev.cellbio.20.010403.113126.

Lowry, O. H., Passonneau, J. V., Hasselberger, F. X. and Schulz, D. W. (1964) ‘Effect of Ischemia on Known Substrates and Cofactors of the Glycolytic Pathway in Brain’, *The Journal of biological chemistry*, 239(1), pp. 18–30.

Lu, Q. R., Sun, T., Zhu, Z., Ma, N., Garcia, M., Stiles, C. D. and Rowitch, D. H. (2002) ‘Common developmental requirement for Olig function indicates a motor neuron/oligodendrocyte connection.’, *Cell*, 109(1), pp. 75–86. doi: 10.1016/S0092-8674(02)00678-5.

MacDonald, B. T., Tamai, K. and He, X. (2009) ‘Wnt/β-Catenin Signaling: Components, Mechanisms, and Diseases’, *Developmental Cell*, 17(1), pp. 9–26. doi: 10.1016/j.devcel.2009.06.016.

Magaki, S. D., Williams, C. K. and Vinters, H. V (2017) ‘Glial function (and dysfunction) in the normal & ischemic brain.’, *Neuropharmacology*. Elsevier Ltd, pp. 1–8. doi: 10.1016/j.neuropharm.2017.11.009.

Magistretti, P. J. (2011) 'Neuron-glia metabolic coupling and plasticity.', *Experimental physiology*, 96(4), pp. 407–10. doi: 10.1113/expphysiol.2010.053157.

Maldonado, P. P., Vélez-Fort, M., Levavasseur, F. and Angulo, M. C. (2013) 'Oligodendrocyte precursor cells are accurate sensors of local K^+ in mature gray matter.', *The Journal of neuroscience : the official journal of the Society for Neuroscience*, 33(6), pp. 2432–42. doi: 10.1523/JNEUROSCI.1961-12.2013.

Marinou, K., Christodoulides, C., Antoniades, C. and Koutsilieris, M. (2012) 'Wnt signaling in cardiovascular physiology', *Trends in Endocrinology and Metabolism*. Elsevier Ltd, 23(12), pp. 628–636. doi: 10.1016/j.tem.2012.06.001.

Martí, E. and Bovolenta, P. (2002) 'Sonic hedgehog in CNS development: One signal, multiple outputs', *Trends in Neurosciences*, 25(2), pp. 89–96. doi: 10.1016/S0166-2236(02)02062-3.

Martin, R. L., Lloyd, H. G. and Cowan, A. I. (1994) 'The early events of oxygen and glucose deprivation: setting the scene for neuronal death?', *Trends in neurosciences*, 17(6), pp. 251–7. doi: 10.1016/0166-2236(94)90008-6.

Matthias, K., Kirchhoff, F., Seifert, G., Hüttmann, K., Matyash, M., Kettenmann, H. and Steinhäuser, C. (2003) 'Segregated expression of AMPA-type glutamate receptors and glutamate transporters defines distinct astrocyte populations in the mouse hippocampus.', *The Journal of neuroscience : the official journal of the Society for Neuroscience*, 23(5), pp. 1750–8. doi: 10.1523/JNEUROSCI.23-05-01750.2003.

McKenzie, I. A., Ohayon, D., Li, H., de Faria, J. P., Emery, B., Tohyama, K. and Richardson, W. D. (2014) 'Motor skill learning requires active central myelination.', *Science (New York, N.Y.)*, 346(6207), pp. 318–22. doi: 10.1126/science.1254960.

McTigue, D. M., Wei, P. and Stokes, B. T. (2001) 'Proliferation of NG2-positive cells and altered oligodendrocyte numbers in the contused rat spinal cord.', *The Journal of neuroscience : the official journal of the Society for Neuroscience*, 21(10), pp. 3392–400. doi: 0270-6474/01/213392-09$15.00/0.

Menn, B., Garcia-Verdugo, J. M., Yaschine, C., Gonzalez-Perez, O., Rowitch, D. and Alvarez-Buylla, A. (2006) 'Origin of oligodendrocytes in the subventricular zone of the adult brain.', *The Journal of neuroscience : the official journal of the Society for Neuroscience*, 26(30), pp. 7907–18. doi: 10.1523/JNEUROSCI.1299-06.2006.

Nager, M., Bhardwaj, D., Cantí, C., Medina, L., Nogués, P. and Herreros, J. (2012) 'β -Catenin Signalling in Glioblastoma Multiforme and Glioma-Initiating Cells', *Chemotherapy Research and Practice*, 2012, pp. 1–7. doi: 10.1155/2012/192362.

Nakajima, K., Honda, S., Tohyama, Y., Imai, Y., Kohsaka, S. and Kurihara, T. (2001)

'Neurotrophin secretion from cultured microglia.', *Journal of neuroscience research*, 65(4), pp. 322–31. doi: 10.1002/jnr.1157.

Neprasova, H., Anderova, M., Petrik, D., Vargova, L., Kubinova, S., Chvatal, A. and Sykova, E. (2007) 'High extracellular K^+ evokes changes in voltage-dependent K^+ and Na^+ currents and volume regulation in astrocytes', *Pflügers Archiv - European Journal of Physiology*, 453(6), pp. 839–849. doi: 10.1007/s00424-006-0151-9.

Nimmerjahn, A., Kirchhoff, F. and Helmchen, F. (2005) 'Resting microglial cells are highly dynamic surveillants of brain parenchyma in vivo.', *Science (New York, N.Y.)*, 308(5726), pp. 1314–8. doi: 10.1126/science.1110647.

Nishiyama, A., Dahlin, K. J., Prince, J. T., Johnstone, S. R. and Stallcup, W. B. (1991) 'The primary structure of NG2, a novel membrane-spanning proteoglycan.', *The Journal of cell biology*, 114(2), pp. 359–71. doi: 10.1083/jcb.114.2.359.

Nishiyama, A., Lin, X. H., Giese, N., Heldin, C. H. and Stallcup, W. B. (1996) 'Co-localization of NG2 proteoglycan and PDGF alpha-receptor on O2A progenitor cells in the developing rat brain.', *Journal of neuroscience research*, 43(3), pp. 299–314. doi: 10.1002/(SICI)1097-4547(19960201)43:3<299::AID-JNR5>3.0.CO;2-E.

Nishiyama, A., Yu, M., Drazba, J. A. and Tuohy, V. K. (1997) 'Normal and reactive NG2+ glial cells are distinct from resting and activated microglia.', *Journal of neuroscience research*, 48(4), pp. 299–312. doi: 10.1002/(SICI)1097-4547(19970515)48:4<299::AID-JNR2>3.0.CO;2-6.

O'Neill, L. A. and Kaltschmidt, C. (1997) 'NF-kappa B: a crucial transcription factor for glial and neuronal cell function.', *Trends in neurosciences*, 20(6), pp. 252–8. doi: 10.1016/S0166-2236(96)01035-1.

Orentas, D. M., Hayes, J. E., Dyer, K. L. and Miller, R. H. (1999) 'Sonic hedgehog signaling is required during the appearance of spinal cord oligodendrocyte precursors.', *Development (Cambridge, England)*, 126(11), pp. 2419–2429.

Orset, C., Macrez, R., Young, A. R., Panthou, D., Angles-Cano, E., Maubert, E., Agin, V. and Vivien, D. (2007) 'Mouse model of in situ thromboembolic stroke and reperfusion.', *Stroke*, 38(10), pp. 2771–8. doi: 10.1161/STROKEAHA.107.487520.

Othman, T., Yan, H. and Rivkees, S. A. (2003) 'Oligodendrocytes Express Functional A1 Adenosine Receptors That Stimulate Cellular Migration', *Glia*, 44(2), pp. 166–172. doi: 10.1002/glia.10281.

Ozerdem, U., Grako, K. a, Dahlin-Huppe, K., Monosov, E. and Stallcup, W. B. (2001) 'NG2 proteoglycan is expressed exclusively by mural cells during vascular morphogenesis.',

Developmental Dynamics, 222(2), pp. 218–27. doi: 10.1002/dvdy.1200.

Paez, P. M., Spreuer, V., Handley, V., Feng, J.-M., Campagnoni, C. and Campagnoni, A. T. (2007) 'Increased Expression of Golli Myelin Basic Proteins Enhances Calcium Influx into Oligodendroglial Cells', *Journal of Neuroscience*, 27(46), pp. 12690–12699. doi: 10.1523/JNEUROSCI.2381-07.2007.

Paolicelli, R. C., Bolasco, G., Pagani, F., Maggi, L., Scianni, M., Panzanelli, P., Giustetto, M., Ferreira, T. A., Guiducci, E., Dumas, L., Ragozzino, D. and Gross, C. T. (2011) 'Synaptic pruning by microglia is necessary for normal brain development.', *Science (New York, N.Y.)*, 333(6048), pp. 1456–8. doi: 10.1126/science.1202529.

Parakalan, R., Jiang, B., Nimmi, B., Janani, M., Jayapal, M., Lu, J., Tay, S. S. W., Ling, E.-A. and Dheen, S. T. (2012) 'Transcriptome analysis of amoeboid and ramified microglia isolated from the corpus callosum of rat brain.', *BMC neuroscience*, 13(1), p. 64. doi: 10.1186/1471-2202-13-64.

Parkhurst, C. N., Yang, G., Ninan, I., Savas, J. N., Iii, J. R. Y., Lafaille, J. J., Hempstead, B. L., Littman, D. R. and Gan, W. (2014) 'Miroglia promote learning-dependent synapse formation through BDNF', *Cell*, 155(7), pp. 1596–1609. doi: 10.1016/j.cell.2013.11.030.Microglia.

Parpura, V., Basarsky, T. A., Liu, F., Jeftinija, K., Jeftinija, S. and Haydon, P. G. (1994) 'Glutamate-mediated astrocyte-neuron signalling.', *Nature*, 369(6483), pp. 744–7. doi: 10.1038/369744a0.

Peters, A. (2004) 'A fourth type of neuroglial cell in the adult central nervous system.', *Journal of neurocytology*, 33(3), pp. 345–57. doi: 10.1023/B:NEUR.0000044195.64009.27.

Petr, G. T., Sun, Y., Frederick, N. M., Zhou, Y., Dhamne, S. C., Hameed, M. Q., Miranda, C., Bedoya, E. A., Fischer, K. D., Armsen, W., Wang, J., Danbolt, N. C., Rotenberg, A., Aoki, C. J. and Rosenberg, P. A. (2015) 'Conditional deletion of the glutamate transporter GLT-1 reveals that astrocytic GLT-1 protects against fatal epilepsy while neuronal GLT-1 contributes significantly to glutamate uptake into synaptosomes.', *The Journal of neuroscience : the official journal of the Society for Neuroscience*, 35(13), pp. 5187–201. doi: 10.1523/JNEUROSCI.4255-14.2015.

Pivonkova, H., Benesova, J., Butenko, O., Chvatal, A. and Anderova, M. (2010a) 'Impact of global cerebral ischemia on K^+channel expression and membrane properties of glial cells in the rat hippocampus', *Neurochemistry International*. Elsevier Ltd, 57(7), pp. 783–794. doi: 10.1016/j.neuint.2010.08.016.

Porter, J. T. and McCarthy, K. D. (1996) 'Hippocampal astrocytes in situ respond to glutamate released from synaptic terminals.', *The Journal of neuroscience : the official journal of the*

Society for Neuroscience, 16(16), pp. 5073–81. doi: 10.1523/JNEUROSCI.16-16-05073.1996

Prajerova, I., Honsa, P., Chvatal, A. and Anderova, M. (2010) 'Distinct effects of sonic hedgehog and Wnt-7a on differentiation of neonatal neural stem/progenitor cells in vitro.', *Neuroscience*. Elsevier Inc., 171(3), pp. 693–711. doi: 10.1016/j.neuroscience.2010.09.023.

Psachoulia, K., Jamen, F., Young, K. M. and Richardson, W. D. (2009) 'Cell cycle dynamics of NG2 cells in the postnatal and ageing brain.', *Neuron glia biology*, 5(3–4), pp. 57–67. doi: 10.1017/S1740925X09990354.

Raff, M. C., Miller, R. H. and Noble, M. (1983) 'A glial progenitor cell that develops in vitro into an astrocyte or an oligodendrocyte depending on culture medium.', *Nature*, 303(5916), pp. 390–6. doi: 10.1038/303390a0.

Regan, M. R., Huang, Y. H., Kim, Y. S., Dykes-Hoberg, M. I., Jin, L., Watkins, A. M., Bergles, D. E. and Rothstein, J. D. (2007) 'Variations in promoter activity reveal a differential expression and physiology of glutamate transporters by glia in the developing and mature CNS.', *The Journal of neuroscience : the official journal of the Society for Neuroscience*, 27(25), pp. 6607–19. doi: 10.1523/JNEUROSCI.0790-07.2007.

Rivers, L. E., Young, K. M., Rizzi, M., Jamen, F., Psachoulia, K., Wade, A., Kessaris, N. and Richardson, W. D. (2008) 'PDGFRA/NG2 glia generate myelinating oligodendrocytes and piriform projection neurons in adult mice.', *Nature neuroscience*, 11(12), pp. 1392–401. doi: 10.1038/nn.2220.

Robins, S. C., Trudel, E., Rotondi, O., Liu, X., Djogo, T., Kryzskaya, D., Bourque, C. W. and Kokoeva, M. V. (2013) 'Evidence for NG2-glia derived, adult-born functional neurons in the hypothalamus.', *PloS one*, 8(10), p. e78236. doi: 10.1371/journal.pone.0078236.

Rodriguez, J. P., Coulter, M., Miotke, J., Meyer, R. L., Takemaru, K.-I. and Levine, J. M. (2014) 'Abrogation of -Catenin Signaling in Oligodendrocyte Precursor Cells Reduces Glial Scarring and Promotes Axon Regeneration after CNS Injury', *Journal of Neuroscience*, 34(31), pp. 10285–10297. doi: 10.1523/JNEUROSCI.4915-13.2014.

Rothwell, N. J. and Hopkins, S. J. (1995) 'Cytokines and the nervous system II: Actions and mechanisms of action.', *Trends in neurosciences*, 18(3), pp. 130–6. doi: 10.1016/0166-2236(95)93890-A.

Ruscher, K., Isaev, N., Trendelenburg, G., Weih, M., Iurato, L., Meisel, A. and Dirnagl, U. (1998) 'Induction of hypoxia inducible factor 1 by oxygen glucose deprivation is attenuated by hypoxic preconditioning in rat cultured neurons.', *Neuroscience letters*, 254(2), pp. 117–20. doi: 10.1016/S0304-3940(98)00688-0.

Sakry, D., Neitz, A., Singh, J., Frischknecht, R., Marongiu, D., Binamé, F., Perera, S. S., Endres,

K., Lutz, B., Radyushkin, K., Trotter, J. and Mittmann, T. (2014) 'Oligodendrocyte Precursor Cells Modulate the Neuronal Network by Activity-Dependent Ectodomain Cleavage of Glial NG2', *PLoS Biology*, 12(11), p. e1001993. doi: 10.1371/journal.pbio.1001993.

Semënov, M., Tamai, K. and He, X. (2005) 'SOST is a ligand for LRP5/LRP6 and a Wnt signaling inhibitor.', *The Journal of biological chemistry*, 280(29), pp. 26770–5. doi: 10.1074/jbc.M504308200.

Semënov, M. V., Tamai, K., Brott, B. K., Kühl, M., Sokol, S. and He, X. (2001) 'Head inducer Dickkopf-1 is a ligand for Wnt coreceptor LRP6.', *Current biology : CB*, 11(12), pp. 951–61. doi: 10.1016/S0960-9822(01)00290-1.

Shen, J. (2013) 'Modeling the glutamate-glutamine neurotransmitter cycle', *Frontiers in Neuroenergetics*, 5(JAN), pp. 1–13. doi: 10.3389/fnene.2013.00001.

Shruster, A., Ben-Zur, T., Melamed, E. and Offen, D. (2012) 'Wnt signaling enhances neurogenesis and improves neurological function after focal ischemic injury.', *PloS one*, 7(7), p. e40843. doi: 10.1371/journal.pone.0040843.

Silbereis, J. C., Huang, E. J., Back, S. A. and Rowitch, D. H. (2010) 'Towards improved animal models of neonatal white matter injury associated with cerebral palsy', *Disease Models & Mechanisms*, 3(11–12), pp. 678–688. doi: 10.1242/dmm.002915.

Simon, C., Götz, M. and Dimou, L. (2011) 'Progenitors in the adult cerebral cortex: cell cycle properties and regulation by physiological stimuli and injury.', *Glia*, 59(6), pp. 869–81. doi: 10.1002/glia.21156.

Sirko, S., Behrendt, G., Johansson, P. A., Tripathi, P., Costa, M., Bek, S., Heinrich, C., Tiedt, S., Colak, D., Dichgans, M., Fischer, I. R., Plesnila, N., Staufenbiel, M., Haass, C., Snapyan, M., Saghatelyan, A., Tsai, L. H., Fischer, A., Grobe, K., Dimou, L. and Götz, M. (2013) 'Reactive glia in the injured brain acquire stem cell properties in response to sonic hedgehog glia', *Cell Stem Cell*, 12(4), pp. 426–439. doi: 10.1016/j.stem.2013.01.019.

Stallcup, W. B. (1981) 'The NG2 antigen, a putative lineage marker: immunofluorescent localization in primary cultures of rat brain.', *Developmental biology*, 83(1), pp. 154–65. doi: 10.1016/S0012-1606(81)80018-8.

Stallcup, W. B. and Beasley, L. (1987) 'Bipotential glial precursor cells of the optic nerve express the NG2 proteoglycan.', *The Journal of neuroscience : the official journal of the Society for Neuroscience*, 7(9), pp. 2737–44. doi: 10.1523/JNEUROSCI.07-09-02737.1987.

Sugimura, R. and Li, L. (2010) 'Noncanonical Wnt signaling in vertebrate development, stem cells, and diseases.', *Birth defects research. Part C, Embryo today : reviews*, 90(4), pp. 243–56. doi: 10.1002/bdrc.20195.

Suzuki, S., Yamashita, T., Tanaka, K., Hattori, H., Sawamoto, K., Okano, H. and Suzuki, N. (2005) 'Activation of Cytokine Signaling through Leukemia Inhibitory Factor Receptor (LIFR)/gp130 Attenuates Ischemic Brain Injury in Rats', *Journal of Cerebral Blood Flow & Metabolism*, 25(6), pp. 685–693. doi: 10.1038/sj.jcbfm.9600061.

Taguchi, A., Kasahara, Y., Nakagomi, T., Stern, D. M., Fukunaga, M., Ishikawa, M. and Matsuyama, T. (2010) 'A Reproducible and Simple Model of Permanent Cerebral Ischemia in CB-17 and SCID Mice.', *Journal of experimental stroke & translational medicine*, 3(1), pp. 28–33. doi: 10.6030/1939-067X-3.1.28.

Tanaka, K., Nogawa, S., Ito, D., Suzuki, S., Dembo, T., Kosakai, A. and Fukuuchi, Y. (2001) 'Activation of NG2-positive oligodendrocyte progenitor cells during post-ischemic reperfusion in the rat brain', *Neuroreport*, 12(10), pp. 2169–2174. doi: 10.1097/00001756-200107200-00025.

Tanaka, Y., Tozuka, Y., Takata, T., Shimazu, N., Matsumura, N., Ohta, A. and Hisatsune, T. (2009) 'Excitatory GABAergic activation of cortical dividing glial cells', *Cerebral Cortex*, 19(9), pp. 2181–2195. doi: 10.1093/cercor/bhn238.

Tillet, E., Gential, B., Garrone, R. and Stallcup, W. B. (2002) 'NG2 proteoglycan mediates beta1 integrin-independent cell adhesion and spreading on collagen VI.', *Journal of cellular biochemistry*, 86(4), pp. 726–36. doi: 10.1002/jcb.10268.

Tomassy, G. S., Berger, D. R., Chen, H., Kasthuri, N., Hayworth, K. J., Vercelli, A., Seung, H. S., Lichtman, J. W. and Arlotta, P. (2014) 'Distinct profiles of myelin distribution along single axons of pyramidal neurons in the neocortex.', *Science (New York, N.Y.)*, 344(6181), pp. 319–24. doi: 10.1126/science.1249766.

Traystman, R. J. (2003) 'Animal models of focal and global cerebral ischemia.', *ILAR journal*, 44(2), pp. 85–95. doi: 10.1093/ilar.44.2.85.

Ueno, M., Fujita, Y., Tanaka, T., Nakamura, Y., Kikuta, J., Ishii, M. and Yamashita, T. (2013) 'Layer V cortical neurons require microglial support for survival during postnatal development.', *Nature neuroscience*. Nature Publishing Group, 16(5), pp. 543–51. doi: 10.1038/nn.3358.

Valny, M., Honsa, P., Kriska, J. and Anderova, M. (2017) 'Multipotency and therapeutic potential of NG2 cells', *Biochemical Pharmacology*. Elsevier Inc., 141, pp. 42–55. doi: 10.1016/j.bcp.2017.05.008.

Varela-Nallar, L., Alfaro, I. E., Serrano, F. G., Parodi, J. and Inestrosa, N. C. (2010) 'Wingless-type family member 5A (Wnt-5a) stimulates synaptic differentiation and function of glutamatergic synapses.', *Proceedings of the National Academy of Sciences of the United*

States of America, 107(49), pp. 21164–9. doi: 10.1073/pnas.1010011107.

Vautier, F., Belachew, S., Chittajallu, R. and Gallo, V. (2004) 'Shaker-type potassium channel subunits differentially control oligodendrocyte progenitor proliferation.', *Glia*, 48(4), pp. 337–45. doi: 10.1002/glia.20088.

de Vivo, L., Melone, M., Bucci, G., Rothstein, J. D. and Conti, F. (2010) 'Quantitative analysis of EAAT4 promoter activity in neurons and astrocytes of mouse somatic sensory cortex.', *Neuroscience letters*, 474(1), pp. 42–5. doi: 10.1016/j.neulet.2010.03.003.

Wakselman, S., Béchade, C., Roumier, A., Bernard, D., Triller, A. and Bessis, A. (2008) 'Developmental neuronal death in hippocampus requires the microglial CD11b integrin and DAP12 immunoreceptor.', *The Journal of neuroscience : the official journal of the Society for Neuroscience*, 28(32), pp. 8138–43. doi: 10.1523/JNEUROSCI.1006-08.2008.

Wang, J., Sinha, T. and Wynshaw-Boris, A. (2012) 'Wnt signaling in mammalian development: lessons from mouse genetics.', *Cold Spring Harbor perspectives in biology*, 4(5), p. 6. doi: 10.1101/cshperspect.a007963.

Wang, S. S.-H., Shultz, J. R., Burish, M. J., Harrison, K. H., Hof, P. R., Towns, L. C., Wagers, M. W. and Wyatt, K. D. (2008) 'Functional trade-offs in white matter axonal scaling.', *The Journal of neuroscience : the official journal of the Society for Neuroscience*, 28(15), pp. 4047–56. doi: 10.1523/JNEUROSCI.5559-05.2008.

Wang, W., Gao, X.-F., Xiao, L., Xiang, Z.-H. and He, C. (2011) 'KV7/KCNQ Channels Are Functionally Expressed in Oligodendrocyte Progenitor Cells', *PLoS ONE*. Edited by Y.-P. Tang, 6(7), p. e21792. doi: 10.1371/journal.pone.0021792.

Wexler, E. M., Paucer, A., Kornblum, H. I., Palmer, T. D., Plamer, T. D. and Geschwind, D. H. (2009) 'Endogenous Wnt signaling maintains neural progenitor cell potency.', *Stem cells (Dayton, Ohio)*, 27(5), pp. 1130–41. doi: 10.1002/stem.36.

WHO.Int. (2016) 'WHO | The Atlas of Heart Disease and Stroke', *WHO*. World Health Organization. Available at: http://www.who.int/cardiovascular_diseases/resources/atlas/en/ (Accessed: 6 February 2018).

Wisniewska, M. B., Nagalski, A., Dabrowski, M., Misztal, K. and Kuznicki, J. (2012) 'Novel β-catenin target genes identified in thalamic neurons encode modulators of neuronal excitability.', *BMC genomics*, 13(1), p. 635. doi: 10.1186/1471-2164-13-635.

Woodruff, T. M., Thundyil, J., Tang, S.-C., Sobey, C. G., Taylor, S. M. and Arumugam, T. V (2011) 'Pathophysiology, treatment, and animal and cellular models of human ischemic stroke', *Molecular Neurodegeneration*. BioMed Central Ltd, 6(1), p. 11. doi: 10.1186/1750-1326-6-11.

Wu, X., Tu, X., Joeng, K. S., Hilton, M. J., Williams, D. A. and Long, F. (2008) 'Rac1 Activation Controls Nuclear Localization of β-catenin during Canonical Wnt Signaling', *Cell*, 133(2), pp. 340–353. doi: 10.1016/j.cell.2008.01.052.

Xiao, L., Hu, C., Yang, W., Guo, D., Li, C., Shen, W., Liu, X., Aijun, H., Dan, W. and He, C. (2013) 'NMDA receptor couples Rac1-GEF Tiam1 to direct oligodendrocyte precursor cell migration', *Glia*, 61(12), pp. 2078–2099. doi: 10.1002/glia.22578.

Xie, M., Lynch, D. and Schools, G. (2007) 'Sodium channel currents in rat hippocampal NG2 glia: Characterization and contribution to resting membrane potential', *Neuroscience*, 150, pp. 853–862. doi: 10.1016/j.neuroscience.2007.09.057.

Xing, Y. L., Röth, P. T., Stratton, J. A. S., Chuang, B. H. A., Danne, J., Ellis, S. L., Ng, S. W., Kilpatrick, T. J. and Merson, T. D. (2014) 'Adult neural precursor cells from the subventricular zone contribute significantly to oligodendrocyte regeneration and remyelination.', *The Journal of neuroscience : the official journal of the Society for Neuroscience*, 34(42), pp. 14128–46. doi: 10.1523/JNEUROSCI.3491-13.2014.

Yang, Z., Suzuki, R., Daniels, S. B., Brunquell, C. B., Sala, C. J. and Nishiyama, A. (2006) 'NG2 glial cells provide a favorable substrate for growing axons.', *The Journal of neuroscience : the official journal of the Society for Neuroscience*, 26(14), pp. 3829–39. doi: 10.1523/JNEUROSCI.4247-05.2006.

Yi, H., Hu, J., Qian, J. and Hackam, A. S. (2012) 'Expression of brain-derived neurotrophic factor is regulated by the Wnt signaling pathway.', *Neuroreport*, 23(3), pp. 189–94. doi: 10.1097/WNR.0b013e32834fab06.

Young, K. M., Psachoulia, K., Tripathi, R. B., Dunn, S.-J., Cossell, L., Attwell, D., Tohyama, K. and Richardson, W. D. (2013) 'Oligodendrocyte dynamics in the healthy adult CNS: evidence for myelin remodeling.', *Neuron*. Elsevier Inc., 77(5), pp. 873–85. doi: 10.1016/j.neuron.2013.01.006.

Yu, A. C., Schousboec, A. and Hertz, L. (1982) 'Metabolic Fate of 14 C-Labeled Glutamate in Astrocytes in Primary Cultures', *Journal of Neurochemistry*, 39(4), pp. 954–960. doi: 10.1111/j.1471-4159.1982.tb11482.x.

Zhang, R. L., Chopp, M., Roberts, C., Wei, M., Wang, X., Liu, X., Lu, M. and Zhang, Z. G. (2012) 'Sildenafil Enhances Neurogenesis and Oligodendrogenesis in Ischemic Brain of Middle-Aged Mouse', *PLoS ONE*, 7(10), pp. 3–8. doi: 10.1371/journal.pone.0048141.

Zhang, Y., Chen, K., Sloan, S. A., Bennett, M. L., Scholze, A. R., O'Keeffe, S., Phatnani, H. P., Guarnieri, P., Caneda, C., Ruderisch, N., Deng, S., Liddelow, S. A., Zhang, C., Daneman, R., Maniatis, T., Barres, B. A. and Wu, J. Q. (2014) 'An RNA-Sequencing Transcriptome and

Splicing Database of Glia, Neurons, and Vascular Cells of the Cerebral Cortex', *Journal of Neuroscience*, 34(36), pp. 11929–11947. doi: 10.1523/JNEUROSCI.1860-14.2014.

Zhou, M., Xu, G., Xie, M., Zhang, X., Schools, G. P., Ma, L., Kimelberg, H. K. and Chen, H. (2009) 'TWIK-1 and TREK-1 Are Potassium Channels Contributing Significantly to Astrocyte Passive Conductance in Rat Hippocampal Slices', *Journal of Neuroscience*, 29(26), pp. 8551–8564. doi: 10.1523/JNEUROSCI.5784-08.2009.

Zhu, X., Bergles, D. E. and Nishiyama, A. (2008) 'NG2 cells generate both oligodendrocytes and gray matter astrocytes.', *Development (Cambridge, England)*, 135(1), pp. 145–57. doi: 10.1242/dev.004895.

Zhu, X., Hill, R. a, Dietrich, D., Komitova, M., Suzuki, R. and Nishiyama, A. (2011) 'Age-dependent fate and lineage restriction of single NG2 cells.', *Development (Cambridge, England)*, 138(4), pp. 745–53. doi: 10.1242/dev.047951.

Zhu, X., Zuo, H., Maher, B. J., Serwanski, D. R., LoTurco, J. J., Lu, Q. R. and Nishiyama, A. (2012) 'Olig2-dependent developmental fate switch of NG2 cells.', *Development (Cambridge, England)*, 139(13), pp. 2299–307. doi: 10.1242/dev.078873.

Ziskin, J. L., Nishiyama, A., Rubio, M., Fukaya, M. and Bergles, D. E. (2007) 'Vesicular release of glutamate from unmyelinated axons in white matter.', *Nature neuroscience*, 10(3), pp. 321–330. doi: 10.1038/nn1854.

Zonouzi, M., Scafidi, J., Li, P., McEllin, B., Edwards, J., Dupree, J. L., Harvey, L., Sun, D., Hübner, C. A., Cull-Candy, S. G., Farrant, M. and Gallo, V. (2015) 'GABAergic regulation of cerebellar NG2 cell development is altered in perinatal white matter injury.', *Nature neuroscience*, 18(5), pp. 674–82. doi: 10.1038/nn.3990.

del Zoppo, G. J. and Hallenbeck, J. M. (2000) 'Advances in the vascular pathophysiology of ischemic stroke.', *Thrombosis research*, 98(3), pp. 73–81. doi: 10.1016/S0049-3848(00)00218-8.

del Zoppo, G. J., Milner, R., Mabuchi, T., Hung, S., Wang, X., Berg, G. I. and Koziol, J. A. (2007) 'Microglial activation and matrix protease generation during focal cerebral ischemia.', *Stroke*, 38(2 Suppl), pp. 646–51. doi: 10.1161/01.STR.0000254477.34231.cb.

Zuo, X.-L., Wu, P. and Ji, A.-M. (2012) 'Nylon filament coated with paraffin for intraluminal permanent middle cerebral artery occlusion in rats.', *Neuroscience letters*. Elsevier Ireland Ltd, 519(1), pp. 42–6. doi: 10.1016/j.neulet.2012.05.017.